VILNIUS UNIVERSITY

VAIDOTAS STANKEVIČIUS

DOSE DELIVERY AND MICROENVIRONMENT DEPENDENT TRANSCRIPTOMIC PROFILES OF TUMOUR CELLS EXPOSED TO IONIZING RADIATION

Doctoral dissertation

Physical sciences, biochemistry (04 P)

Vilnius, 2016

The work presented in doctoral dissertation has been carried out at Vilnius university Department of Natural Sciences and National Cancer Institute during 2011-2015.

Scientific supervisor

Prof. dr. **Kęstutis Sužiedėlis** (Vilnius University, physical sciences, biochemistry – 04 P) 2011-2015.

Scientific advisor

Prof. dr. **Kęstutis Sužiedėlis** (Vilnius University, physical sciences, biochemistry – 04 P) 2016.

VILNIAUS UNIVERSITETAS

VAIDOTAS STANKEVIČIUS

Mikroaplinkos įtakos vėžinių ląstelių atsakui į jonizuojančiąją spinduliuotę transkriptominis tyrimas

Daktaro disertacija
Fiziniai mokslai, biochemija (04 P)

Vilnius, 2016

Daktaro disertacija rengta 2011-2015 m. Vilniaus universiteto Gamtos mokslų fakultete bei Nacionaliniame vėžio institute ir ginama eksternu.

Mokslinis vadovas

Prof. dr. **Kęstutis Sužiedėlis** (Vilniaus universitetas, fiziniai mokslai, biochemija – 04 P) 2011-2015 m.

Mokslinis konsultantas

Prof. dr. **Kęstutis Sužiedėlis** (Vilniaus universitetas, fiziniai mokslai, biochemija – 04 P) 2016 m.

Contents

LIST OF ABREVIATIONS

2D – two-dimensional

3D – three-dimensional

aRNA – antisense RNA

BER - base excision repair

SBBR - single-strand DNA break repair

BME - basement membrane extract

BSA - bovine serum albumin

CAF - cancer associated fibroblasts

Cdk - cyclin dependent kinase

Cip – Calf intestine phosphatase

CRC – colorectal cancer cells

CTOS - cancer tissue originated spheroid

Cy3/Cy5 - Cyanine fluorescent dyes

DDR - DNA damage response

DLD1 - Human colon adenocarcinoma cell line

DMEM - Dulbecco's Modified Eagle Medium

DSB - double-strand break

ECM – extracellular matrix

FBS – fetal bovine serum

FD – fractionated dose

Gy – Gray; SI unit of absorbed radiation, it is equal to the absorption of one joule of radiation energy per kilogram of absorbing material

HNSCC - Head and neck squamous cell carcinoma cell line

HRR - homologous recombination repair

HT29 - Human colon adenocarcinoma cell line

IR – ionizing radiation

IRIF- ionizing radiation induced foci

KEGG - Kyoto encyclopedia of genes and genomes

LLC1 - mouse Lewis lung carcinoma cell line

lr-ECM 3D – laminin-rich extracellular matrix 3D culture

MAPK - mitogen-activated protein kinase

MCS – multicellular tumor spheroids

microT - CDS – algorithm for miRNA target prediction

miRNA – small non-coding RNA molecule

NHEJ - non-homologous end joining

Oligo(dT) - a short sequence of deoxy-thymidine nucleotides

qPCR - Reverse transcription polymerase chain reaction

ROS – reactive oxygen species

RT – radiotherapy

SD – single dose

SD10 – single dose of 10 Gy

SSB - single strand DNA breakages

INTRODUCTION

After more than 100 years since the first applications of ionizing radiation (IR) in medicine, discoveries made in the field of radiobiology have led to the development of the modern radiation therapy (Purdy 2008). This type of therapy is one of the most precise and reliable methods of treating cancer, the therapy being received by about a half of all cancer patients. To improve the effectiveness of the treatment, radiation therapy is often be combined with chemotherapy, surgery and hormone therapy based on individual characteristics of the tumour (Delaney et al. 2005).

The exposure to X-ray irradiation induces the ionization of DNA in cells which results in various forms of DNA damage (Lord and Ashworth 2012). However, although cancer cells are usually more sensitive to IR than normal cells (Barcellos-Hoff et al. 2005), ionizing radiation induces DNA damage in the surrounding normal tissue cells as well. Thus, to allow repair and recovery of radiation-induced damage in normal tissue cells, radiotherapy is administered in fractions of ~2 Gy every 24 hours, 5 days per week for up to 7 weeks (Feofanova et al. 2014). The efficiency of radiotherapy is highly dependent on a variety of molecular processes which are activated in cells in response to ionizing radiation eventually leading to decreased tumor cell sensitivity to IR. Despite the fact, that ionizing radiation is most often applied in clinical practice in the form of fractionated dose (FD) irradiation, a vast amount of the knowledge in radiobiology is accumulated during investigations of cellular responses to single dose (SD) treatment of ionizing radiation. Therefore, to better predict the outcome of radiotherapy and to develop more efficient radiotherapy strategies, a better understanding of FD radiation mediated molecular changes in cancer cells is still required.

In order to investigate the molecular networks in cancer cells after exposure to ionizing radiation it is important to choose an appropriate model system which would reflect *in vivo* processes occurring in the tumor cells as close as possible.

Traditionally, the most common cancer cell based *in vitro* assays are performed using 2D monolayer forming cell cultures, where cells are often grown on plastic substrates. However, 2D cell cultures poorly mimic biological processes occurring in tumour tissue, due to the artificial environment and standardized growing conditions (Nyga et al. 2011). 3D cell cultures retain many characteristics typical of tumour tissue *in vivo*. Cells cultured under 3D conditions demonstrate heterogeneity, different growth and division rates, as well as changes in cell morphology and gene expression (Storch ir Cordes, 2012). These features may affect cellular response to anticancer treatment and result in different outcomes in tumors/3D cell cultures compared to 2D cell cultures. Therefore, tumour cell response to IR evaluated in cells grown in 3D cell cultures could better reflect the response of tumour cells *in vivo*.

Therefore, in order to elucidate potential molecular targets for the development of more efficient radiotherapy, **the aim of this study** was to evaluate the changes in genome-wide gene and miRNA expression in tumour cells cultivated under different cellular microenvironment conditions after the exposure to a single dose or a fractionated dose irradiation.

Objectives:

1. To evaluate survival fractions of mouse Lewis lung carcinoma LLC1 cells cultivated in a monolayer forming cell culture after the exposure to a single or a fractionated dose irradiation;
2. To evaluate genome-wide gene and miRNA expression profiles of mouse Lewis lung carcinoma LLC1 cells cultivated in a monolayer forming cell culture after the exposure to a single or a fractionated dose irradiation;
3. To evaluate genome-wide gene and miRNA expression profiles of mouse Lewis lung carcinoma LLC1 cells cultivated in lr-ECM 3D cell culture compared to cells grown in a monolayer forming cell culture;

4. To evaluate genome-wide gene expression profiles of human colon carcinoma DLD1 and HT29 cells cultivated in lr-ECM 3D cell culture compared to cells grown in a monolayer forming cell culture;
5. To evaluate survival fractions of human colon carcinoma DLD1 and HT29 cells cultivated in monolayer forming or lr-ECM 3D cell culture after the exposure to a single or a fractionated dose irradiation;
6. To evaluate genome-wide gene expression profiles of human colon carcinoma DLD1 and HT29 cells cultivated in lr-ECM 3D cell culture after the exposure to a single or a fractionated dose ionizing irradiation;
7. To identify the potential molecular targets for the further development of more efficient radiotherapy.

Scientific novelty

In this study we applied genome-wide transcriptomic analysis to elucidate molecular processes of the cellular response to IR delivered as a single or a fractionated dose irradiation. Similar attempts aiming to the development of a more efficient radiotherapy strategy have already demonstrated striking differences between cells cultured *in vitro* and tumor xenografts after exposure to irradiation (Camphausen et al. 2005, Tsai et al. 2007). Therefore, in this study we for the first time utilized a syngeneic murine Lewis lung carcinoma LLC1 tumor model. Although our data confirmed the previous indications that cellular response is irradiation dose delivery type dependent, this study for the first time provided a comprehensive analysis of gene and miRNA expression profiles of LLC1 cells exposed to different irradiation regimens. In addition, our study demonstrated that the fractionated dose irradiation treatment response of LLC1 cells cultivated in monolayer cell culture does not reflect the syngeneic LLC1 tumor response to fractionated dose irradiation.

Despite the fact that cell lines of different origin were utilized, the present genome-wide transcriptomic analysis indicates that key pathways including cell adhesion, MAPK and immune response-related are most significantly altered in

an extracellular matrix (ECM) dependent manner in murine (LLC1) and human (DLD1 and HT29) carcinoma cell lines cultured in three-dimensional (3D) cell cultures compared to cells grown in 2D. In addition, our present data show that the expression of selected genes and miRNAs differentially expressed in LLC1 cells grown in lr-ECM 3D cell culture correspond the expression levels of these genes and miRNAs in a syngeneic LLC1 tumor model compared to expression levels in cells grown in 2D.

Furthermore, our study for the first time indicated that treatment with a fractionated dose irradiation resulted in the upregulated expression of prosurvival cell cycle/DNA damage or immune response pathway genes in an ECM-dependent manner in human colon carcinoma DLD1 and HT29 cells, respectively.

Together our novel observations not only indicate the existence of common extracellular matrix dependent regulatory networks in tumor cells but also provide the insights for the development of more efficient targeted radiotherapy.

Defense statements

1. Lewis lung carcinoma LLC1 and human colon carcinoma DLD1 and HT29 cell response to irradiation is dose delivery type dependent;
2. Cellular response to fractionated dose irradiation in a monolayer forming LLC1 cell culture does not reflect the syngeneic LLC1 tumor response to fractionated dose irradiation;
3. Common ECM-dependent regulatory networks exist in mouse (LLC1) and human (DLD1, HT29) cancer cells;
4. Cellular response to fractionated dose irradiation in human colon carcinoma DLD1 and HT29 cells is ECM-dependent.

LITERATURE REVIEW

1.1 Radiotherapy. Mechanism of action

Ionizing radiation (IR) can be considered as a sub-group of electromagnetic radiation, as it consists of only x-rays (wavelength 0.01-10 nm) and γ radiation (wavelength <10 pm) and a stream of elementary particles, which are able to ionize atoms and molecules (Baskar et al. 2012). The sources of these types of radiation are different: x-rays are created by accelerating and stopping electrons in a linear accelerator, when high-energy photons are produced; γ radiation comes from the decay of radioactive isotope nuclei. The stream of elementary particles, also called corpuscular radiation, consists of electrons, protons, alpha particles, neutrons, negatively charged mesons and ions. In clinical anticancer radiotherapy, x-rays are most widely used. The effectiveness of radiotherapy is based on the mechanism of action of IR (Morgan and Sowa 2005). When the molecules of the cell are exposed to IR, it can have a direct or an indirect effect (**Fig. 1.1**). The direct effect of IR arises from the interactions

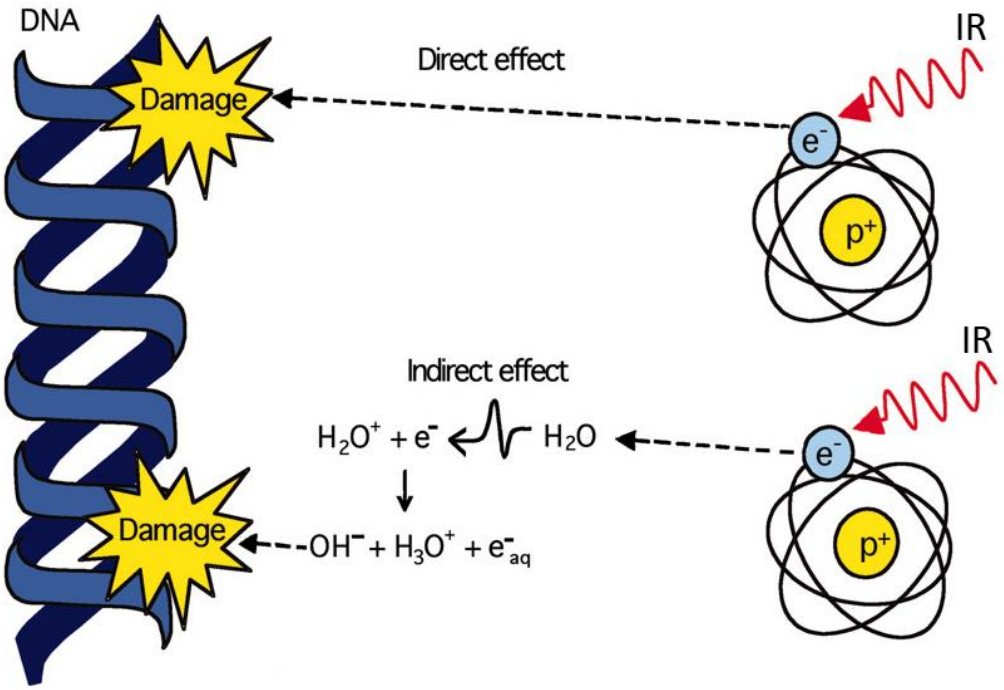

Figure 1.1 Radiation-induced direct and indirect effect on DNA damage (Morgan and Sowa 2005).

between high energy photons and various molecules inside the cell. The probability of damage depends on the size of the molecules and their concentration in the cell (Jackson and Bartek 2009). Therefore, DNA molecules are excellent targets for IR, which can induce various alterations in the nucleotide chain.

The mechanism of the indirect effect of IR arises from the interactions of high-energy photons and the water molecules inside and around the cell. The ionization of water produces active hydroxyl radicals which start a chain reaction, producing various other reactive oxygen species (ROS) (Morgan and Sowa 2005). ROS act on various biologically active molecules, including DNA. It has been shown, that about two thirds of the DNA damage induced by IR can be attributed to indirect effects (Barcellos-Hoff et al. 2005). In addition, it has been suggested, that the formation of ROS has an effect on the induced changes in the cellular microenvironment, which can promote cancerogenesis or alter the cellular response to other anticancer treatments (Najafi et al. 2014). To overcome disruption of normal cellular function caused by IR, special damage protection mechanisms are activated in irradiated cells (Feofanova et al. 2014, Nikjoo et al. 2016).

IR can also cause complex aggregations of DNA damage, where DNA breaks are a few bases apart from each other. Complex DNR damage together with double-stranded DNA breaks are considered to be the most complex forms of DNA damage in the cell (Singleton et al. 2002). Therefore IR may damage genomic integrity and induce various gene mutations. Mutations in genes associated with cellular survival, tumor suppressors and proto-oncogenes, can affect the proliferation of cancer cells, the further development of the tumor and cellular radioresistance (Lord and Ashworth 2012, Tian et al. 2015). Therefore, research focused on the molecular mechanisms involved in cellular response to IR has yielded substantial knowledge about the processes of IR response: DNA damage recognition and repair, cell cycle regulation and cell death.

1.2 Cellular response to ionizing radiation

As mentioned previously, the DNA of cancer cells is the main target of IR therapy. Ionizing radiation causes nucleotide base damage, single and double chain breakages, which in eukaryotic cells activate the mechanism of DNA damage response (DDR) (Tian et al. 2015). DDR is a complex signaling pathway that helps the cell keep its genetic integrity. During the cellular response to IR a lot of DDR genes are activated, which are involved in DNA damage recognition and repair, cell cycle regulation and cell death (Ciccia and Elledge 2010). It has been shown, that a lot of DDR genes also activate RNA metabolism regulating spliceosome assembly, RNA splicing and polyadenylation of mRNA. All of these processes help keep genetic information intact (Zlotorynski 2015).

The whole DNA damage response system can be divided into three groups (**Fig. 1.2**) (Ciccia and Elledge 2010): 1) sensors that recognize DNA damage and initiate DNA damage response; 2) transducer proteins, that strengthen and transmit the signal from the sensors; 3) effectors, that initiate DNA damage

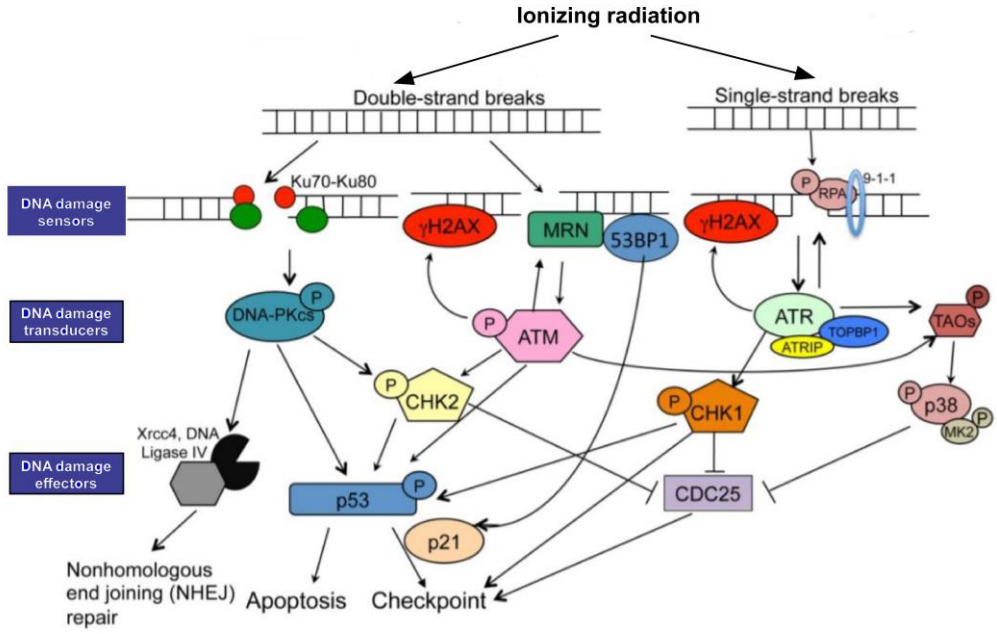

Figure 1.2. Schematic representation of DDR signaling pathways. DNA-PK responds to DNA double-strand breaks (DSB) and regulates nonhomologous end joining (NHEJ). ATM responds to DNA DSB; phosphorylates H2AX, which is localized to sites of DNA damage. ATR is activated in response to SSB. Arrows show the flow of the corresponding DDR pathways (E and Kowalik 2014)

repair, activate temporary or continuous cell cycle arrest or activate processes leading to cell death.

There are three known kinases, belonging to the PI3-like kinase family, that participate in DNA damage recognition and further signaling – ATR (*ataxia telangiectasia and Rad3-related*), ATM (*ataxia telangiectasia-mutated*) and DNA-PK (*DNA-dependent protein kinase*). The activation of these kinases in the cell depends on the type of DNA damage. ATR kinase is activated by single strand DNA breaks, double strand DNA breaks with sticky ends or DNA fractures, due to fallacies during DNA replication (Fokas et al. 2014), while ATM and DNA-PK kinase complexes are activated in the presence of double strand DNA breakages (Santivasi and Xia 2014, Xiaofei and Kowalik 2014).

1.3 DNA damage recognition

In eukaryotic cells most of the proteins, involved in DNA damage response, are present in the cell throughout the whole cell cycle, but when the response is „turned on“, a fast activation of DNA repair factors is observed. The amount of these factors in the cell is usually constant, but during DDR activation they accumulate in DSB site, forming Ionizing Radiation Induced Foci (IRIF) (Lisby and Rothstein 2009).

One of the earliest events during IRIF formation (**Fig. 1.3**) is histone H2A type H2AX ser-139 phosphorylation, resulting in γ-H2AX (Kinner et al. 2008). It has been suggested, that H2AX phosphorylation ensures DNA repair protein complex assembly at the site of double strand breakage and stabilizes protein interactions in the IRIF complex (Dickey et al. 2009). Right after DSB formation MRN (Mre11-Rad50-Nbs1) protein complex recognizes DSB and, interacting trough Nbs1 with ATM, pulls it towards DSB. This causes ATM dimmer autophosphorylation and dissociation of inactive ATM dimers to active monomers, which further phosphorylate H2AX (Bonner et al., 2008). Then

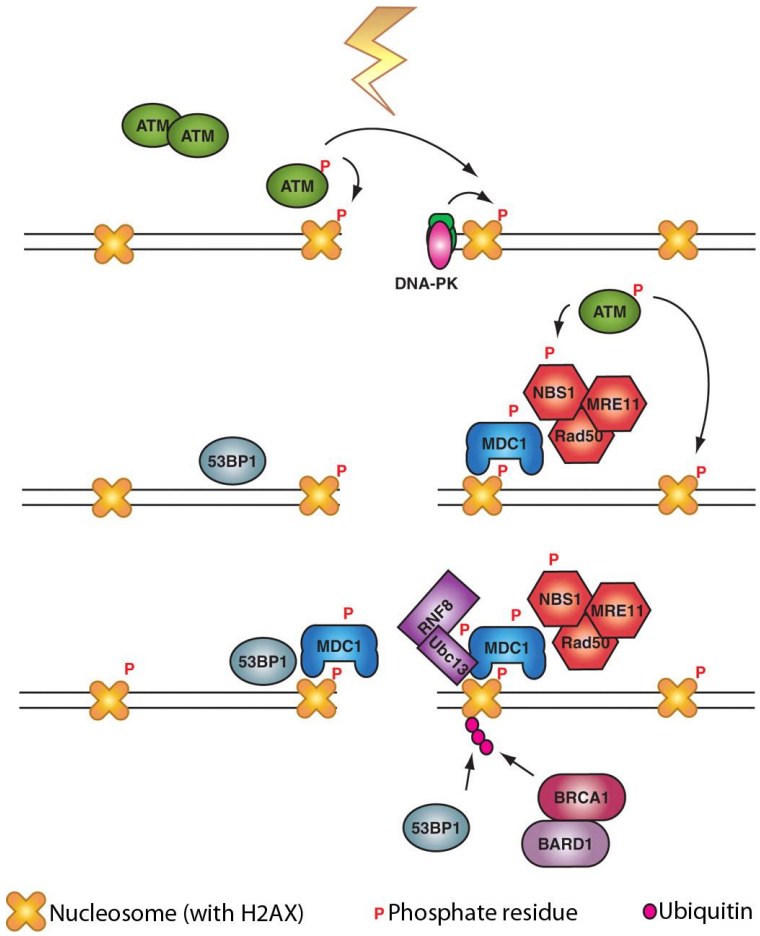

Figure 1.3. The formation of IRIF. After the initial phosphorylation of H2AX by ATM, or DNA-PK, MDC1 is recruited and attracts MRN complex to further activate ATM. This leads to further phosphorylation of H2AX and the chromatin modifications required for the recruitment of 53BP1. The activation cascade ends up with the recruitment of RNF8 to phosphorylated MDC1 and the polyubiquitination of H2AX to recruit BRCA1/BARD1 (Kinner et al. 2008).

γ-H2AX is recognized by MDC1 (mediator of DNA damage checkpoint), which interacts with MRN complex (Grabarz et al. 2012). MRN complex recruits more ATM molecules which induce the further spread of γ-H2AX signal bidirectionally around the DNA break site. Also, MDC1 attracts E3 ubiquitin ligases to the site, namely RNF8 and RNF168, which start ubiquitination of histones H2A and H2AX at the DSB site. Likely, this histone modification affects conformational changes in chromatin and the accumulation of repair protein 53BP1 and complex BRCA1-BARD1 at the DSB site (Kinner et al. 2008, Grabarz et al. 2012).

1.4 DNA damage repair

Single strand and double strand breaks in the cell are repaired by different mechanisms. Single strand breaks are repaired by base excision repair/single-strand break repair mechanism (BER/SBBR). During this process damaged bases or damaged nucleotides firstly are removed from the DNA chain, and afterwards, using the undamaged DNA strand as a template, new DNA is synthesized (Lord and Ashworth 2012). The recognition and removal of the damaged base is performed by glycosylase enzymes, forming apurinic/apyrimidinic (AP) sites. After that enzymes AP endonuclease (APE) and/or Polynucleotide kinase (PNK) depending on the damage type, modifies the structure of AP and prepares it for the incorporation of complementary nucleotide by polymerase using the undamaged strand as a matrix. There are several sub-variants of the BER mechanism, using different polymerases, including DNA polymerase β (Pol β) and proliferating cell nuclear antigen (PCNA) PCNA-Pol δ and PCNA-Pol ε complexes. Then DNA ligase facilitates the joining of DNA strands together. It is suggested, that other proteins, e.g. XRCC1 and PARP1 participate in the recognition of SSB and the activation of other repair proteins (Begg et al. 2011). Unrepaired or faultily repaired single strand breaks can result in the formation of double strand breaks after the replication of the damaged DNA strand (Begg et al. 2011).

Homologous recombination (HR) (**Fig. 1.4A**) – is a very precise DSB repair mechanism (Jasin and Rothstein 2013). HR is initiated by the MRN complex which binds to the loose ends of the break and induces the processing of DNA ends by CtIP and RECQ family helicases and Exo1 and Dna2 nucleases in order to create single stranded DNA overhangs. Then the main HR enzyme is activated — recombinase Rad51. Together with supporting proteins Rad52, Rad54, BRCA1, BRCA2 and other Rad51 paralogs (Rad51C, XRCC2, XRCC3) it recognizes the complementary DNA sequence in a homologous chromosome and forms a D-loop. In this way the homologous sequence is used as a matrix for DNA polymerase Pol δ to synthesize the damaged strand. The repair process is

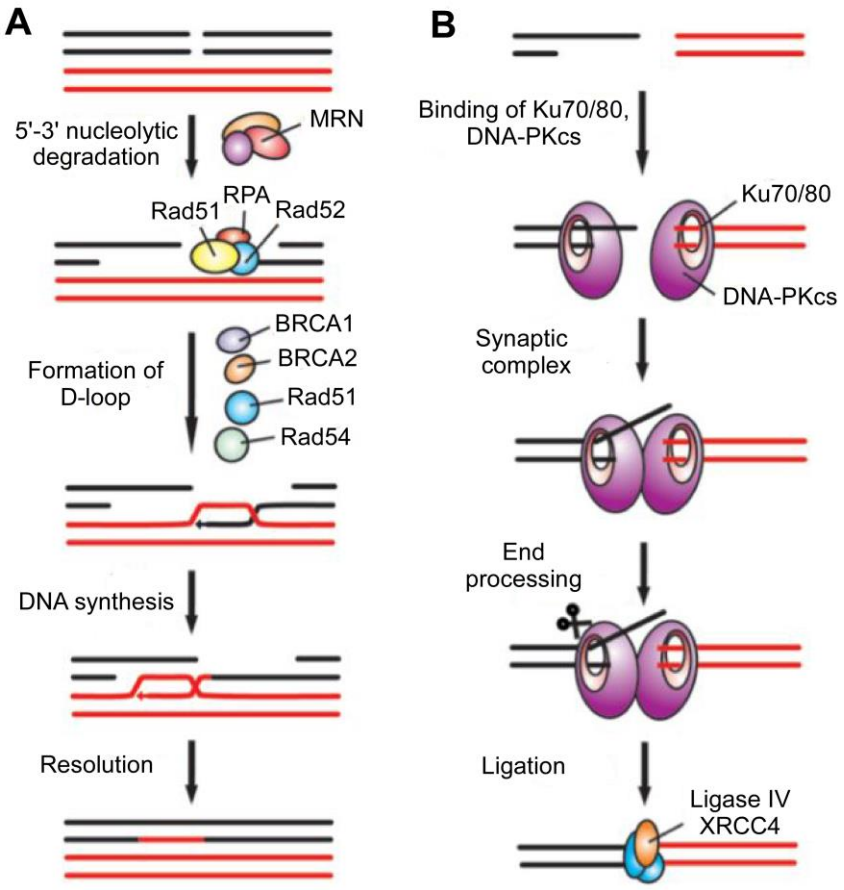

Figure 1.4 Simplified overview of A) homologous recombination (HR) repair and B) non-homologous end-joining (NHEJ) repair (Weterings and Chen 2008).

finalized by DNA ligase I that facilitate the joining of the synthesized DNA ends together (Lord and Ashworth 2012).

During NHEJ (**Fig. 1.4B**) repair DNA double strand break ends are ligated together directly. The main proteins active in this process are Ku70/Ku80 heterodimers, which quickly binds to the DSB ends and activate protein kinase DNA-PKcs. DNA-PKcs pulls the break ends together, and then specific DNA end processing enzymes process the DNA break ends by synthesizing or removing a few nucleotides. Thus the DNA break ends are prepared for ligation and finally they are joint by XRCC4-DNA ligase IV complex (Weterings and Chen 2008). This process does not require matrix DNA, therefore NHEJ can be performed at any point during the cell cycle (Couedel et al. 2004).

NHEJ repair is error-prone process leading to the formation of DNA deletions or insertions (Lieber 2010). Since the HR repair requires a homologous

DNA sequence, repair by this process is only possible when the double strand DNA break is formed after DNA replication: at late S or G2 phase. It has been noted, that HR is also used to repair DNA damage that forms during replication (Couedel et al. 2004).

1.5 Cell cycle regulation

During cell division, DNA damage might facilitate the loss of genetic material or the formation and accumulation of new mutations, hence daughter cells can inherit genetic changes caused by DNA damage or even die. To ensure genetic integrity cells have developed very strict cell cycle control mechanisms that make sure the cell cycle is stopped in the case of DNA damage (Jackson and Bartek 2009). This protective function in the cell is performed by DNA damage checkpoints. They make sure, that the cell cycle is halted when DNA damage is present and the DNA damage is not transferred to the daughter cells (Curtin 2012) (**Fig. 1.5**).

The transit from one cell cycle phase to another is regulated by three main protein categories, which are closely related: 1) cyclins – low molecular mass proteins, whose concentration in the cell fluctuates during the whole cycle; 2) cyclin-dependent kinases (Cdk), that interacting with cyclins are activated and promote cell cycle progression; 3) various cell cycle modulators, that regulate cyclin-dependent kinase activity under stress conditions. Single and double strand breaks, formed due to exposure to IR, initiate the activation of ATR and ATM kinases – the main cell cycle checkpoint regulators. These kinases halt the cell cycle by inhibiting cyclin and cyclin-dependent kinase complex formation or Cdk activity (Brown and Baltimore 2003). Sustainable cell cycle progression control in response to DNA damage is performed by three main cell cycle checkpoints:

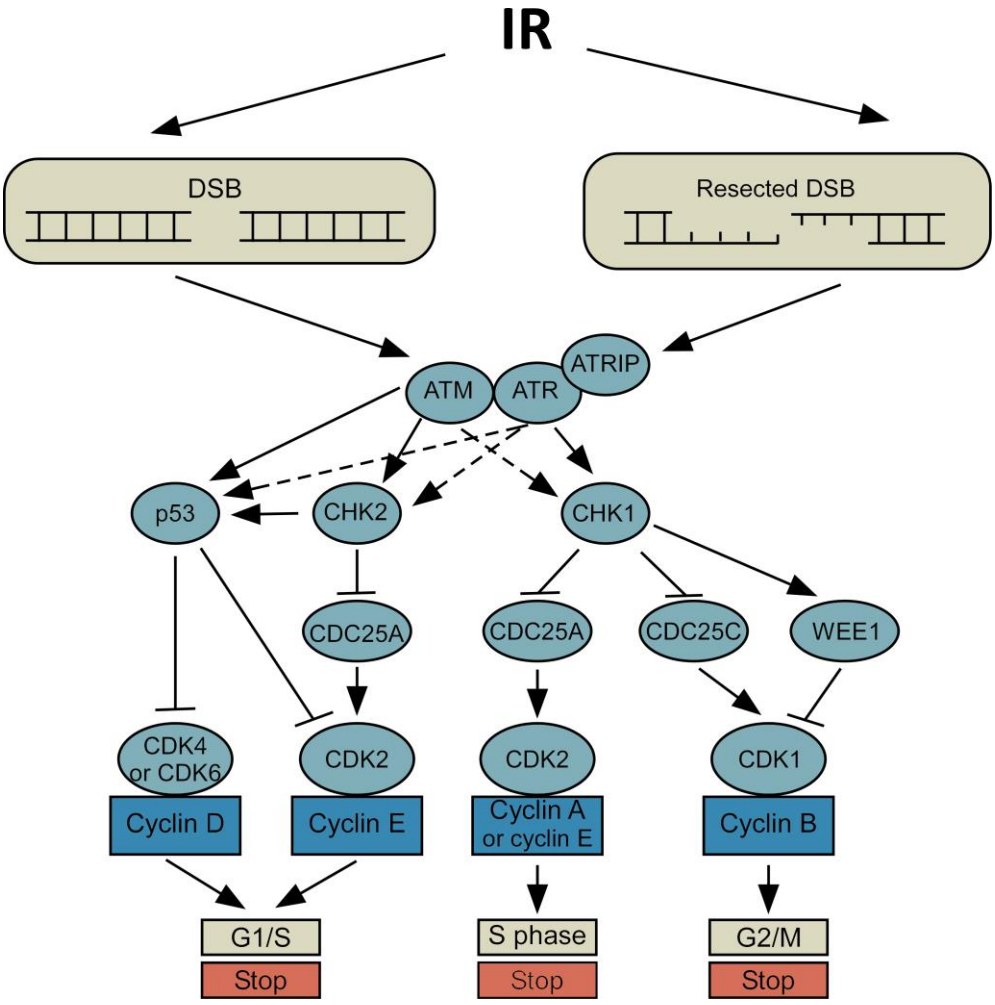

Figure 1.5. Schematic overview of radiation-induced activation of cell cycle checkpoints. ATM activated by DSBs triggers the G1 checkpoint by phosphorylating CHK2 and P53. ATR is activated by SSBs, which are formed at stalled replication forks or resected DSBs. This triggers the intra S phase and the G2 checkpoints via phosphorylation of CHK1, which in turn phosphorylates WEE1 kinase and CDC25 phosphatases to inhibit cell cycle progression through the coordinate suppression of cyclin-dependent kinase (CDK) activity. Arrows indicate secondary targets (Curtin 2012).

1) G1/S checkpoint;

2) S phase checkpoint;

3) G2/M checkpoint.

A fourth cell cycle checkpoint is functions in M phase, although it has been shown, that it does not protect from DNA damage transmission to daughter cells (Zhao et al. 2012, Spoerri et al. 2015).

When DNA damage is induced during the G1 phase of the cell cycle, G1/S checkpoint protects from the initiation of damaged DNA replication and inhibits

CyclinD/Cdk4/6 and CyclinE/Cdk2 complexes that promote the transition to S phase. Active CyclinD/CDK4/6 and CyclinE/CDK2 complexes phosphorylate pRb proteins, thus breaking pRB/E2F interaction and activating E2F family transcription factors, which promote the expression of many proteins, necessary for cell cycle continuation (Dyson 1998). Two G1/S checkpoint activation mechanisms were identified. During the first pathway ATM or CHK2 kinases phosphorylate and activate tumor suppressor P53 – a transcription factor, regulating the expression of genes involved in cell death, senescence or cell cycle control (Surget et al. 2013). One of the main P53 targets is the CDK inhibitor p21 that inactivates cyclinD/Cdk4/6 and cyclinE/Cdk2 complexes, thus preventing the transition to S phase. This mechanism of cell cycle control is relatively inert, but in the case of complex DNA damage it ensures long term DNA damage control during the G1 phase. During the second pathway CHEK2 phosphorylates CDC25A phosphatase. Phosphorylated Cdc25A is further polyubiquitinated and degraded, the inhibiting phosphate group cannot be removed from Cdk2 kinase, thus cyclinE/Cdk2 complex cannot be formed. This pathway results in a rapid cell cycle halt in the G1 phase (Deckbar et al. 2011).

S phase checkpoint ensures the inhibition of damaged DNA replication. During replication, disrupted due to DNA damage, ATR kinase is activated and phosphorylates CHK1 kinase. This kinase further phosphorylates Cdc25A phosphatase, thus Cdk2 kinase is not dephosphorylated and cannot interact with CyclinE. This inhibits the replication of damaged DNA (Krempler et al. 2007).

When DNA damage is induced in the G2 phase, G2/M checkpoint initiates inhibition of CyclinB/Cdk1 complex that promotes cell cycle transition to the M phase (Deckbar et al. 2011). The activity of the CyclinB1/Cdk1 complex is regulated by Cdc25C phosphatase and kinases Wee1 and Myt1. When DNA damage is present, ATM and ATR kinases activate Chk2 and Chk1 kinases that further phosphorylate Cdc25C and promote its transport from the nucleus. Chk1 and Chk2 kinases also activate kinases Wee1 and Myt1, which further phosphorylate Cdk1 kinase. Phosphorylated Cdk1 remains inactive in the nucleus

and does not form a complex with cyclin B. Thus the cell cycle is stopped and does not transit to mitosis (Sarcar et al. 2011).

The cell cycle at the checkpoint is halted, until DNA damage is repaired, or mechanisms of cell death are initiated (Eriksson and Stigbrand 2010)

Cell senescence is a process, when the cell, due to accumulated DNA damage, „gets stuck“ in either G1 or G2 phase (Campisi and d'Adda di Fagagna 2007). These cells keep up their metabolic activity, but stop proliferation. One of the main cell senescence biomarkers is an increased expression of senescence-associated β-galactosidase (SA-β-galactosidase). It has been suggested, that senescence in the cell is initiated by P53-P21 and P16-Rb pathways, which is activated by IR induced DNA damage (Campisi 2013). Cancer cells, which exhibit the senescence phenotype, secrete various cell survival stimulating factors to the extracellular medium and also cytokines and chemokines, that stimulate the proliferation of nearby cells, tumor angiogenesis or inhibit the immune response to cancer cells (Eriksson and Stigbrand 2010, Rodier and Campisi 2011). It has also been demonstrated, that senescent cancer cells, after IR induced DNA damage repair, can return to the active proliferation (Gewirtz et al. 2008). Therefore, cancer cell senescence can be considered as one of mechanisms of cancer renewal after radiotherapy.

1.6 Cell death

The main goals of anticancer therapy are the inhibition of cancer cell proliferation and the initiation of cell death. Ionizing radiation can activate a few different cell death mechanisms in cancer cells: apoptosis, necrosis, autophagy dependent cell death or mitotic catastrophe (Minafra and Bravatà 2014). Cell death starts not right after exposure to IR, the process usually takes about 3-4 cell divisions to begin (West and Barnett 2011). The amount of time between the exposure to IR and cell death and the exact mechanism of cell death depends on radiation type and dose, the nature of the cells, cell cycle phase, the ability of the

DNA repair system to correct double strand DNA breaks and various gene mutations, related to resistance to IR. (Eriksson and Stigbrand 2010).

Apoptosis – programmed cell death – is characterized by cell shrinkage, membrane wrinkling and DNA fragmentation (Czabotar et al. 2014). It can be activated by internal or external mechanisms, where the main role is played by the cysteine-aspartic family peptidases - caspases. The intrinsic apoptotic pathway is initiated by the formation of active apoptosome complex. When cell death signaling is present, cytochrome c (CytC) relocates from the mitochondria to cytosol and together with apoptotic protease activating factor 1 (Apaf1) and procaspase-9 forms an apoptosome, which turns inactive procaspase-9 into apoptosis initiating caspase-9 (Casp9). The extrinsic apoptosis pathway is induced trough transmembrane death receptors, belonging to the TNF receptor superfamily, when they are activated by ligands, such as FASL. The cytosolic fragments of the active receptor attract FAS-associated death domain protein (FADD), which attracts initiator procaspase-8 and stimulates pro-Casp8 autoactivation. Then both internal and external apoptosis pathway initiator caspases Casp8 and Casp9 activate effector caspases Casp3, Casp6 and Casp7, that carry out further substrate breakdown and DNA fragmentation (Minafra and Bravatà 2014).

Mitotic catastrophe is one of the main forms of IR induced cell death. It has been noted, that during mitotic catastrophe cells die in a way very similar to the internal apoptosis pathway, and hence this type of cell death is often considered as a separate type of apoptosis (Castedo et al. 2004). One of the main reasons for mitotic catastrophe in cancer cells are defects in the cell cycle checkpoints (Eriksson and Stigbrand 2010). It has been demonstrated, that G2/M checkpoint does not halt the cell cycle progression through the M phase, if cells have less than 10-20 double strand DNA breaks (Deckbar et al. 2011). G1/S checkpoint regulation is often disrupted in cancer cells due to the mutations in the P53 gene. Therefore, the cell cycle progression to mitosis may become impaired in cells with unrepaired DNA damage (Eriksson and Stigbrand 2010). Due to the

formation of chromosome damage, cell division proceeds asymmetrically – the genetic material in the daughter cells is unevenly distributed (Lara-Gonzalez et al. 2012). After the first uneven cell division tetraploid cells with double nuclei forms (Castedo and Kroemer 2004). These cells can immediately initiate apoptotic or necrotic cell death pathways or continue the cycle into G1 phase. Following few uneven divisions aneuploidy, polyploidy or modified nucleus morphology forms and cell death mechanisms are activated (Eriksson and Stigbrand 2010).

During necrosis the function of mitochondria is disrupted, plasma membrane deteriorates and cell contents leak into the extracellular space, but differently from apoptosis, no DNA fragmentation is observed (Nagata et al. 2010). Cancer cell necrosis is most often initiated by large radiation doses, which induce an inflammatory reaction in the surrounding tissue (Minafra and Bravatà 2014).

Autophagy is a process, during which certain components of the cell are disassembled by autolysosomes. Autophagy in cells is initiated when various stress signals are present, for example the lack of nutrition, hypoxia or damage to cellular components (Eskelinen 2008). During autophagy cellular components are encapsulated by double membrane autophagosomes that later on merge with lysosomes, forming autolysosomes, and degeneration products can be reused in other catabolic processes of the cell. When a strong stress signal is present, autophagy dependent cell death is the consequence of high (above the survival threshold) turnover rate of proteins and organeles (Wirth et al. 2013). Apart from DNA damage in the cells IR initiated oxidative stress can cause damage to the membranes of mitochondria, structural changes in various proteins and endoplasmic reticulum stress. It has been demonstrated, that these factors can participate in autophagy cell death (Fulda et al. 2010). Despite that, molecular mechanisms of IR induced autophagy remains unknown. It has been demonstrated, that autophagosome formation depends on delivered IR dose. In addition, it has been reported that the activity of autophagy after IR exposure can

be stimulated by P53 and PARP1 (Zois and Koukourakis 2009, Minafra and Bravatà 2014).

1.2.4 P53 structure and functions

Transcription factor P53 is a tumor suppressor, that ensures cell division is halted in cells that have sustained genetic damage, therefore it is considered as the guardian of the genome (Surget et al. 2013). When various cell stress signals are present, such as DNA damage, oncogene expression changes, nutritional and oxygen deficiency P53 can activate the processes of cell death and cell senescence, which promotes the removal of damaged cells (Vousden and Ryan 2009). Although when the DNA damage is not severe, P53 dependent cell cycle block, DNA damage repair and the expression of genes that regulate cellular response to oxidative stress are activated. In this way P53 supports genomic integrity and promotes cell survival (Brady and Attardi 2010).

The structure of P53 is common transcription factor like (**Fig. 1.6**) (Joerger and Fersht 2007). At the N-terminus of the protein two transcription coactivation domains are located – TAD1 and TAD2, that promote target gene transcription, by attracting chromatin modifying complexes and other transcription activating factors (Gamper and Roeder 2008). The most important domain of P53 is the region responsible for the interaction with target gene promotor. This domain is the hotspot for the accumulation of mutations. It has been noted, that the bulk of mutations, implied in the transformation of normal cells to cancer cells, accumulate in this region (Hainaut and Hollstein 2000). Tet domain is responsible for P53 tetramerisation (Brady and Attardi 2010). PRD domain, located at the N-terminus of P53 is responsible for the interaction with other proteins (Toledo and Wahl 2007), and the basic region located at the C-terminus interacts with DNA in a sequence independent manner and aids in strengthening the interaction with the target gene promoter sequence (Kruse and Gu 2009).

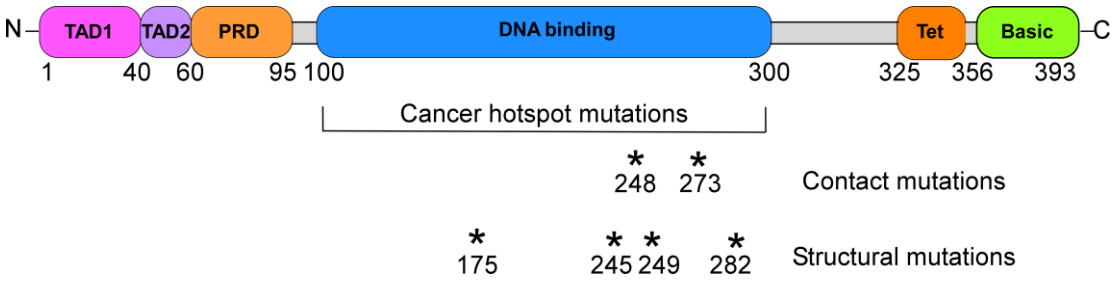

Figure 1.6. The domain organization of P53 (Brandy and Attardi, 2010).

Under normal conditions, the amount of P53 protein in the cell is regulated by stimulating constant degradation of the protein or by inhibiting the interaction of p53 with its target proteins (Helton and Chen 2007). Ubiquitin ligase mouse double-minute 2 (Mdm2) directs P53 for degradation in proteasomes by ubiquitination (Brooks and Gu 2006) or interferes with the attachment of transcription factor coactivators while interacting with P53. When a stress signal is present in the cell P53 is activated by posttranslational protein modifications. For example, DNA damage formed after the exposure to IR promotes the activation of various kinases (ATM, ATR, DNA-PK, Chk1, Chk2) which participate in DNA damage repair, that phosphorylate N-terminus amino acids in the P53 molecule (Appella and Anderson 2000). The phosphorylation of P53 N-terminus inhibits the its interaction with Mdm2, while also protecting it from degradation (el-Deiry et al. 1992). Active P53 can attach to DNA and activate the transcription of target genes or miRNAs (Huarte et al. 2010).

Transcription factor P53 is one of the most important factors in cellular response to IR induced DNA damage (**Fig. 1.7**). Depending on the amount of damage within the cell, P53 can activate different cellular response pathways. When the amount of DNA damage is not severe, P53 can promote cell survival by initiating the transcription of genes, involved in cell cycle checkpoints and DNA damage repair processes (Frantz et al. 2010). Also P53 regulates the transcription of genes, involved in the antioxidative stress response – namely sestrin 1 and 2, GPX1, TIGAR. These proteins inhibit the accumulation of ROS in the cell and support genome integrity (Liu et al. 2008). When severe DNA damage accumulates in the cell, P53 promotes cell senescence, apoptosis or

autophagy (Green and Kroemer 2009). It has been demonstrated, that IR induced DNA damage can initiate apoptosis by P53 dependent or independent pathways. P53 promotes the expression of genes, encoding for proteins in the proapoptotic family Bcl-2, such as Bax, PUMA, NOXA, APAF1 and P53AIP1, which are involved in the intrinsic apoptosis pathway (Harms et al. 2003). Extrinsic apoptosis pathway can be promoted by P53 mediated expression of death receptors (e.g.: DR5) (Kuribayashi et al. 2011). It has also been demonstrated, that P53 can promote apoptosis, by regulating cytochrome c release from mitochondria (Mihara et al. 2003).

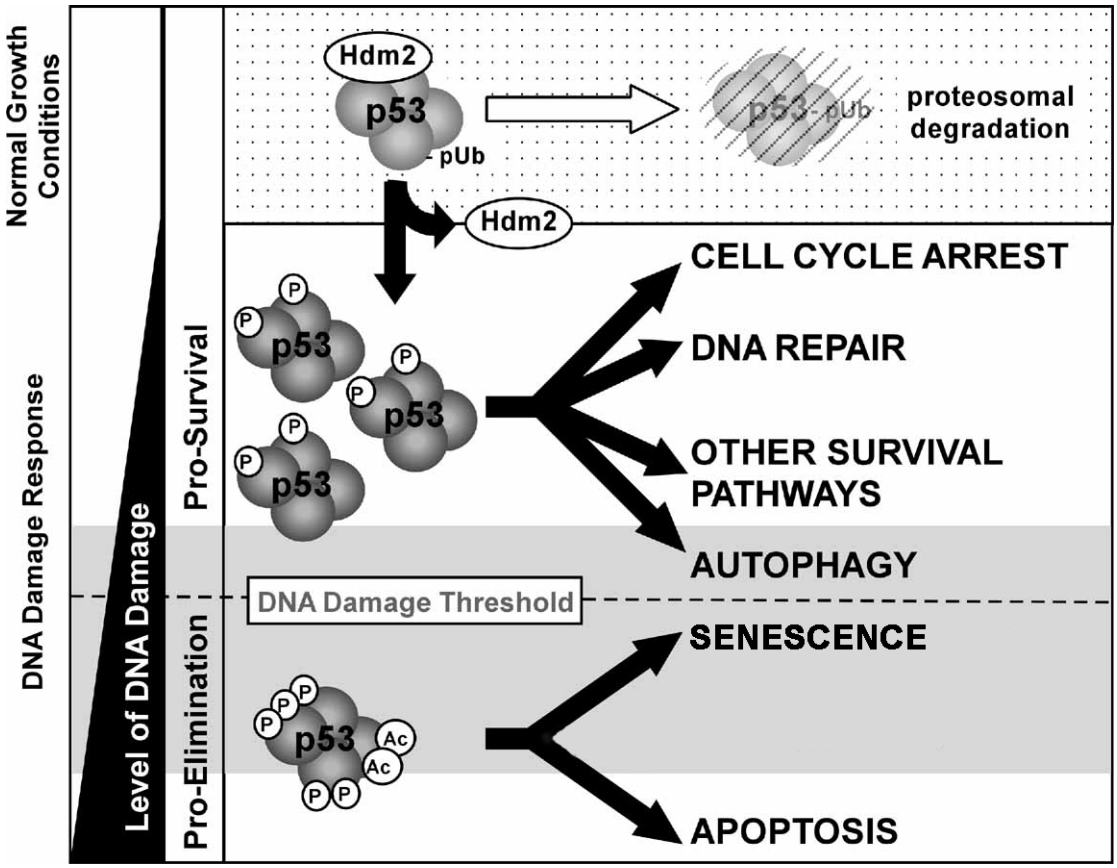

Figure 1.7. P53 modulates the radiation-induced DNA damage response. Under normal cell growth conditions P53 protein levels are kept low by ubiquitin-mediated protein degradation. Phosphorylation of P53 following DNA damage stabilizes and activates P53. If DNA damage is not severe, P53 promotes cell survival by initiating cell cycle arrest, regulating DNA repair and inducing other pro-survival pathways, including autophagy. If DNA damage is severe, P53 induce programmed cell death. Autophagy, and senescence may also utilized as alternative mechanisms to eliminate damaged cells (Heldon and Chen, 2007).

1.7 Tumor microenvironment

Seeking to uncover the molecular processes, promoting normal tissue cell transformation to cancer cells, in the recent decades the research was mainly focused on the genetic changes in the cells. The research was mainly directed towards identification of tumor development promoting or suppressing gene functions and various mutations, responsible for cancerogenesis as it was shown, that the deregulated expression of such genes could lead to the cellular transformation into cancer cells (Tredan et al. 2007). Although later on it was noticed, that during tumour development the tumor microenvironment, in which the cells proliferate, is a major factor (Hanahan and Coussens 2012). It was noted, that cancer cells on their own cannot complete transformation and form tumors, for that normal tissue cell extracellular matrix and a vascular system are necessary (Bissell et al. 2002). In the tumor microenvironment, besides the cancer cells, various other types of cells are found. These include immune cells (e.g. neutrophils, basophiles, T and B lymphocytes, dendritic cells) and various connective tissue cells (e.g. endothelial cells and their precursors – pericytes, smooth muscle cells, fibroblasts, myofibrioblasts) (Mbeunkui and Johann 2009) (**Fig. 1.8).** The interactions between cancer cells and corresponding normal cells, such as macrophages, fibroblasts, endothelial cells, promote tumor genesis and development (Lorusso and Ruegg 2008).

The components of the tumor microenvironment can be classified into three main groups: cells of hematopoietic, mesenchymal origin and non-cellular components. Tumors of different origin and at different stages differ in the composition of their components, but these three classes of components are abundant in the microenvironment of all tumors (Pattabiraman and Weinberg 2014).

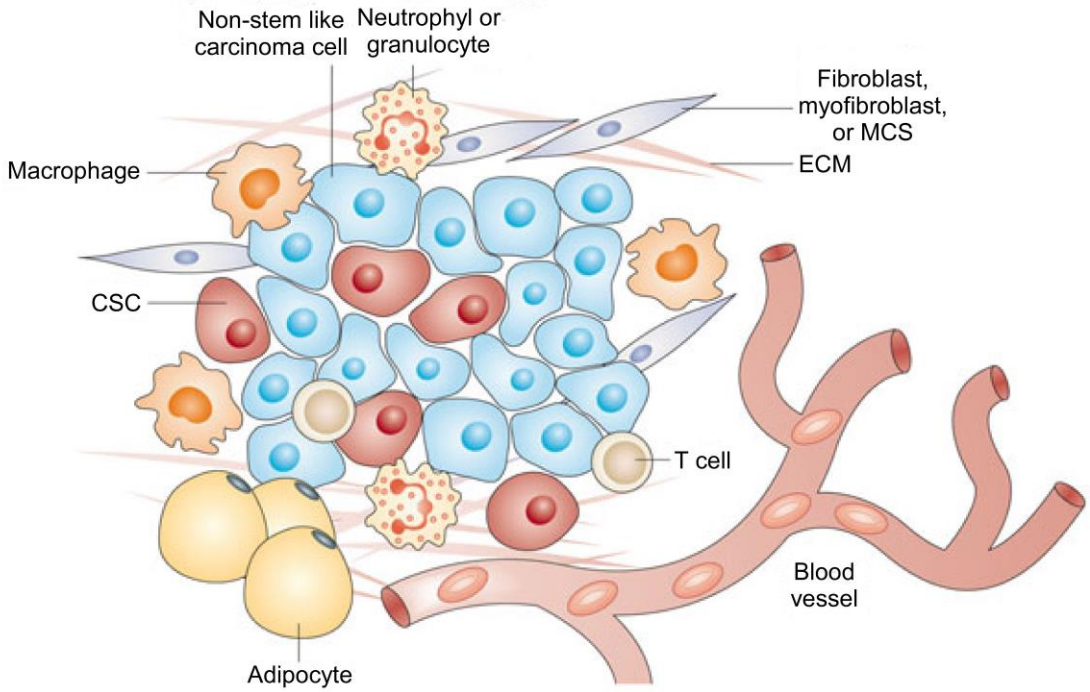

Figure 1.8. Tumor microenvironment (Pattabiraman and Weinberg, 2014).

Cells of a hematopoietic origin. Immune cells found in the tumor microenvironment are very important for tumor development and proliferation to surrounding tissue. This group of cells is formed from cells originating in bone marrow, and it can be divided into lymphoid – T, B, and K cells, and myeloid – macrophage, granulocyte and neutrophil and myeloid-derived suppressor cells (MDSC). Immune cells are supposed to identify and destroy cancer cells, but it has been noted, that antigens on the surface of cancer cells, differently from various pathogens are considered as "native" (Whiteside 2008). Therefore, the immune cells in the tumor microenvironment not only do not destroy the cancer cells, but can even promote their proliferation and further tumor development (Albini and Sporn 2007). Immune cells, while interacting with cancer cells, excrete growth factors (e.g. epidermal growth factor), chemokines (e.g. CCL2, CCL4) (Robinson and Coussens 2005) and extracellular medium degenerating ligands, hence modifying the tumor microenvironment (Coussens and Werb 2002, Pollard 2004). These factors activate tumor cell invasion into surrounding

tissue, angiogenesis and support a constant inflammatory state in the tumor microenvironment (Robinson and Coussens 2005).

Cells of a mesenchymal origin – are connective tissue cells (fibroblasts, myofibroblasts, mesenchymal stem cells MSCs), adipocytes and endothelium cells. In damaged tissue fibroblasts, reacting to paracrine signaling, differentiate into myofibroblasts (Li and Wang 2011). They are also called cancer associated fibroblasts (CAF). Myofibroblasts and their secreted factors together with stem-cell like cancer cells create niche, that stimulates tumor development and angiogenesis (Quante et al. 2011). Myofibrioblasts secrete growth factors (e.g. HGF, FGF and IGF1), which stimulate cancer cell proliferation (Spaeth et al. 2009). Until very recently it was thought, that adipocytes perform the function of energy accumulation, but recent data shows, that adipocyte secreted hepatocyte growth factor (HGF) is important during tumor development (Dirat et al. 2011). Endothelial cells and pericytes, which form blood vessel walls, play an important role in stimulating angiogenesis, and regulating cancer cell spread to the tissues of other organs (Armulik et al. 2005).

Non cellular components. For cancer cell survival, migration and invasion into other tissues, not only immune or connective tissue cells in the tumor microenvironment are important, but also the extracellular medium surrounding the tumor cells (Hanahan and Weinberg 2011). Changes in the usual cell microenvironment, which are caused by structural changes in the extracellular microenvironment, can activate the transformation of normal cells into cancer cells or stimulate cancer cell proliferation, the formation of metastases or the formation of new blood vessels in the tumor (Frantz et al. 2010). All this can be induced by changes in the composition of the extracellular matrix (Wozniak et al. 2003, Paszek et al. 2005, Levental et al. 2009), or changes in the activity of various components of the extracellular matrix or matrix metalloproteinase (MMP), which deteriorate the extracellular matrix (Lu et al. 2011). Therefore, in order to evaluate tumor development and progression and to prescribe the most effective anticancer therapy, it is important to focus not just on

the cancer cell properties, but also the tumor microenvironment should be considered.

1.8 Extracellular matrix and its composition

Extracellular matrix is a complex and dynamic macromolecular structure found in the extracellular space that regulates many cell functions and has various biophysical and biochemical properties (Ozbek et al. 2010). Even though for a long time the extracellular matrix was thought to be just an inert supplementary structure, it's importance in cell biology has been substantially recognized in the last two decades. This macromolecular structure is specific for different tissues, hence forming a niche for the cells they contain, which is vital to the supporting the biological functions of the cells. The extracellular matrix regulates the behavior of the cells – it is important for the formation of cell-cell connection, cell-cell interaction and signaling. This non cellular structure connects tissue cells into a whole, participates in tissue morphogenesis, and is responsible for tissue homeostasis.

The main components of the ECM are fibril glycoproteins (collagens and a variety of non-collagenous proteins such as fibronectin and laminin), and proteoglycans (Järveläinen et al. 2009). Collagens are the main structural elements of the ECM and often form the majority of ECM proteins. Collagen molecules closely interact with elastin, which together determine the elasticity of the tissue (Wise and Weiss 2009). Fibronectin is a protein that have collagen and glycosaminoglycan (GAG) binding sites. Through these sites, fibronectins interact with other molecules in the ECM. In addition, fibronectin also has cell surface receptor binding sites, which facilitate the cell-ECM interactions (Smith et al. 2007, Rozario and DeSimone 2010). Laminin is a part of the basal membrane and affects its formation and physiological functions (Aumailley et al. 2003). Proteoglycans are proteins, covalently linked with glycosaminoglycan molecules. They fill the space between protein fibrils in the tissue, in the form of a hydrated gel.

It is worth noting, that the structure of the extracellular matrix is not constant, it is constantly modified by MMP proteins (Mott and Werb 2004), lysine oxidases (LOX), transglutaminases and their inhibitors (Lucero and Kagan 2006). This ensures a two-way interaction between the cell and its surrounding microenvironment.

1.9 Functions of the extracellular matrix

The ECM has distinct biological, biomechanical and physical properties, which determine its importance to cell functions **(Fig. 1.9).** First of all, the ECM serves as a cell adhesion substrate. Cell adhesion to the basal lamina ensures the asymmetric division of stem cells and determines tissue polarity. Depending on the circumstances, the ECM can act as a barrier, halting cell migration or alternatively – act as a moving direction for migrating cells (Lu et al. 2012). Various fibril proteins in the ECM are also vital to ensure regular tissue structure, that determines resistance to stretching and elasticity and also ensures the functionality of the tissue (Mithieux and Weiss 2005). Proteins of the ECM, rich in polysaccharide modifications, interact with growth factors, such as bone morphogenetic protein (BMP), fibroblast growth factor (FGF), Sonic hedgehog (Sh), Wnt signal proteins (Hynes 2009) and transmit signals to cell surface receptors, hence initiating intracellular changes in the cell (Rozario and DeSimone 2010). The components of the ECM (heparan sulfate proteoglycans or hyaluronic acid receptors) also act as docking molecules - binding various growth factors and concentrating them – acting as depository of signal molecules. Such binding regulates the diffusion of these molecules and, depending on the conditions, can regulate the distribution of growth factors in cell surrounding microenvironment.

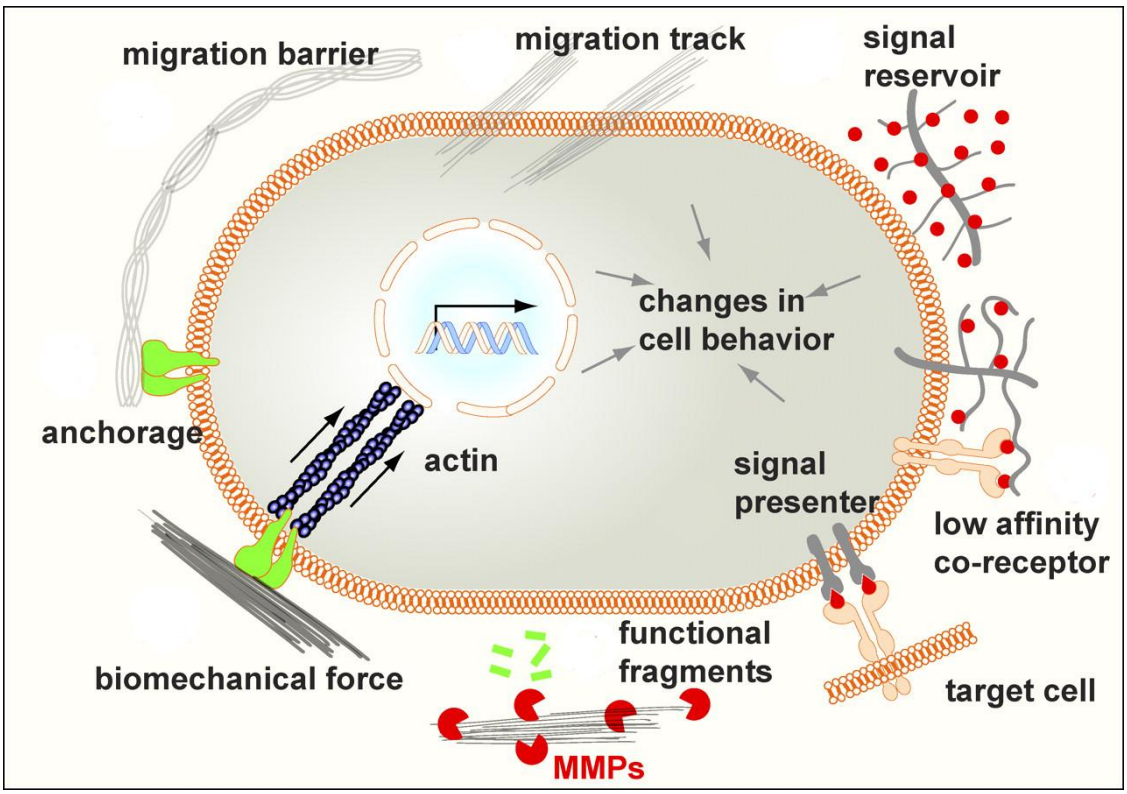

Figure 1.9. Representative ECM functions (Lu et al., 2012).

The tumor microenvironment also affects the impact of anticancer drugs and can stimulate cell migration and cancer metastasis (Gu and Mooney 2016). Structural changes in the ECM are common in the tumor microenvironment. The increased expression of ECM components and their receptors, responsible for signal transmission and a greater MMP activity can induce the transformation of the normal cells into cancer cells in that microenvironment or create better conditions for the existing cancer cells to form a tumor (Stauder et al. 1995, Kauppila et al. 1998, Butcher et al. 2009). Tumor cells must constantly be provided with nutrition, hence the changes in growth factor secretion, such as vascular endothelial growth factor (VEGF) together with ECM reorganization stimulate the migration of endothelial cells to tumor tissue and blood vessel formation, which supports both tumor development and metastasis (Quail and Joyce 2013).

1.10 Cell interactions with ECM proteins

Cells that form tissue *in vivo* are involved in various complex interactions. Cells interact with each other and form cell junctions – adherent junctions, desmosomes, tight or gap junctions. The cells also interact with the ECM and results in the formation of focal adhesions and hemidesmosomes. Cell junctions are important for tissue formation, nutrition and signal transmission. When contact with the surrounding cells is lost, cell death often occurs (Gattazzo et al. 2014).

The most important receptor proteins, involved in cell-cell interactions and cell-ECM interactions are called integrins – heterodimeric transmembrane proteins, consisting of two transmembrane polypeptides - α and β subunits (Hynes 2009, Moser et al. 2009). Both receptor subunits are formed of C-terminus intracellular and N-terminus extracellular domains (Miranti and Brugge 2002). Integrins are unique receptor proteins, distinguished by their ability to transmit the signal both ways while interacting with the ECM – "outside-in" and "inside-out" signaling (Zaidel-Bar et al. 2007).

Depending on the distribution of the subunits, integrins can be in an open or closed conformation **(Fig. 1.10)** (Moser et al. 2009, Shattil et al. 2010). Closed conformation integrins are inactive, the subunits are close together (α subunit arginine and β subunit lysine form a salt bridge). This subunit conformation blocks ECM proteins or other cell receptors from binding to it. Closed conformation integrin heterodimers are stabilized by the binding of cytoplasmic sharpin, mammary-derived growth inhibitor (MDGI), integrin cytoplasmic domain-associated ICAM-1 and filamin proteins. Sharpin and MDGI proteins interact with integrin α subunits and protect the salt bridge between integrin domains, prohibiting the subunits from moving apart and forming an open conformation. ICAM-1 and filamin interact with integrin β subunits and compete with integrin activating protein talin, which also binds to the β subunit. These inhibitors are of biological importance, because they regulate integrin activity.

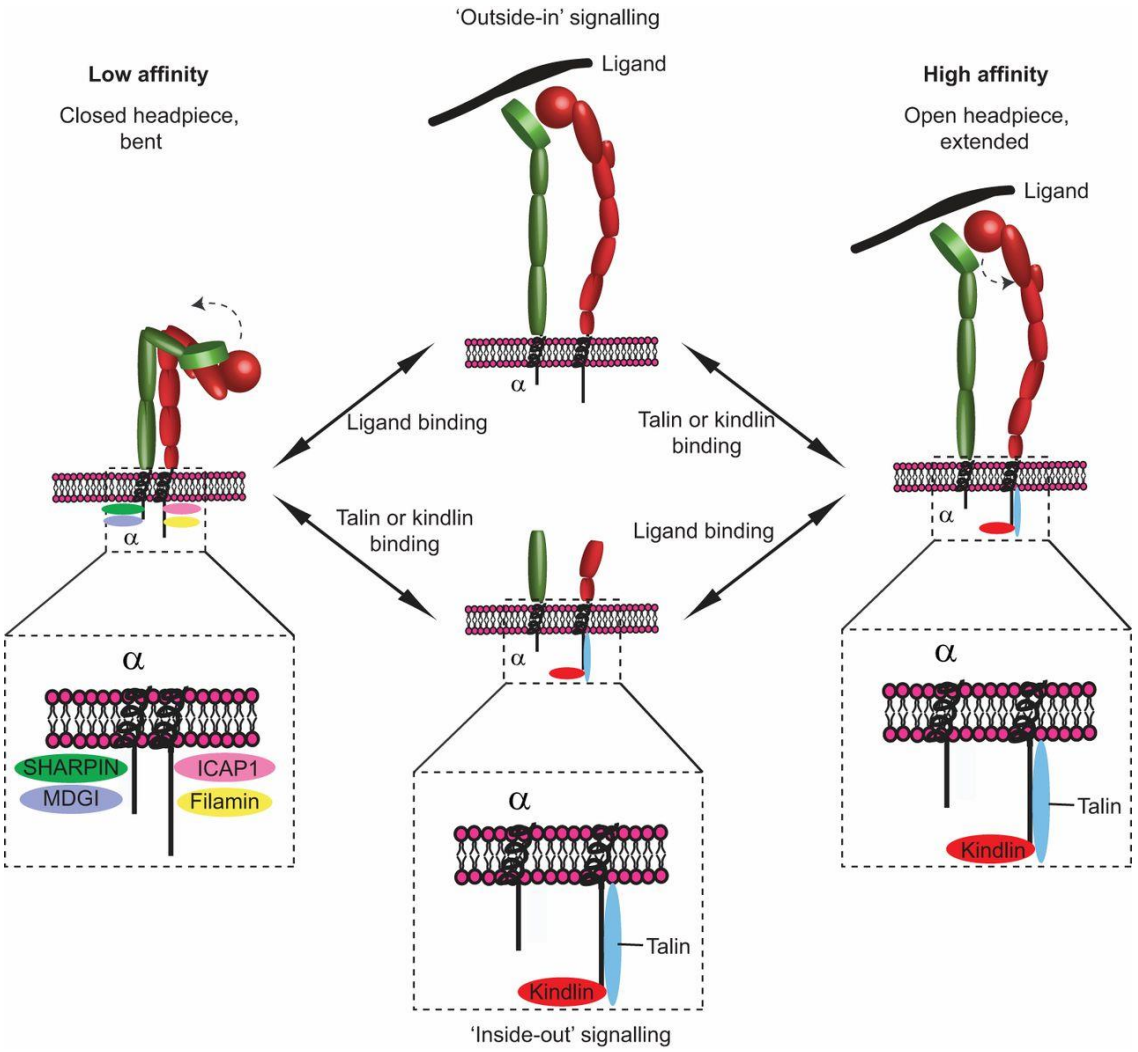

Figure 1.10 A schematic representation of integrin conformation switch. (Pouwels et al., 2012**).**

Integrins assume their active form by changing conformation – their chains straighten and move away from each other (Pouwels et al. 2012). Depending on the transmitted signal, integrins can be activated in different ways – by interacting with intracellular ligands, when the signal is transmitted to the outside, or by interacting with ECM ligands, when the signal is transmitted to the inside of the cell. Ligand binding induces conformational changes in intracellular and extracellular domains, which leads to α and β subunit separation, and then they can interact with various structural and signal proteins in the cell cytoplasm (Lau et al. 2009). In the first case, integrins are activated by the binding of the intracellular protein talin. Talin binds to the cytoplasmic β integrin site and changes the conformation of integrin (Critchley 2009). Another intracellular

protein acts together with talin – kindlin, which also binds to the integrin β subunit and coactivates integrins. When both of these proteins are bound the maximum activity of integrin is achieved (Moser et al. 2009). Talins are important not only to the support of the active integrin conformation, but also to signal transmission. Trough talin, integrins interact with various intermediate cytoskeleton proteins (vinculin, paxillin, α-actinin), which bind to actin strands or interact with signal proteins: FAK, Src, MAP kinases, other regulatory proteins (Li et al. 2005). Hence integrins mediate, together with intermediate proteins that interact with them, the transmission of signals from the ECM to the cell, that mediate cell division, gene expression changes and cell death. (Berrier and Yamada 2007).

Cell-ECM interactions are very important to various intracellular processes, responsible for normal cell function. However, it has been noted that that the interaction between cancer cells and the ECM differs from the normal cell-ECM interaction. A different signal transduction from the cell to the ECM and vice versa has also been noted (Lu et al. 2012). It was also demonstrated, that the expression of integrins that mediate the cell-ECM interactions is different in cancer cells compared to normal tissue cells (Gabarra-Niecko et al. 2003). For example, in colon cancer cells the expression of the β6 subunit is elevated, hence the cells interact more strongly with fibronectin, vitronectin and other ECM proteins (Zhu et al. 2014). Due to stronger interactions intracellular signal proteins are activated, which promote the proliferation, survival, mobility and angiogenesis of cancer cells in tumors *in vivo* (Mitra and Schlaepfer 2006).

1.11 Tumor models

The most common model system in *in vitro* research of various molecular processes is a 2D model system, where cancer cells are cultured in a monolayer. 2D *in vitro* models assume, that cancer cells grown in a monolayer resemble the morphology and response to IR of actual tumor cells (Kahn et al. 2012). However, 2D monolayer cultures do not resemble the complex microenvironment

of the tumor (Nyga et al. 2011). Cells grown in such model systems predominantly interact with the plastic surface and growth medium, enriched with concentrated nutrients resulting in only partial cell-cell interactions. While native tumor cells interact with the most of their membrane with nearby cells and the ECM and the distribution and availability of nutrition is uneven (Tibbitt and Anseth 2012). Cellular microenvironment affects the intracellular processes of cancer cells, therefore 2D cell culture do not represent all the cellular processes occurring in the tumor tissue.

Therefore, animal models are applied in cancer research. Human tumor xenografts are the most widely used in cancer research. For these models, laboratory mice (Mus musculus) are subcutaneously (or in a different tissue or organ) injected with a human cancer cell suspension, which forms a tumor in the mice (Rygaard and Povlsen 1969). Since the immune system of regular mice would reject human cancer cells, genetically modified mice with an inhibited Foxn1 gene, responsible for the normal development of the thymus, are used. These mice do not have mature or well-functioning T cells, which lessens the immune response to xenograft cells (Sausville and Burger 2006). However, the immune system plays an important role in tumor development, hence xenografts cannot accurately represent tumor formation in the human body (Chen et al. 2014). Even though mice xenografts represent the complex microenvironment of the tumor and allow the observation of cancer cell migration in the body *in vivo*, in such systems, due to complex physiological and biochemical processes, experiments are hard to control. Therefore, as an alternative to *in vivo* and 2D *in vitro* models, 3D model systems are being developed (Katt et al. 2016). This system is easily manipulated, experimental conditions are easily changed and cancer cell response can be quickly evaluated. In addition, on the contrary to 2D model systems, 3D models allow for a microenvironment representative of that of an actual tumour.

3D *in vitro* models are used in cancer research as an intermediate model between cancer cell lines and tumours *in vivo*. There are four types of 3D multi-

cell models, used in cancer research: multicellular tumor spheroids (MCS), tumorospheres, tissue-derived tumor spheres (TDTS) and organotypic tumor spheroids (CTOS). Models are characterized by their structure, properties and the presence of cancer cells (Weiswald et al. 2015).

Multicellular tumour spheroids (MCS) are a 3D model system, formed from a cancer cell culture suspension. There are several ways, used for tumour spheroid formation, but all the main methods are based on the same principle – to ensure conditions, in which cells do not form connections with the surface of the culturing dish. This facilitates cell-cell adhesion which is the reason for the forming of spherical cultures (Friedrich et al. 2009). Spheroids formed in such a 3D culture exhibit characteristics common to *in vivo* tumours – the spheroids are distinguished by cellular heterogeneity, different cell proliferation zones on the outer and inner segments of the spheroid. A different gradient of various substances has also been noted in different zones of the spheroid. Besides that, it has been noted that cells in such a molecular system start producing ECM on their own (Gong et al. 2015). Hence, in the MCS model system cells form cell-cell contacts, and contact with self-produced ECM.

To evaluate the cell-ECM interaction, the effect of the tumor microenvironment in tumorigenesis and tumor development, other 3D models are applied, which are formed using ECM protein mixture extracted form tumours *in vivo*. ECM protein mixtures contain ECM components: laminins, type IV collagens, entactins, heparan sulfate proteoglycans, and various growth factors. These components ensure most of the cell-ECM interactions, also the present signal molecules increase cell survival, proliferation, affect cell function and development (Tibbitt and Anseth 2012). In addition, to maintain 3D model systems synthetic compounds e.g. polylactide, polyglicolide and polylactide and polyglicolide co-polymers, analogous to ECM proteins can be used. These compounds are mechanically more resilient than natural ECM proteins, but the cell interaction with them is far lesser, hence their surface must be modified by binding certain functional groups (Tibbitt and Anseth 2009).

2 MATERIALS AND METHODS

2.1 Materials

All chemicals used in the present study were purchased from Carl ROTH, Sigma-Aldrich and ThermoFisher Scientific.

2.1.1 Materials for cell culture

DMEM – Dulbecco's Modified Eagle Medium, stored at 4°C (Biochrom AG, Germany);

RPMI 1640 – Roswell Park Memorial Institute cell culture medium, stored at 4°C (ThermoFisher Scientific, USA);

Antibiotics – streptomycin, penicillin – powder, stored at 4°C (Sigma-Aldrich, USA);

FBS – fetal bovine serum, stored at -20°C or 4°C (Biochrom AG);

GlutaMAX – a stabilized form of L-glutamine, 200 mM L-alanyl-L-glutamine solution, stored at room temperature (ThermoFisher Scientific);

Sodium pyruvate – 100 mM solution, stored at 4°C (ThermoFisher Scientific).

Low melting agarose – powder, stored at room temperature (Carl ROTH, Germany);

Geltrex™ – soluble form of laminin-rich extracellular matrix (lr-ECM) isolated from Engelbreth-Holm-Swarm (EHS) murine tumors (ThermoFisher Scientific);

Cell culture dishes – 25 cm^2 cell culture flasks; 6, 24 ir 96 well culture plates (Biochrom AG);

Trypsin – powder, stored at 4°C (Biochrom AG);

EDTA (Ethylenediaminetetraacetic acid) – powder, stored at room temperature (Carl ROTH).

2.1.2 Other materials

Buffer solutions: PBS – saline solution (pH 7,4) containing 137 mM NaCl, 2.7 mM KCl, 10 mM Na_2HPO_4, 1.8 mM KH_2PO_4, stored at room temperature; **DPBS -** saline solution (pH 7.4) containing 137 mM NaCl, 2.7 mM KCl, 8.1 mM Na_2HPO_4, 1.47 mM KH_2PO_4 , stored at room temperature;

Crystal violet ([4-[bis[4-(dimethylamino) phenyl] methylidene] cyclohexa-2,5-dien-1-ylidene] - dimethylazanium chloride) 0,5% solution prepared in distilled water and stored at room temperature (Carl ROTH);

Agarose gel – 1% low melting point (LMP) agarose prepared in PBS (Carl ROTH);

Triton X-100 – nonionic surfactant, stored at room temperature (Carl ROTH);

Roti-Histofix – paraformaldehyde 10 % solution, stored at room temperature (Carl ROTH);

BSA – Bovine serum albumin powder, stored at 4°C (Carl ROTH).

2.1.3 Cell cultures and experimental animals

DLD1 – Human colon adenocarcinoma cell line (ATCC® CCL221™). The base medium for this cell line is RPMI 1640 containing 10% FBS, 100 U/ml penicillin, 100 μg/ml streptomycin, 3.5 g/l glucose, 2 mM L-alanyl-L-glutamine, 2 g/l $NaHCO_3$.

HT29 – Human colon adenocarcinoma cell line (ATCC® HTB-38™). The base medium for this cell line is DMEM containing 10% FBS, 100 U/ml penicillin, 100 μg/ml streptomycin, 3.5 g/l glucose, 2 mM L-alanyl-L-glutamine, 3.7 g/l $NaHCO_3$.

LLC1 – mouse Lewis lung carcinoma cell line established from the lung of a C57BL mouse bearing a tumor resulting from an implantation of primary Lewis lung carcinoma (ATCC® CRL-1642™). The base medium for this cell line is DMEM containing 10% FBS, 100 U/ml penicillin, 100 μg/ml streptomycin, 3.5 g/l glucose, 2 mM L-alanyl-L-glutamine, 3.7 g/l $NaHCO_3$.

C57BL/6 mice (Vilnius University Institute of Biochemistry, Lithuania) – 10-12 weeks male mice (19-22g) were used for experiments *in vivo*. Animals have been utilized according Lithuania Animal Protection Association recommendations.

2.2 Methods

2.2.1 Cell culture maintenance

Cells were maintained in a CO_2 incubator at 37ºC, 5% CO_2 and 95% humidity. Cell growth was observed using inverted microscope Nikon TS 100-F (Nikon, Japan).

For the 2D cell culture, cells were passaged 3 times in a week. Briefly, cell culture medium was discarded from 25 cm^2 cell culture flasks and cells were washed 3 times in 5 mL of PBS. Then cells were treated with 1 mL of 0.5% trypsin and 0.02% EDTA solution in PBS. After cell detachment, the trypsin solution was neutralized with 4 mL of fresh complete growth medium followed by gentle pipetting. Cell suspension was transferred into 15 mL tubes and centrifuged at 500xg for 5 min. The supernatant was discarded and cells were resuspended in fresh complete growth medium, counted and plated for experiments or plated in 25 cm^2 cell culture flasks for the further passage maintenance.

For the lr-ECM 3D cell culture, cells were utilized only during experiments. Briefly, cells were embedded in 0.5 mg/ml laminin rich extracellular matrix (lr-ECM; Geltrex®, ThermoFisher Scientific) solution in complete cell culture medium in a cell culture plates precoated with 1 % agarose solution in PBS to avoid cell attachment on plastic surface. If needed, cells were transferred into 15 mL tubes and centrifuged at 1000xg for 5 min. The supernatant was discarded and cells were utilized for corresponding experimental procedures.

2.2.2 Animal model maintenance

C57BL/6 mice were injected subcutaneously with Lewis lung carcinoma (LLC1) cells ($1x10^6$ cells suspended in DMEM medium) in the right groin. Animals were sacrificed, tumors excised, homogenized and resuspended in normal saline 10 days following the implantation. Experimental group of mice was injected with 0.2 ml of the obtained suspension in the right groin. Mice were housed at a constantly maintained temperature (22±1 ◦C), relative humidity (55±10%) and photoperiod (12 h light/dark cycle) in the Open Access Centre at National Cancer Institute, Lithuania. The animals were fed standard rodent chow and purified water ad libitum. Tumor volume was determined by measuring the diameter with vernier calipers and calculating the volume according to the following formula: tumor volume = L x W x H x π/6 (L is length, W is width and H is height of tumor). Tumors reached 400-600 mm^3 volume in 10 days following implantation. Then animals were irradiated. All animal procedures were performed in accordance with the guidelines established by the Lithuanian Care Committee which approved the study (No.0190)

2.2.3 Experimental design of 2D and 3D cell culture models

All experiments were performed according to the scheme shown in **Figure 2.1**. For the 2D cell culture, cells were plated in 25 cm^2 flasks. The plating density was as follows: DLD1 ir HT29 – $3x10^4$ cells per cm^2; LLC1 – $2,5x10^4$ cells per cm^2. For the lr-ECM 3D cell culture, cells were embedded in 1 mL of 0.5 mg/ml lr-ECM/complete growth medium in 24 well plates pre-coated with agarose layer. The plating density was as follows: DLD1 ir HT29 – $5x10^4$ cells per mL; LLC1 - $2,5x10^4$ cells per mL. 48 h following cell growth, the morphology of cells grown under different cell culture conditions was evaluated using inverted microscope Nikon TS 100-F (Nikon) or confocal microscope Zeiss 7Duo Live (Zeiss, Germany). Then cells were harvested for the isolation of RNA as described in section 2.2.1. Total RNA was isolated from DLD1 and HT29 cells

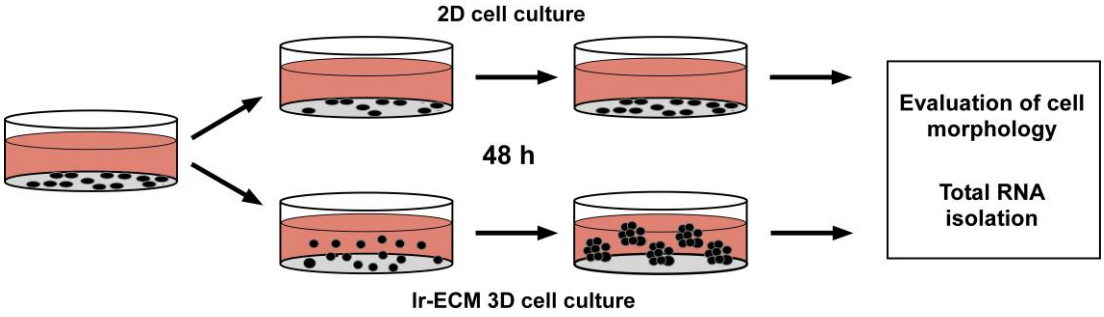

Figure 2.1. Experimental scheme of cells grown under 2D or lr-ECM 3D cell culture conditions.

as described in section 2.2.7. Total RNA enriched in small noncoding RNAs was isolated from LLC1 cells as described in section 2.2.7.

2.2.4 Irradiation scheme

Cell culture irradiation. All experiments were performed according to the scheme shown in **Figure 2.2**. Cells were irradiated with a single dose of up to 10 Gy or a fractionated dose course of 2 Gy daily for up to 5 days using Varian 6MV Clinac 600 C/D linear accelerator X-ray system at room temperature. The dose rate was approximately 3 Gy/min. To evaluate clonogenic survival, cells were plated into the cell culture dishes 24 h before irradiation. To evaluate transcriptomic profiles of cells exposed to irradiation, cells were plated into the cell culture dishes 48 h before irradiation. For the 2D cell culture, cells were seeded into 25 cm^2 cell culture flasks for RNA isolation or 6-well plates for clonogenic survival assay (500 - 10000 cells per well). For total RNA isolation, the plating density was as follows: for both cells lines (DLD1 and HT29) – $3x10^4$ or 0.4 $x10^4$ cells per cm^2 for SD or FD irradiation regimen, respectively. For the isolation of total RNA enriched in miRNAs, LLC1 cells were seeded at the density of $2.5x10^4$ or 0.35 $x10^4$ cells per cm^2 for SD or FD irradiation regimen, respectively. For the 3D cell culture, cells were embedded into 0.5 mg/ml lr-ECM solution in complete growth medium in 24-well cell culture plates for RNA isolation (5 $x10^4$ and 1 $x10^4$ cells per well for SD or FD, respectively) or in a 96-well plate for clonogenic survival (500-1000 cells per well). 24 – 48 h after cell growth, cells were exposed to SD or FD irradiation. Clonogenic survival was

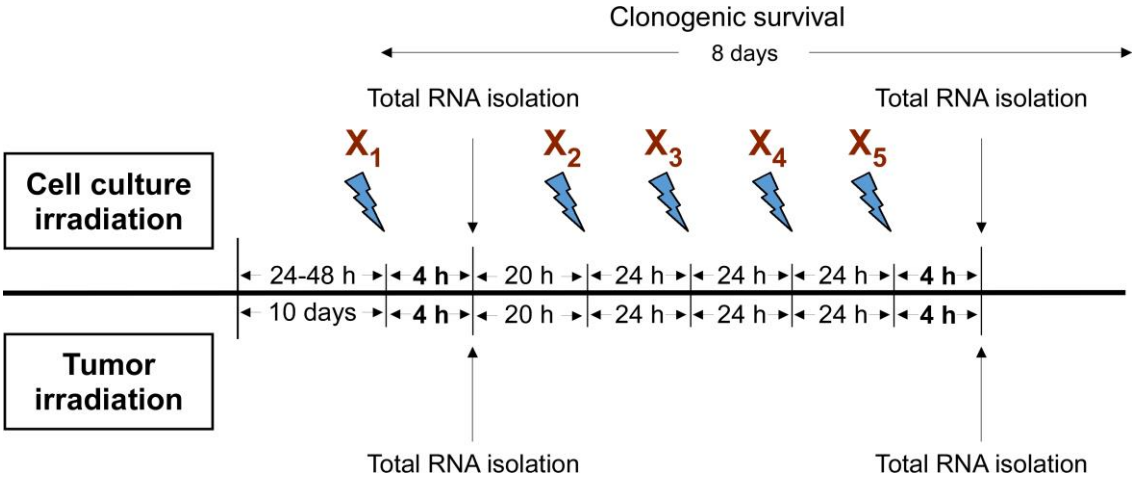

Figure 2.2. Irradiation scheme. LLC1, DLD1 and HT29 cells grown in 2D and lr-ECM 3D cell culture or LLC1 tumors were exposed to a single dose of up to 10 Gy or a fractionated dose course of 2 Gy daily up to five days. X_1 represents treatment with single dose or the first dosage of 2 Gy of fractionated dose irradiation. X_2 - X_5 represent the corresponding fractions of fractionated dose treatment.

evaluated counting colonies formed following 8 days after the start of irradiation. RNA was isolated at 4 h following treatment with SD or FD irradiation. In all experiments the same experimental design and separate controls of non-irradiated cells were used for SD or FD regimens.

Tumor irradiation. All experiments were performed according to the scheme shown in **Figure 2.2**. Briefly, before irradiation, animals were tied in a customized harness that allowed the groin to be exposed to irradiation, whereas the rest of the body was shielded by lead. LLC1 tumors were exposed to a single dose of 2 and 10 Gy or a fractionated dose course of 2 Gy daily for up to 5 days using Varian 6MV Clinac 600 C/D linear accelerator X-ray system (Varian, Palo Alto, CA, USA) at room temperature. The dose rate was approximately 3 Gy/min. 4 h following treatment with SD or FD irradiation animals were sacrificed, tumors excised and utilized to isolate total RNA. Over all of the experiments separate controls were used for SD or FD regimens.

2.2.5 Clonogenic survival assay

For the 2D cell culture, a single cell suspension was plated in 6 well plates at the range of 500-10000 cells per well accordingly to a dose of irradiation. 24 h

after, cells were exposed to a single dose of up to 10 Gy or a fractionated dose course of 2 Gy daily up to 5 days. Immediately after the exposure to irradiation, cell culture medium was removed and cells were washed twice by 1 mL of PBS. Then 2 ml of fresh cell culture medium was added and plates were placed in an incubator (37ºC, 5% CO_2). 8 days after the start of irradiation, cells were washed by 1 mL of PBS and fixed by 1 mL of 50% methanol for 10 min. Methanol was removed and plates were left to dry. Then cells were stained with 1 mL 0,5% crystal violet solution for 30 min. Colonies (>50 cells per colony) were counted and clonogenic survival was evaluated as described previously (Buch et al. 2012).

For the 3D cell culture, a single cell suspension was embedded in 200 µL of 0.5 mg/ml lr-ECM solution in complete growth medium in 96 well plates precouted with 1% agarose gel layer at the range of 500-1000 cells per well accordingly to a dose of irradiation. 24 h after, cells were exposed to a single dose of up to 10 Gy or a fractionated dose course of 2 Gy daily up to 5 days. Immediately after the exposure to irradiation, a half cell culture medium was removed and cells were washed twice by 100 µL of fresh cell culture medium. Plates were placed in an incubator (37ºC, 5% CO_2). 8 days after the start of irradiation, formed colonies were counted and clonogenic survival was evaluated as described previously (Eke et al. 2012).

2.2.6 Fluorescence microscopy

Cells plated on glass cover were washed twice with PBS and fixed with 4% paraformaldehyde (PFA) (diluted in PBS). Fixed cells were washed 3 times for 5 min. with PBS. Cell permeabilization was performed with ice-cold 0.1% Triton X-100 in PBS for 10 min. Staining was accomplished with Alexa®633 Phalloidin (ThermoFisher Scientific) in PBS containing 1% BSA for 30 min and 5 µg/ml Dapi (Sigma-Aldrich) in PBS for 3 min at room temperature. All staining steps were followed by 3 wash steps in PBS for 5 min at room temperature. Finally, slides were mounted with Roti®-MountFluorCare mounting media (Carl ROTH). Images were obtained using Zeiss LSM 7 Duo Live confocal microscope

(Zeiss) and 40x/1.3 immersion objective and excitation wavelengths of 405 nm and 633 nm.

2.2.7 RNA and miRNA extraction

Total RNA isolation. Approximately a total of 1 x 10^6 cells were harvested and total RNA was isolated using GeneJET RNA Purification Kit (ThermoFisher Scientific) according to the manufacturer‘s instructions. Before lysis, cells were harvested as described in section 2.2.1. Briefly, pelleted cells were lysed in 600 µl of Lysis buffer. 360 µl of 96% EtOH was added and each sample was mixed well by pipetting. Each 700 µL of lysates was transferred into the GeneJET RNA Purification Column and centrifuged at 12000×g for 1 min. Total RNA purification columns were washed according to manufacturer’s instructions and transferred into a sterile 1.5 mL RNase-free microcentrifuge tube. For the elution of total RNA, 50 µL of nuclease-free water was added and samples were centrifuged for 1 min at 12000×g. Collected total RNA was stored at –70°C.

Isolation of total RNA enriched in miRNAs. Approximately a total of 1 x 10^6 cells of 100 mg cells from tumor *in vivo* were harvested and total RNA enriched with small noncoding RNAs was isolated using mirVana RNA isolation kit (ThermoFisher Scientific) according to the manufacturer’s instructions. Pelleted cells were lysed in 600 µl of Lysis buffer. 60 µl of Lysis buffer additive was added to lysate. Each sample was resuspended well by pipetting and incubated on ice for 10 min. Then 600 µl of Acid-Phenol:Chloroform was added. To separate the aqueous and organic phases, all samples were vortexed for 40 s following centrifugation at 12000×g for 5 min at room temperature. The aqueous phase was mixed with 750 µl of 96% EtOH in a fresh nuclease-free tube. Each sample mixture was transferred into the Filter Cartridges then centrifuged at 12000×g for 15 s. Filter Cartridges containing total RNA were washed according to manufacturer’s instructions and transferred to a fresh nuclease-free tube. Total RNA enriched in miRNAs was eluted with 50µl of pre-heated (95°C) nuclease-

free H_2O following centrifugation for 30 s at 12000×g. Collected RNA stored at –70°C.

The quantity and purity of total RNA was determined using spectrophotometer Nanodrop 2000 (Thermo Scientific) and Agilent 2100 bioanalyzer (Agilent Technologies, USA).

2.2.8 Analysis of total RNA by capillary electrophoresis

Capillary electrophoresis was performed using a RNA 6000 Nano Kit (Agilent Technologies) in Agilent 2100 bioanalyzer (Agilent Technologies) according to manufacturer‘s instructions. Briefly**,** 550 µl of Agilent RNA 6000 Nano gel matrix were centrifuged at 1500×g for 10 min in a spin filter cartridge. Then 65 µL of filtered gel was mixed with 1 µL of the RNA dye concentrate. The mixture was vortexed well and spun down at 13000×g for 10 min at room temperature. To denaturate the secondary structures of RNA which can modify RNA mobility during electrophoresis, RNA samples were heated at 70°C for 2 min. and cooled down in ice bath. The RNA chip was prepared as follows: corresponding chip wells were primed with 9 µl of the gel-RNA dye mixture. Sample wells were filled with 5 µl of RNA marker and 1 µl of RNA. Then 1 µl of Agilent RNA 6000 Ladder was added to a corresponding well and the RNA chip was vortexed at 2400 rpm for 1 min. Capillary electrophoresis was performed using Agilent 2100 bioanalyzer (Agilent Technologies). The data obtained were analyzed using Agilent 2100 Expert ver. B.02.08 (Agilent Technologies) software. In order to evaluate integrity and quality of RNA, RIN (RNA integrity number) was calculated. RIN values of all RNA samples which were further utilized for microarray hybridization were >9.5.

2.2.9 Genome-wide gene expression analysis

2.2.9.1 Antisense mRNA synthesis

MessageAmpTM II aRNA Amplification Kit (Ambion) was used for aRNA synthesis according to manufacturer’s instructions.

First strand cDNA synthesis. Briefly, each 20 µl of the FS RT reaction mix in the FS buffer contained 1 µg of total RNA, 1 µl of T7-Oligo(dT) primer; 4 µl of dNTP mix; 1 µl of RNase inhibitor and 1 µl of ArrayScript reverse transcriptase. The first strand cDNA synthesis was performed at 42°C for 2 hours following short centrifugation (~5 sec) to collect the contents at the bottom of the tubes. Then the samples were placed on ice and the synthesis of second strand cDNA was proceeded immediately.

Second strand cDNA synthesis. Briefly, each 100 µl of SS reaction mix in SS buffer contained 20 µl of FS cDNA; 4 µl of dNTP mix; 2 µl of DNA polymerase and 1 µl of RNase H. SS cDNA synthesis was performed at 16°C for 2 h. Double-stranded cDNA were purified immediately after incubation.

dsDNA purification. 250 µL of cDNA Binding Buffer was added to each sample and mixed thoroughly by pipetting. The cDNA sample/cDNA Binding Buffer was pipetted onto the center of the cDNA Filter Cartridge and centrifuged at 10,000×g for 1 min. cDNA Filter Cartridges were washed according to manufacturer's instructions and transferred into a sterile 1.5 mL RNase-free microcentrifuge tube. cDNA was eluted with 18 µL of preheated Nuclease-free Water (55°C) at 10,000×g for 1 min. The synthesis of aRNA was proceeded immediately.

***In vitro* transcription.** Each 40 µl of aRNA synthesis reaction mix in the IVT reaction buffer contained 16 µl of cDNA, 4 µl of ATP, 4 µl of CTP, 4 µl of GTP, 4 µl of UTP and 4 µl of T7 RNA polymerase. The aRNA synthesis was performed at 37°C for 8 hours. The synthesis reactions were stopped adding 60 µl of Nuclease-free H_2O to each aRNA sample. Next, samples were proceeded to the aRNA purification immediately.

Antisense RNA (aRNA) purification. Briefly**,** each of the aRNA samples was mixed with 350 µL of aRNA Binding Buffer and 250 µL of 96% ethanol. Then, each of sample mixture was transferred to the aRNA Filter Cartridge tubes and spun down at 10,000×g for 1 min. aRNA Filter Cartridges were washed according to manufacturer's instructions and transferred into a sterile 1.5 mL

RNase-free microcentrifuge tube. aRNA was eluted in 50 µL of preheated nuclease-free water (55°C) at 10,000×g for 1.5 min.

The quantity and the quality of aRNA samples were determined using spectrophotometer Nanodrop 2000 (Thermo Scientific) and Agilent 2100 bioanalyzer (Agilent Technologies). Collected aRNA stored at –70°C.

2.2.9.2 Fluorescent labeling of aRNA

aRNA was labeled with fluorescent Cy3/Cy5 dyes using Arcturus® TURBO labeling™ Cy™3/Cy™5 Kit (ThermoFisher Scientific) according to manufacturer's instructions. Briefly, each 20 µl of the reaction mix in the labeling buffer contained 2 µg of aRNR, 5 µl of Turbo Cy3 (for control samples) or 5 µl of Turbo Cy5 Reagent (for treated samples). The aRNA labeling reactions were performed at 85°C for 15 min. The excess of Cy3 and Cy5 dyes was removed by the purification according to manufacturer's instructions.

2.2.10 mRNA microarray hybridization

Each 30 µl of the fragmentation reaction mixture in the fragmentation buffer contained 825 ng of aRNR labeled with Cy3, 825 ng of aRNR labeled with Cy5 and 6 µl of 10x blocking agent. The aRNA fragmentation was at 60ºC for 30 min. The fragmentation reaction was stopped adding 30 µl of 2x GEx HI-RPM hybridization buffer (Agilent Technologies). Then samples were centrifuged at 13000×g for 1 min and kept on ice until the hybridization. The hybridization was performed in an automated HS 400™ Pro hybridization station (Tecan, Switzerland) using Agilent Mouse Whole Genome 4x44k Oligonucleotide Microarrays (Agilent Technologies) for LLC1 samples or Agilent Human Whole Genome 4x44k ver2 Microarrays (Agilent Technologies) for DLD1 and HT29 samples. Briefly, the microarrays were pre-washed with prehybridization buffer (Agilent Technologies) at 65ºC for 1 min. Each 55 µl of aRNA prepared for hybridization was pipetted into the corresponding hybridization chambers. The microarray hybridization was performed at 65ºC for 17 hours. Then microarrays

were washed with gene expression wash buffer 1 (Agilent Technologies) for 1.5 min at room temperature, gene expression wash buffer 2 (Agilent Technologies) for 1.5 min at 37ºC and dried at 30ºC for 2 min in N_2 atmosphere. After hybridization, microarrays were kept at room temperature in the dark.

The microarrays were scanned using LS Reloaded™ sanner (Tecan, Switzerland), at 6 μm resolution and were managed by Array-Pro Analyzer ver. 4.5.1.73 software (MediaCybernetics, USA). Received images were saved in 16-bit TIFF format. ImaGene™ ver. 9.0 software (BioDiscovery, USA) was used for microarray image analysis; generated data was further processed using GeneSpring GX ver. 11.0 software (Agilent Technologies). Loess normalization was performed to adjust microarray data for variation. Fold change above 1.5 (with p-value <0.05) was defined as differentially expressed between two conditions. P values were adjusted with Benjamini-Hochberg multiple testing correction.

2.2.11 Global miRNA expression analysis

2.2.11.1 Fluorescent labeling of miRNA

miRNA was labeled using miRNA Complete Labeling and Hyb Kit (Agilent technologies) according to manufacturer's instructions. Briefly, each 4 μl of CIP reaction mixtures in the CIP buffer contained 100 ng of total RNA and 0.5 μl of calf intestinal phosphatase. The reactions were incubated at 37°C for 30 minutes to dephosphorylate the samples and stopped transferring samples on ice. Next, to denaturate RNA, 2.8 μl of DMSO was mixed with each sample. Samples were incubated at 100°C for 5 minutes and immediately transferred to ice-water bath. Then the ligation reaction was started immediately. Each 11.3 μL of ligation reactions in the T4 RNA ligase buffer contained 6.8 μl of denaturated RNA, 3 μl of Cyanine 3-pCp and 0.5 μl of T4 ligase. The reaction mixtures were gently mixed by pipetting and gently spun down. Then the RNA ligation was performed at 16°C for 2 hours. After the incubation, each sample was dried completely in a vacuum concentrator (Eppendorf, Germany) at 55ºC.

2.2.11.2 miRNA microarray hybridization

The hybridization mix was prepared as follows: dried samples were resuspended in 18 µl nuclease-free water and mixed with 4.5 µl of Gene Expression Blocking Agent and 22.5 µl of 2x Hi-RPM Hybridization Buffer following the incubation at 100ºC for 5 min. Each reaction mix was cooled down in ice bath for 5 min and centrifuged for 1 min. at 12000×g. Each 35 µl of Cyt3 labelled miRNA samples was kept on ice until the hybridization. In a further step samples were hybridized to Agilent mouse miRNA 8x15K microarrays containing probes for 627 mouse miRNAs from Sanger database v.12 (Agilent Technologies) for 20 h at 55°C in a rotating hybridization oven. Then microarrays were washed in slide-staining dishes with gene expression wash buffer 1 in at room temperature for 5 min and with gene expression wash buffer 2 at 37ºC for 5 min. The microarrays were scanned immediately.

Global miRNA expression microarrays were scanned with Agilent SureScan Microarray Scanner (Agilent Technologies). Microarray images were extracted using Extraction Feature v10.7.3.1 software (Agilent Technologies). To normalize raw probe values, experimental samples were scaled to mean of control samples using GeneSpring GX v11.0 software (Agilent Technologies). miRNAs that showed expression values above fold change 2 (with P-value <0.05) were defined as differentially expressed between two conditions. P values were adjusted with Benjamini-Hochberg multiple testing correction.

2.2.12 Gene and miRNA expression analysis by RT-qPCR

2.2.12.1 cDNA synthesis

RevertAid RT Kit (ThermoFisher Scientific) was used for the cDNA synthesis according to the manufacturer's instructions.

cDNA synthesis for evaluation of the mRNA expression. Briefly, 1 µg of total RNA was added to 20 µL reverse transcription (RT) reaction volume containing 5 µM random hexamer primers, 1 µM of dNTP mix, 20 U RNase inhibitor and 20 U reverse transcriptase. Then the RT reaction mixtures were

incubated at 25 ºC for 5 min followed by cDNA synthesis at 42 ºC for 60 min. and terminated by heating at 70 ºC for 5 min. The RT reaction samples were stored at -70 °C.

cDNA synthesis for evaluation of the miRNA expression. Briefly, 0.2 µg of total RNA was added to 20 µL RT reaction volume containing 1 µM specific RT primer, 1 µM of dNTP mix, 20 U RNase inhibitor and 20 U reverse transcriptase. The mixture was incubated at 25 ºC for 20 min followed by synthesis at 37 ºC for 60 min. and terminated by heating at 70 ºC for 10 min. The reverse transcription reaction product was stored at -70 °C. The sequences of specific RT primers are shown in supplementary table 1.

2.2.12.2 RT-qPCR

Real time qPCR for evaluation of the mRNA expression. RT-qPCR was performed on MasterCycler RealPlex^4 RT-PCR system (Eppendorf) using 2x KAPA SYBR FAST qPCR Master Mix (KAPA Biosystems, USA) according to manufacturer's instructions. To validate differential expression of genes obtained from microarray data, all reactions were performed in a 10 µL reaction volume containing 5 µL 2x KAPA SYBR FAST qPCR Master Mix, 1 µL 5-fold diluted cDNA, 0.2 µL volume of 10 µM forward and reverse primer mixture and 3.8 µL nuclease-free water. The reaction conditions were as follows: pre-denaturation at 95 ºC for 3 min. followed by amplification of 40 cycles of 3s at 95 ºC and 30 s min at 60 ºC. The relative changes in gene expression were evaluated by $\Delta\Delta C_t$ method as described previously (Livak and Schmittgen 2001). For the normalization of the expression data, Hprt1 or Gapdh were used as reference genes. The sequences of primers used for the amplification are shown in supplementary table 2.

Real time qPCR for evaluation of the miRNA expression. To validate differential expression of miRNA obtained from microarray data, all reactions were performed in a 10 µL reaction volume containing 5 µL 2x KAPA SYBR FAST qPCR Master Mix, 1 µL 2-fold diluted cDNA, 0.2 µL volume of 10 µM

forward and reverse primer mixture and 3.8 μL nuclease-free water. The reaction conditions were as follows: pre-denaturation at 95 ºC for 3 min, followed by amplification of 3 cycles 15s at 95 ºC, 1 min at 55 ºC, 30 s at 60 ºC and 32 cycles 10s at 95 ºC, 30 s at 60 ºC. The relative changes in miRNA expression were evaluated by $\Delta\Delta C_t$ method. For the normalization of the expression data, SnoRNA-135 was used as a reference gene. The sequences of primers used for the amplification are shown supplementary table 3

2.2.13 Pathway enrichment analysis

The functional significance of differentially expressed genes (fold change >1.5; P<0.05) following SD and FD irradiation was evaluated using WebGestalt (WEB-based GEne SeT AnaLysis Toolkit; www.webgestalt.org) online source toolkit as described previously (Wang et al. 2013). Data sets were uploaded into WebGestalt toolkit and mapped to the functional KEGG pathway categories. P values were calculated using hypergeometric test and adjusted with Benjamini-Hochberg multiple testing corrections. Functional categories associated in at least 5 genes and P<0.05 were considered as significant. The miRNA target enrichment analysis was performed with Diana Tools (Diana.imis.athena-innovation.gr) using microT-CDS algorithm, as described previously (Vlachos et al. 2012, Paraskevopoulou et al. 2013).

2.2.14 Statistical analysis

Data were analysed using GraphPad v6.0 software (Graphpad Software, USA). Student's t test was used to compare the two groups. P<0.05 was considered as statistically significant. All experiments were independently repeated at least 3 times.

2.2.15 Open access microarray data deposition

All microarray generated data were uploaded in GEO database (www.ncbi.nlm.nih.gov/geo). GEO accession numbers for the corresponding global expression studies are:

GSE84108 - Gene expression profile of mouse Lewis lung carcinoma cell line treated with single or fractionated ionizing radiation doses;

GSE84109 - miRNA expression profile of mouse Lewis lung carcinoma cell line treated with single or fractionated ionizing radiation doses;

GSE75863 - Gene expression profile of mouse Lewis lung carcinoma cell line cultivated in 2-dimensional or 3-dimensional cell culture enriched with laminin rich extracellular matrix proteins;

GSE75862 - miRNA expression profile of mouse Lewis lung carcinoma LLC1 cell line cultivated in 2-dimensional or 3-dimensional cell culture enriched with laminin rich extracellular matrix proteins;

GSE75551 - Gene expression profile of two colorectal cancer HT29 and DLD-1 cell lines cultivated in 2-dimensional or 3-dimensional cell culture enriched with laminin rich extracellular matrix proteins;

GSE75915 - Gene expression profile of two colorectal cancer HT29 and DLD-1 cell lines treated with single or fractionated ionizing radiation doses under 3D cell culture conditions.

3 RESULTS

3.1 Gene and miRNA expression profiles of mouse Lewis lung carcinoma LLC1 cells following single or fractionated dose irradiation

There is an emerging body of knowledge on the comprehensive molecular mechanisms involved in the cellular response to FD irradiation as well as the mechanisms associated with resistance to RT. Previous reports have shown that treatment with multiple fractions of irradiation had a different gene expression signature in several cancer cell lines when compared to the exposure to SD irradiation (Tsai et al. 2007, John-Aryankalayil et al. 2010). For instance, exposure to 10 Gy delivered as fractionated irradiation resulted in more robust changes in differential gene expression in prostate cancer PC3 and DU145 cells (Simone et al. 2013). In addition, as demonstrated by the gene expression profiles, exposure to FD irradiation also induced a significantly different miRNA expression profile compared to cells exposed to SD (John-Aryankalayil et al. 2012, Palayoor et al. 2014). miRNAs play an important role in the regulation of the expression of genes involved in cellular response to radiation-induced DNA damage (Zhao et al. 2013). Previous studies have also reported that the modulation of miRNA expression levels in cancer cells can alter their sensitivity to irradiation (Weidhaas et al. 2007, BALÇA-SILVA et al. 2012, Gong et al. 2015). Therefore, the integration of gene and miRNA signatures of radiosensitivity could lead to a more reliable strategy for predicting radiation-induced cellular response. Furthermore, the interference of radiation-specific miRNAs could be implemented in direct antitumor effects and improve the response of tumor cells to RT.

Several previous studies using the gene expression microarray approach indicated a different set of genes in several human cancer cell xenografts after exposure to irradiation compared to cells irradiated *in vitro* suggesting that tumor microenvironment might influence the outcome of irradiation (Camphausen et al. 2005, Tsai et al. 2007) . LLC1 cell line was established from the lung of a C57BL

mouse bearing a tumor of primary Lewis lung carcinoma. This cell line is highly tumorigenic and the implanted cells are immunologically compatible with the murine immune system, unlike the widely used human cancer xenograft models. Consequently, it is primarily used as syngeneic animal model to evaluate efficacy of anticancer treatment *in vivo* (Pawlik et al. 2009). Therefore, in order to integrate miRNA and mRNA expression profiles of cancer cells exposed to IR to improve the development of more efficient radiotherapy, in this study we analysed genome-wide gene and miRNA expression changes in LLC1 cells exposed to single dose of 2 Gy or 10 Gy and fractionated dose of 5x2 Gy irradiation using a syngeneic animal model. All experiments were performed according to experimental design described in Methods section 2.2.4.

3.1.1 Clonogenic survival

Clonogenic survival analysis was performed as described in Methods section 2.2.5. The results showed that LLC1 cells were more sensitive to exposure to single dose (SD) irradiation compared to treatment with fractionated dose (FD) irradiation. The surviving fractions of LLC1 cells following 2-10 Gy single dose irradiation were 0,622 ± 0,041 – 0,0011 ± 0,00051. LLC1 cell survival decreased to 0,1981 ± 0,0465 following fractionated dose (FD) irradiation up to 5x2 Gy. Survival data of LLC1 cells exposed to IR is depicted in supplementary table 4.

3.1.2 Genome-wide mRNA expression changes

Genome wide mRNA expression analysis was performed as described in Methods section 2.2.9. The microarray data analysis revealed that a total of 2294 genes were differentially expressed (fold change > 1.5; $P < 0.05$) in LLC1 cells 4h following treatment of single dose (of 2 Gy (SD2) or 10 Gy (SD10)) or fractionated dose of 5x2 Gy (FD) irradiation compared to untreated cells (**Fig. 3.1**). The amount of differentially altered genes was irradiation dose

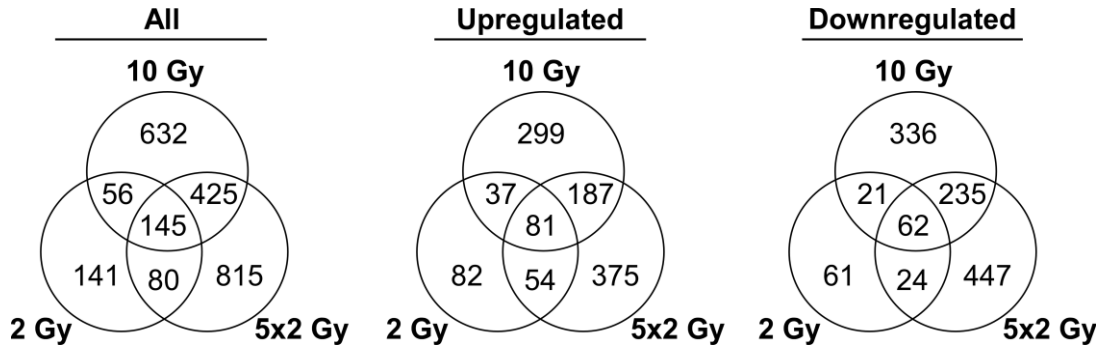

Figure 3.1 Venn diagrams. Venn diagrams showing the number of genes (fold change is at least 1.5 and p<0.05) differently expressed in LLC1 cells after SD (2 Gy and 10 Gy) and FD (5x2 Gy) irradiation.

delivery dependent. The exposure of LLC1 cells to 2 Gy SD resulted in differential expression of 422 genes. By contrast, the expression of 1258 and 1465 genes was significantly altered after the exposure to SD10 and FD irradiation, respectively. The ratio of upregulated and downregulated genes was similar following all irradiation regimens. The microarray data analysis also revealed that 145 differently expressed genes were common between all irradiation regimens.

3.1.3 KEGG pathway enrichment analysis

In order to elucidate which pathways were significantly affected by irradiation treatment, genes found to be differentially expressed (fold change > 1.5; P < 0.05) in LLC1 cells following SD or FD irradiation protocols were grouped into functional KEGG pathway categories as described in Methods section 2.2.13 (**Table 3.1**). The KEGG pathway enrichment analysis revealed that the cell cycle and P53 signaling pathway categories were the most significantly altered following all irradiation regimens, and P53 related DNA replication and apoptosis categories were also significantly altered after SD10 and FD irradiation regimens. Genes associated with "Pathways in Cancer" were most significantly enriched among all KEGG categories following SD10 and FD irradiation. Furthermore, after exposure to SD10 or FD the second most significantly altered functional categories were related to DNA repair (Mismatch repair, Nucleotide excision repair, Base excision repair) and Immune response (Cytokine-cytokine

receptor interaction, Hepatitis C, Chemokine, B cell receptor, Jak-STAT and Toll-like receptor signaling pathways). The pathway enrichment data in **Table 3.1** also revealed that irradiation of SD10 or FD significantly altered the expression of genes involved in MAPK, TGF-beta, VEGF, WNT and insulin signaling pathways.

Table 3.1. KEGG pathway enrichment categories of genes differentially expressed in LLC1 cells following SD (2Gy or 10 Gy) or FD (5x2 Gy) irradiation.

Category	**2 Gy**		**10 Gy**		**5x2 Gy**	
	Genes	p value	Genes	p value	Genes	p value
Pathways in cancer	11	0.0005	38	1.76E-16	53	3.50E-27
Cell cycle	5	0.0069	25	2.88E-16	28	3.48E-18
P53 signaling pathway	10	2.37E-09	15	2.07E-10	24	2.46E-20
MAPK signaling pathway	0	NS	20	2.73E-06	29	8.91E-11
Cytokine-cytokine receptor interaction	7	0.0066	19	2.84E-06	26	1.35E-09
DNA replication	0	NS	8	2.09E-06	10	3.89E-08
TGF-beta signaling pathway	3	NS	14	1.92E-08	14	6.72E-08
Apoptosis	6	0.0007	16	3.41E-10	17	1.40E-10
VEGF signaling pathway	0	NS	9	7.35E-05	12	8.71E-07
Hepatitis C	0	NS	16	1.63E-07	19	4.13E-09
Mismatch repair	0	NS	7	1.10E-06	8	1.20E-07
Nucleotide excision repair	0	NS	7	7.45E-05	12	1.72E-09
Wnt signaling pathway	0	NS	9	0.0076	15	1.24E-05
Chemokine signaling pathway	0	NS	15	2.07E-05	16	2.50E-05
B cell receptor signaling pathway	5	0.0022	11	1.96E-06	10	3.51E-05
Base excision repair	2	NS	8	3.42E-06	7	7.77E-05
Jak-STAT signaling pathway	6	0.0035	14	1.13E-05	14	4.64E-05
Insulin signaling pathway	4	NS	17	2.63E-08	17	1.20E-07
RIG-I-like receptor signaling pathway	0	NS	2	NS	6	0.01
Toll-like receptor signaling pathway	0	NS	7	0.008	9	0.0013
Homologous recombination	0	NS	5	0.0006	5	0.0009

Enrichment significance of KEGG gene categories was calculated by hypergeometric distribution. KEGG categories were assign as significant when associated with at least 5 genes, $p<0.05$. NS, no significance; MAPK – mitogen activated protein kinase; TGF – transforming growth factor; VEGF – vascular endothelium growth factor; Wnt – wingless-type MMTV integration site family; Jak – janus kinase; STAT – signal transducer and activator of transcription.

3.1.4 Heat map analysis

Radiation-induced changes in the expression of individual genes from P53, cell cycle, apoptosis and immune response related KEGG pathway categories, which were the most significantly altered following SD and FD irradiation regimens in LLC1 cells, were color coded to demonstrate the expression patterns of genes within each category following exposure to both SD and FD protocols (**Fig. 3.2)**. In general, the heat maps showed that the differential expression of genes peaked in cells exposed to SD10 or FD irradiation. In addition, the extent of some differentially expressed genes was different in cells irradiated with FD compared to SD.

The microarray data indicated that a total of 27 genes involved in the P53 signaling pathway were significantly altered in LLC1 cells exposed to both irradiation regimens (**Fig. 3.2A**). Exposure to radiation also induced the expression of a total of 34 genes involved in cell cycle regulation (**Fig. 3.2B**). The majority of the differentially expressed genes were down-regulated, whereas the expression of only 9 genes was up-regulated. Heat map analysis also demonstrated that 19 apoptosis related genes were differentially expressed in cells following irradiation (**Fig. 3.2C**). The expression of a total of 14 genes was up-regulated including pro-apoptotic Fas, Bad, Bid, Casp7, Trp53, Tradd, Thfrsf10b and anti-apoptotic Bcl2l1 and Cfalr genes. In addition, the expression of 5 apoptosis related genes was down-regulated in cells after exposure to irradiation. The down-regulation of genes involved in inhibition of apoptosis including Bcl2 and Xiap peaked in cells following SD10. **Fig. 3.2D** depicts a total of 77 genes related to immune response regulation that were differentially expressed in LLC1 cells following irradiation treatment. The present subset of the heat map shows that the expression of 51 genes was up-regulated and 26 genes were down-regulated. The expression of chemokines Ccl7 and Ccl9 also peaked in response to 10 Gy, whereas FD also induced the expression of Cxcl5. Both irradiation regimens also induced the expression of tumor necrosis factor related cytokines

Tnfrsf10b and Tnfrsf19 which peaked following irradiation of 10 Gy, whereas FD also significantly altered the expression of Tnfrsf9, Tnfrsf18 and Tnfrsf25.

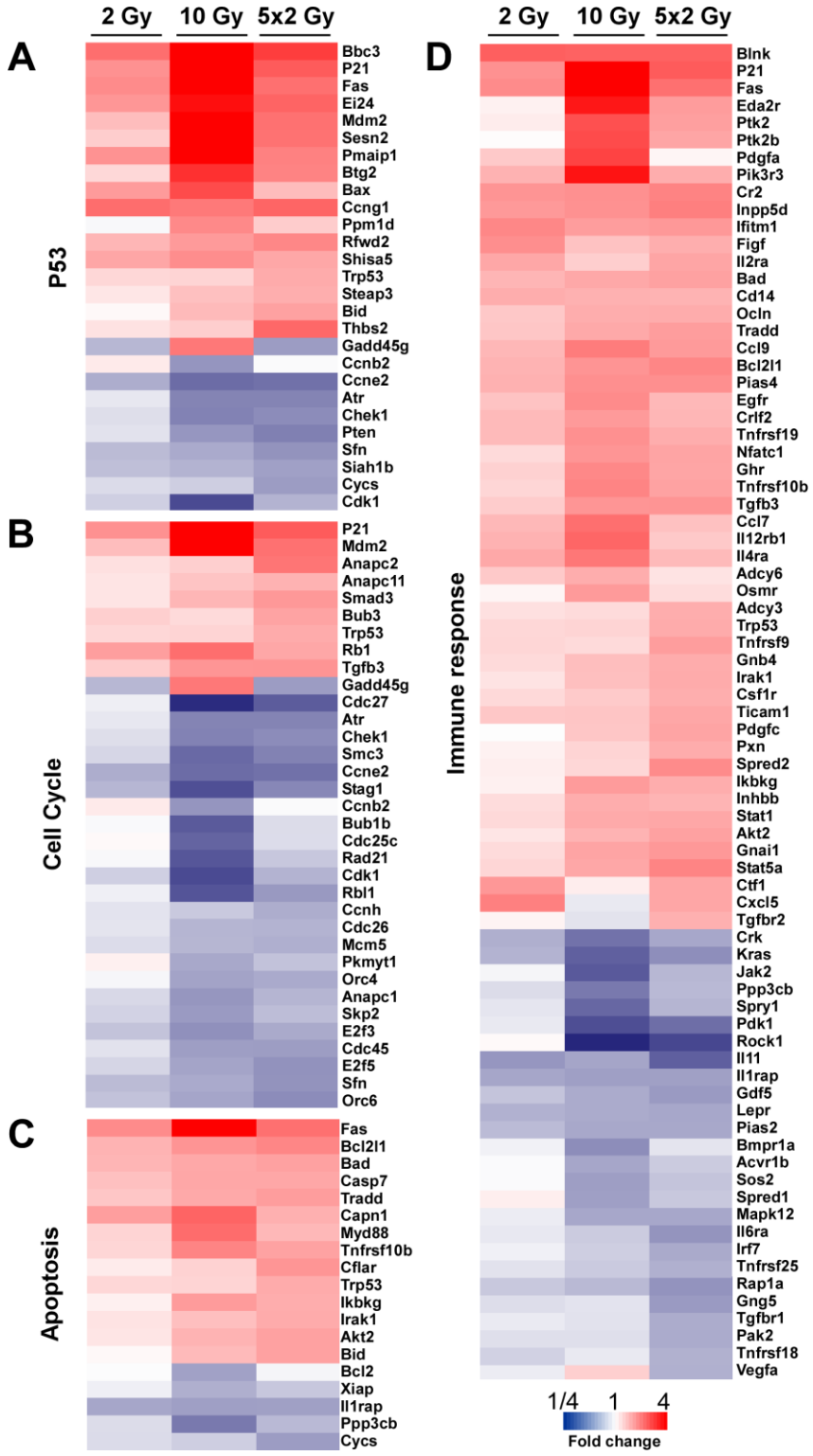

Figure 3.2 Heat maps show differentially expressed genes from (A) P53 signaling pathway; (B) Cell cycle regulation; (C) Apoptosis and (D) Immune response categories in LLC1 cells following SD (2 Gy or 10 Gy) or FD (5x2 Gy) irradiation.

The expression of cytokines including Figf, Vegfa, Pdgfc, Ctf1, Il11 was significantly altered in LLC1 cells in response to FD. Both regimens induced the expression of transcription factors Nfatc1 and Stat1 which peaked after SD10. In addition, FD also significantly induced the expression of Stat5a.

3.1.5 Global miRNA expression changes

Global miRNA expression analysis was performed as described in Methods section 2.2.11. The miRNA microarray data revealed that a total of 18 miRNAs were differentially expressed (> 2 fold, $P < 0.05$) in the LLC1 cells 4 h following all irradiation protocols compared to expression levels in untreated cells (Supplementary table 5). The expression of 2 miRNAs including miR-34c-5p and miR-145a-3p was significantly altered between all irradiation protocols, whereas miR-34c-3p and miR-34b-3p were both up-regulated in LLC1 cells following exposure to SD10 and FD. Data in supplementary table 5 also revealed that the highest number of miRNAs was differently altered in LLC1 cells after exposure to FD resulting in deregulated expression of 7 unique miRNAs. The expression of miR-186-5p, miR-145a-5p, miR-129-5p, miR-192-5p, miR-129-2-3p, miR-30c-5p was up-regulated and miR-105 was down-regulated in LLC1 cells following the FD regimen.

3.1.6 miRNA target filter analysis

In order to determine functions of the 15 miRNAs significantly altered after exposure to SD and FD radiation in the post transcriptional regulation of gene expression, we identified 6343 individual target genes potentially regulated by these miRNAs using in silico miRNA target filter analysis as described in Methods section 2.2.13. Next, we identified negative correlations between all differently expressed genes and miRNAs related to cell cycle regulation, the P53 signaling pathway, apoptosis and immune response subsets to indicate any potential miRNA-mRNA connections in these processes.

Table 3.2. Target filter analysis of differentially expressed target genes and miRNAs from cell cycle, P53, apoptosis and immune response categories showing inverse correlation in LLC1 cells exposed to irradiation of SD (10 Gy) or FD (5x2 Gy).

Category	10 Gy		5x2 Gy	
	miRNA	**Target gene**	**miRNA**	**Target gene**
Cell cycle	miR-34c-5p↑	E2f3↓; E2f5↓; Ccne2↓	miR-30c-5p↑	Ccne2↓; Stag1↓; Orc4↓; Skp2↓
			miR-34c-5p↑	Ccne2↓; E2f3↓
			miR-129-5p↑	Stag1↓; Orc4↓
			miR-145a-5p↑	Orc4↓
			miR-186-5p↑	Cdc27↓; Stag1↓
P53 signaling pathway	miR-34c-5p↑	Ccne2↓	miR-30c-5p↑	Ccne2↓
			miR-34c-5p↑	Ccne2↓
			miR-129-5p↑	Pten↓
			miR-145a-3p↓	Pmaip1↑; Sesn2↑
Apoptosis			miR-30c-5p↑	Ppp3cb↓
Immune response	miR-34b-3p↑	Spred1↓	miR-30c-5p↑	Lepr↓; Kras↓; Ppp3cb↓
	miR-34c-3p↑	Spred1↓	miR-34c-3p↑	Gng5↓
	miR-34c-5p↑	Pdk1↓	miR-34c-5p↑	Pdk1↓
	miR-136-5p↓	Eda2r↑	miR-129-5p↑	Il6ra↓; Rock1↓
	miR-145a-3p↓	Cr2↑; Inpp5d↑	miR-186-5p↑	Vegfa↓; Pias2↓
	miR-466a-5p↓	Eda2r↑; Egfr↑; Inhbb↑	miR-192-5p↑	Crk↓; Pias2↓
	miR-710↓	Stat1↑; Pik3r3↑	miR-105↓	Tgfbr2↑; Stat1↑
			miR-145a-3p↓	Tgfbr2↑; Cr2↑; Inpp5d↑; Ticam1↑

The miRNAs showing inverse correlation with differently expressed target genes involved in selected pathways are shown in the **Table 3.2**. A negative correlation was identified between differential expression of 6 miRNAs and 10 mRNAs in cell cycle, the P53 signaling pathway and apoptosis functional categories. The miRNA target analysis also revealed that 20 differentially expressed genes from the immune response category inversely correlated with the differential expression of 12 miRNAs.

3.1.7 Microarray data validation

To validate the microarray data, we selected 4 up-regulated genes and miRNAs for qRT-PCR analysis as described in Methods section 2.2.12. Our results indicated that the expression of genes involved in the P53 signaling pathway including the BTG family member Btg2, cyclin Ccng1, cyclin-dependent kinase inhibitor P21 was significantly up-regulated in LLC1 cells following

irradiation treatment compared to expression levels in untreated cells (**Fig. 3.3A**). In addition, treatment with FD induced the up-regulation of trombospondin Thbs2 (**Fig. 3.3A**). qPCR analysis also revealed that miR-34b-3p and miR-34c-5p were significantly up-regulated in LLC1 cells after exposure of both SD of 10 Gy and FD, whereas miR-186-5p and miR-145a-5p were significantly up-regulated following FD treatment compared to the expression levels of those miRNAs in untreated cells (**Fig. 3.3B**). qRT-PCR analysis confirmed gene and miRNA microarray data (Supplementary table 6).

Furthermore, we also compared the expression changes of selected genes and miRNAs in LLC1 cells grown *in vitro* and LLC1 tumors *in vivo* irradiated with SD10 and FD (**Fig 3.3A** and **B**). The qRT-PCR analysis revealed that the expression of Btg2, Ccng1 and P21 was up-regulated in tumors after the treatment of 10 Gy, likewise observed in LLC1 cells. Thbs2 was also up-regulated *in vivo*

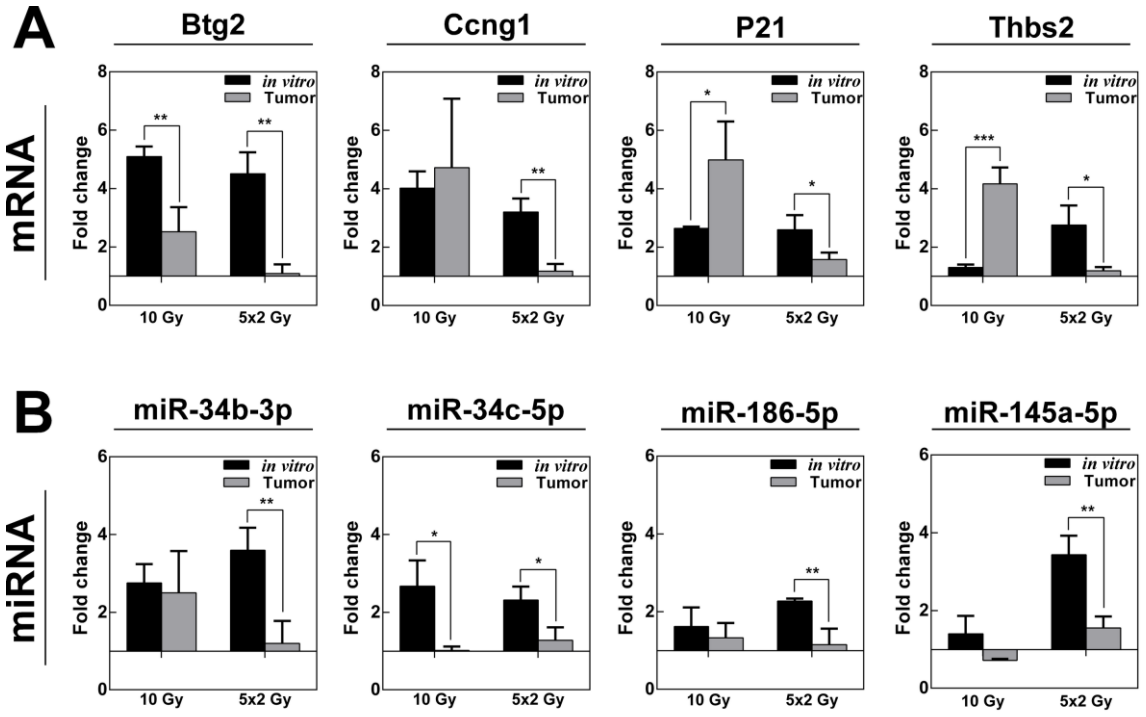

Figure 3.3 Validation of Microarray gene and miRNA expression data by qPCR. Graph showing relative expression of selected A) genes (Btg2, Ccng1, P21 and Thbs2) and B) miRNAs (miR-34b-3p, miR-34c-5p, miR186-5p and miR-145a-5p) in LLC1 cells and in mouse LLC1 tumors following exposure to SD of 10 Gy or FD of 5x2 Gy compared to the expression levels in untreated cells. Results show mean ±SD (n=3; t-test; *P<0.05; **P<0.01; ***P<0,001).

following irradiation of 10 Gy, whereas the expression of Thbs2 was significantly altered *in vitro* only following FD. Surprisingly, the expression of all selected genes was not significantly altered in LLC tumors following the FD irradiation regimen in contrast to expression data in LLC1 cells. Moreover, the qRT-PCR analysis also indicated no significant changes in the expression of all selected miRNAs in LLC1 tumors following both irradiation regimens (**Fig. 3.3B**).

In summary, our results revealed that the gene and miRNA signatures of LLC1 cells exposed to irradiation were dose delivery type dependent. The gene pathway enrichment analysis indicated that the extent of differential expression of genes involved in the P53, cell cycle, apoptosis and immune response categories was the most robust after exposure to FD. Furthermore, the miRNA target analysis demonstrated a significant correlation between differential expression of genes and miRNAs. Therefore, despite the indication that the LLC1 tumor response to fractionated irradiation could be extensively influenced by tumor microenvironment, the present study suggests key pathways involved in radiation induced response of murine cancer cells exposed to irradiation. Data presented in this study can be further applied to improve the outcome and the development of radiotherapy in preclinical animal model settings.

3.2 Transcriptomic signatures of murine and human cells grown in extracellular matrix enriched microenvironment

The extracellular matrix (ECM), as one of the key components of tumor microenvironment, has a significant impact on cancer development and highly influences tumor cell features and therefore the response to treatment (Hanahan and Weinberg). ECM contributes not only structural support of growing tumor cells, but also affects other cellular functions such as cell differentiation, migration, survival or proliferation (Weaver et al. 1997, Hehlgans et al. 2007, Yamada and Cukierman 2007). Moreover, gene and protein expression levels are regulated in a cell-ECM interaction dependent manner (Zschenker et al. 2012, Luca et al. 2013). Not surprisingly, clinical trials based on preclinical two-dimensional (2D) monolayer cell culture models which lack representation of ECM dependent molecular processes occurring in tumors currently have a failure rate of up to 95%. Cancer cell growth under three-dimensional (3D) culture conditions simulating ECM microenvironment better resembles tumor cell properties *in vivo* (Fournier and Martin 2006). Thus, investigations using such 3D cell culture models are expected to result in more successful clinical trials.

A vast amount of evidence indicates the superiority of 3D cell cultures over 2D models for the investigation of cancer tumor microenvironment dependent cancer cell properties (Abbott 2003, Friedrich et al. 2007). Obvious advantages of 3D cell culture models are the cellular-ECM interactions and cell-cell contacts, the formation of active proliferation, quiescent viable cell and necrotic cell zones, as well as the formation of nutritional, oxygen and drug gradients better reflecting cellular organization and the microenvironment in tumor tissue (Lin and Chang 2008). Nevertheless, the 3D cell cultures do not resemble the full complexity of tumor tissue environment *in vivo*. Few obvious limitations of 3D cell cultures as a cancer research model are the lack of vasculature, host immune response and other cell-cell interactions that occur between cancer and stromal cells in tumors (Mehta et al. 2012). Recognized advantages and limitations of 3D cell culture models suggest that the most

successful directions of 3D model application include the development of new anticancer treatment strategies. Hence, detailed analysis at the molecular level of 2D/3D cell cultures and tumors *in vivo* are still needed to unlock the power of 3D cell culture models in translational research.

In order to elucidate which biological pathways are altered in an ECM dependent manner, we have analyzed genome-wide mRNA and miRNA expression changes in murine Lewis lung cancer LLC1 cells following of 48 h of cellular growth under laminin rich ECM (lr-ECM) 3D cell culture conditions compared to cells grown in 2D as described in Methods section 2.2.3. In addition, we have applied the same experimental design to evaluate genome-wide mRNA expression changes in human colorectal carcinoma DLD1 and HT29 cells.

3.2.1 Cell morphology

To elucidate structural changes in cellular morphology we examined mouse Lewis lung carcinoma LLC1, human colon carcinoma DLD1 and HT29 cells grown under 2D or lr-ECM 3D cell culture conditions as described in Methods section 2.2.6. Cells lost their flat elongated morphology and gained 3-dimensional characteristic mass view following 48 hours of cell growth in 3D conditions (**Fig. 3.4A**). Furthermore, in order to visualize cell actin cytoskeleton changes, we also performed confocal microscopy of cells stained with phalloidin (**Fig. 3.4B**). Images showed that cells had undergone a significant actin cytoskeleton rearrangement and actin stress fibers were lost under 3D culture conditions.

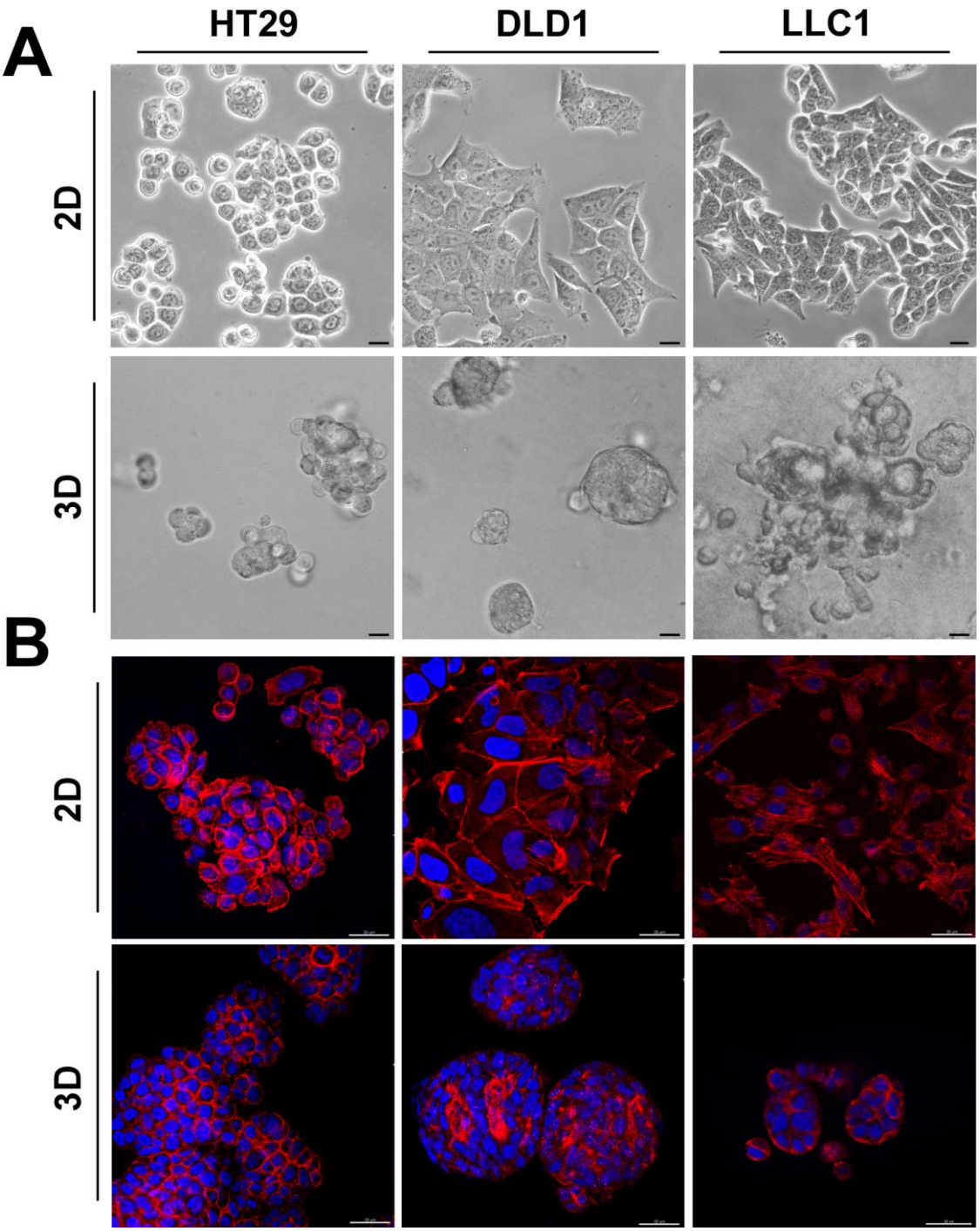

Figure 3.4 Cell morphology of human colon carcinoma DLD1 and HT29 cells and mouse Lewis lung carcinoma LLC1 cells grown under 2D or laminin-rich extracellular matrix (lr-ECM) 3D cell culture conditions. Prior to imaging, cells were cultivated in 2D (upper panel) and 3D (lower panel) conditions for 48 hours. A) Representative phase-contrast images of cell growth in 2D and 3D cell culture. B) Representative confocal laser scanning microscopy images of cell growth in 2D and 3D cell culture. F-Actin was stained with AlexaFluor 633 Phaloidin (red). Nuclei were counterstained with 4’6-diamino-2-phenylindole (DAPI) (blue).

3.2.2 mRNA expression profile of LLC1 cells grown in lr-ECM 3D

Microarray data revealed that the expression of 1884 genes was significantly altered (>1.5 fold change, $p<0.05$) in LLC1 cells following 48 h cell growth under lr-ECM 3D conditions compared to expression levels in cells grown in 2D (**Table 3.3**). Differences in cell culture conditions resulted in a greater number of down-regulated than up-regulated genes (1052 and 832, respectively).

Table 3.3. Number of differentially expressed genes and miRNAs in LLC1 cells after 48 h growth under 2D and lr-ECM 3D conditions.

	All	Up-regulated	Down-regulated
Genes	**1884**	**832**	**1052**
miRNAs	**77**	**41**	**36**

Gene and miRNA expression values are above 1.5 and 2 fold change, respectively, $p<0.05$.

3.2.3 Pathway enrichment analysis

In order to evaluate which biological pathways were affected in LLC1 cells between 2D and 3D cell growth conditions, we performed KEGG pathway enrichment analysis of all 1884 differentially expressed genes. KEGG pathway enrichment analysis revealed that a total of 74 KEGG pathway categories were enriched where each of these categories was represented by at least five or more genes in the functional category with $p<0.05$. A greater number of genes were down-regulated in all categories. Next, we grouped similar KEGG pathway categories into three subsets of major functional groups, which could be related to tumor development and progression: 1) MAP kinase; 2) Cell adhesion and 3) Immune response related pathways (**Table 3.4).** The MAP kinase signaling pathway was the second most significantly altered KEGG category ($p=6.23e-08$) and resulted in 25 genes (11 up-regulated and 14 down-regulated) differently expressed in LLC1 cells cultured under lr-ECM 3D and 2D culture conditions. Differences in cell culture conditions also altered the expression of 48 unique (22 up-regulated and 26 down-regulated) genes related to

Table 3.4. KEGG pathway enrichment analysis of genes differentially expressed in LLC1 cells between lr-ECM 3D and 2D cell culture conditions.

Category groups	All		Up-regulated		Down-regulated	
	Genes	p value	Genes	p value	Genes	p value
MAP Kinase						
MAPK signaling pathway	25	6.23e-08	11	0.0010	14	0.0002
Cell adhesion						
Regulation of actin cytoskeleton	20	1.35e-06	6	0.0404	14	3.76e-05
Focal adhesion	17	3.33e-05	7	0.0148	10	0.0018
Cell adhesion molecules (CAMs)	10	0.0062	5	0.0368	5	NS
Gap junction	7	0.0103	2	NS	5	0.0174
Tight junction	9	0.0103	5	NS	4	NS
ECM-receptor interaction	6	0.0237	4	0.0257	2	NS
Immune response						
Cytokine-cytokine receptor interaction	18	0.0001	6	NS	12	0.0011
T cell receptor signaling pathway	11	0.0003	3	NS	8	0.0011
VEGF signaling pathway	9	0.0004	5	0.0062	4	NS
Cytosolic DNA-sensing pathway	7	0.0013	4	0.0111	3	NS
B cell receptor signaling pathway	7	0.0058	3	NS	4	NS
RIG-I-like receptor signaling pathway	6	0.0121	5	0.0045	1	NS
Natural killer cell mediated cytotoxicity	8	0.0153	3	NS	5	0.0435
Jak-STAT signaling pathway	9	0.0159	3	NS	6	0.0336
Fc epsilon RI signaling pathway	6	0.0186	2	NS	4	NS
Chemokine signaling pathway	9	0.0362	3	NS	6	NS
Toll-like receptor signaling pathway	5	0.0401	4	NS	2	NS

Functional groups of all genes, differentially expressed in LLC cells under 3D cell culture conditions, were assign as significant when enriched in at least 5 genes, $p<0.05$

cell adhesion. These genes were significantly associated with cell adhesion molecules, gap and tight junctions, ECM-receptor interaction functional

categories, with “Regulation of actin cytoskeleton” (p=1.35e-06) and “Focal adhesion” (p=3.33e-05) categories being the most significantly altered in the “cell adhesion” subset. Furthermore, we indicated that the differences in cell culture conditions also altered the expression of 44 (16 up-regulated and 28 down-regulated) genes involved in immune response signaling pathways including cytokine-cytokine receptor, chemokine, T and B cell receptor and Jak-STAT signaling categories (**Table 3.4)**. Differently expressed genes associated to MAP kinase, cell adhesion and immune response pathway categories are listed in supplementary table 7.

3.2.4 miRNA expression pattern in LLC1 cells grown lr-ECM 3D

miRNA expression analysis demonstrated that the expression of 77 miRNAs was significantly altered (>2 fold change, $p<0.05$) in LLC1 cells following 48 h of cell growth under lr-ECM 3D culture conditions compared to miRNA expression levels in cells cultured on plastic (**Table 3.3**). The expression of 41 miRNAs was up-regulated and 36 down-regulated miRNAs in LLC1 cells cultivated in 3D. Next, to obtain a better overview of miRNA expression signature, we further checked which members of miRNA cluster were co-expressed (Supplementary table 8). We found that 16 up-regulated miRNAs were associated to 3 clusters, located in chromosome 2 (miR-466~467~669 cluster), 9 (miR-34 cluster) and 12 (miR-376 cluster) while members (10 miRNAs) of 3 miRNA clusters located in chromosomes 2, 12 and X were down-regulated.

3.2.5 RNA-miRNA regulatory network analysis

To better understand the biological processes which could be regulated by the 77 miRNAs deregulated in LLC1 cells between 2D and 3D cell culture conditions, we identified 8629 unique target genes potentially regulated by these miRNA using in silico miRNA target analysis. Next, miRNA pathway enrichment analysis indicated 69 KEGG categories significantly enriched in targeted genes revealing that pathways related to MAPK, cell adhesion and immune response

Table 3.5. Target genes and miRNAs from MAP Kinase, Cell Adhesion and Immune Response category groups showing inverse correlation in LLC1 cells after 48 h growth between lr-ECM 3D and 2D cell culture conditions.

Category	Differentially expressed genes	Differentially expressed miRNAs
MAP kinase	**Cacna1d ↑**	miR-137-3p↓; miR-448-3p↓; miR-495-3p↓
	Ikbkg ↑	miR-137-3p↓
	Traf6↑	miR-590-3p↓
	Kras↓	**miR-761↑**
	Mknk1↓	**miR-195-5p↑**
	Pak2↓	**miR-297a-3p↑**
	Sos2↓	**miR-34b-3p↑, miR-34c-3p↑, miR-466f-3p↑, miR-500-3p↑**
Cell adhesion	**Arhgef4↑**	miR-135a-5p↓, miR-448-3p↓, miR-200b-3p↓, miR-20b-3p↓
	Col1a1↑	miR-135a-5p↓, miR-137↓, miR-590↓
	Itpr1↑	miR-544-3p↓
	Pard3↑	miR-495-3p↓
	Slc9a1↑	miR-9-5p↓
	Vegfa ↑	miR-1a↓
	Tmsb4x↓	**miR-448↑**
	Flna↓	**miR-328-3p miR-761↑**
	Gnas↓	**miR-877-3p↑**
	Htr2c↓	**miR-466d-3p↑**
	Pak2↓	**miR-297a-3p↑**
	Pak3↓	**miR-297a-3p↑**
	Rhoa↓	**miR-466f-3p↑**
	Ssh1↓	**miR-467b↑**
Immune resopnse	**Pard3↑**	miR-495-3p↓
	Eif2ak1↓	**miR-500-3p↑**
	Oas3↓	**miR-297a-3p↑, miR-466b-3p↑, miR-466d-3p↑, miR-466f-3p↑, miR-466g↑, miR-467d-3p↑, miR-467e-3p↑**
	Ppp2r1b↓	**miR-195-5p↑, miR-672-5p↑**
	Ppp2r2b↓	**miR-466g↑**
	Xcr1↓	**miR-669b↑**

Up-regulated genes and miRNAs are shown in bold

were also among the most significantly altered functional categories.

Finally, we investigated correlations between differently expressed genes and miRNAs related MAP kinase, Cell adhesion and Immune response subsets

which were the most significantly altered in an ECM dependent manner to indicate any potential miRNA-mRNA connections in these processes (**Table 3.5).** In the MAP kinase pathway, a negative correlation was observed between differential expression of 11 miRNAs and 7 mRNAs. In addition, 14 mRNA targets associated with cell adhesion pathways reversely correlated with 18 miRNAs. Target analysis also revealed that 6 differentially expressed genes from the immune response category reversely correlated with 13 miRNAs.

3.2.6 Gene expression pattern in DLD1 and HT29 cells grown in lr-ECM 3D

In order to evaluate the impact of the cellular microenvironment on gene-expression levels in human DLD1 and HT29 CRC cells, we compared genome-wide expression levels in these cells following 48 hours of growth in 2D and lr-ECM 3D cell culture conditions. Microarray data revealed that the expression of 841 and 1190 genes was significantly altered (>1.5 fold-change, $p<0.05$) in an ECM-dependent manner in DLD1 and HT29 cells, respectively (**Fig. 3.5**). Most of these genes (637 in DLD1 cells and 804 in HT29 cells) were down-regulated. The Venn diagrams also revealed that the expression of 383 genes was significantly altered in both DLD1 and HT29 cells grown under 3D versus 2D conditions. However, in both cell lines, only 37 common genes were found to be up-regulated in contrast to 346 commonly down-regulated genes.

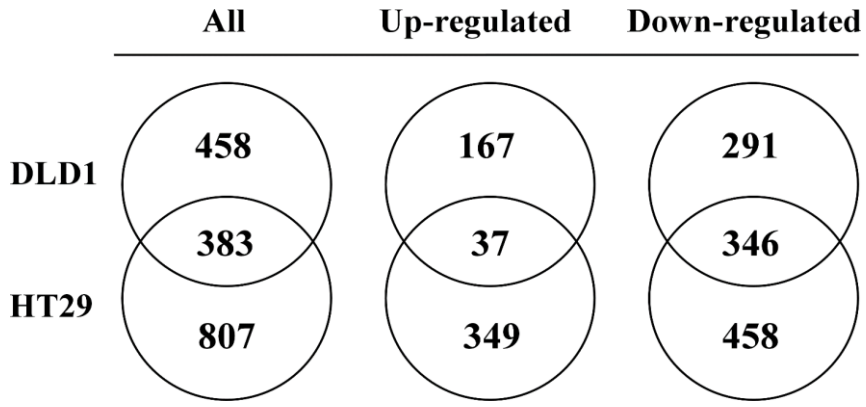

Figure 3.5. Venn diagrams showing the number of deregulated, up-regulated and down-regulated differentially expressed genes (fold change of at least 1.5 and $P<0.05$) in HT29 and DLD1 cells following 48 h growth under laminin-rich extracellular matrix (lr-ECM) 3D and 2D cell culture conditions.

3.2.7 Pathway enrichment analysis

KEGG pathway enrichment results revealed 45 and 35 significantly altered functional categories in DLD1 and HT29 cells, grown under 3D versus 2D culture conditions, respectively. **Table 3.6** presents 13 common functional categories significantly altered in both CRC cell lines. The "Metabolic pathways" category involved the highest number of differentially expressed genes (44 and 48 genes in DLD1 and HT29 cells) between 2D and lr-ECM 3D. Nevertheless, KEGG pathway enrichment analysis revealed that the most significantly altered functional categories were related to cell–cell and cell–ECM interactions. The focal adhesion category was most significantly altered in CRC cells (DLD1: $p<7.47\times10^{-6}$; HT29: $p<1.59\times10^{-5}$) and resulted in significantly altered expression of 17 genes in DLD1 cells and 19 in HT29 cells. The present findings also indicated that functional categories adhesion junction, tight junction, ECM–receptor interaction and regulation of actin cytoskeleton were also prominently altered in an ECM-dependent manner. The majority of genes in these categories were down-regulated in CRC cells grown in lr-ECM 3D cell culture compared to 2D conditions. In addition, mitogen-activated protein kinase (MAPK) signaling pathway (DLD1: $p<0.0056$; HT29: $p<9.9x10^{-7}$) was among next the most significantly altered KEGG categories and comprised 13 differentially regulated genes in DLD1 cells and 25 in HT29 cells. Inflammatory response-related categories significantly altered in both CRC cell lines were "chemokine signaling pathway" and "cytokine–cytokine receptor interaction". Our results also indicated that P53 and WNT signaling pathways were commonly altered in both cell lines. KEGG pathway classification also revealed that the number of differentially expressed genes in all categories and the significance and the extent of enrichment were similar in both cell lines. These findings indicate biologically related gene-expression changes during cellular adaptation to lr-ECM 3D cell culture conditions which could implicate cellular response to treatment and survival.

Table 3.6. KEGG pathway enrichment analysis of genes differentially expressed in HT29 and DLD1 cells between lr-ECM 3D and 2D cell culture conditions.

Functional category	**DLD1**		**HT29**	
	Genes, n	P-value	Genes, n	P-value
Focal adhesion	17	7.47e-06	19	1.59e-05
MAPK signaling pathway	13	0.0056	25	9.90e-07
Pathways in cancer	17	0.0005	25	1.59e-05
Metabolic pathways	44	1.95e-05	48	0.0012
Adherens junction	9	0.0001	10	0.0002
P53 signaling pathway	8	0.0003	7	0.0092
Tight junction	11	0.0003	10	0.0092
ECM–receptor interaction	9	0.0003	7	0.0207
Regulation of actin cytoskeleton	14	0.0003	18	0.0001
Endocytosis	13	0.0005	17	0.0002
Chemokine signaling pathway	11	0.0034	11	0.0247
Cytokine–cytokine receptor interaction	12	0.0115	14	0.0207
WNT signaling pathway	7	0.0387	9	0.0394

3.2.8 Heat map analysis

ECM-induced expression changes of individual genes associated with the most significantly altered KEGG pathway categories, including cell adhesion, MAPK and inflammatory response subsets, were depicted to demonstrate expression patterns within each category subset (**Figure 3.6**). **Figure 3.6A** shows a heat map of a total of 59 genes from the cell adhesion subset, which includes genes involved in focal adhesion, adhesion junction, tight junction, ECM–receptor interaction and regulation of actin cytoskeleton functional categories. Although the expression of some individual genes did not pass the expression threshold (fold change>1.5 and $p<0.05$), the majority of genes from the cell adhesion subset were down-regulated in DLD1 and HT29 cells grown in lr-ECM 3D compared with 2D cell culture conditions. Some of the down-regulated genes associated with cell–cell and cell–matrix junctions included integrins ITGA3, ITGA5, ITGB4, ITGB5 and ITGB7; filamins FLNA and FLNB; laminins LAMA3,

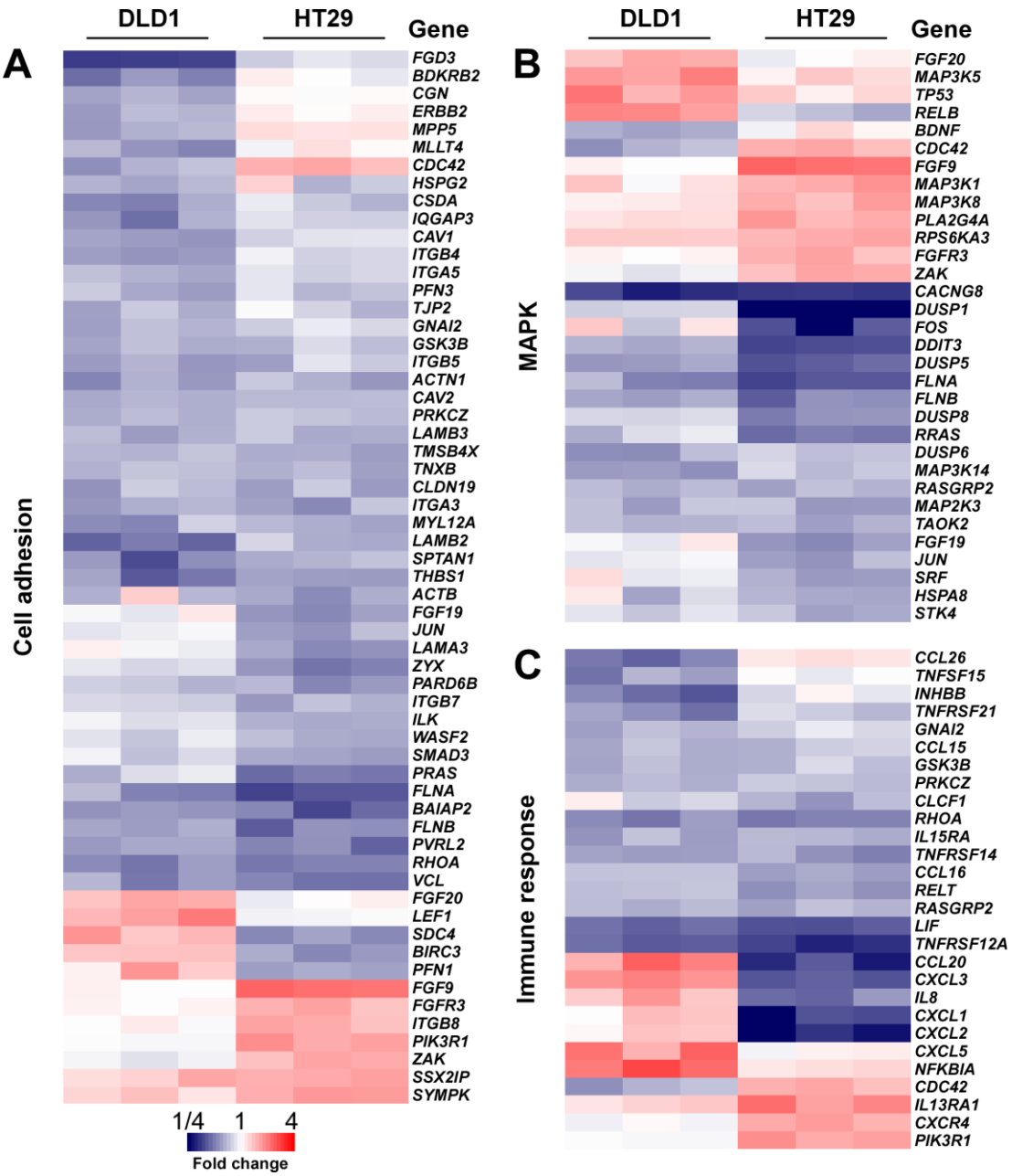

Figure 3.6. Heat map analysis of selected KEGG categories. Heat maps representing the expression profile for cell adhesion (A), MAPK signaling (B), immune response (C) genes following 48 hours of DLD1 and HT29 cell growth under 3D cell culture conditions compared to 2D. Red and blue indicate an increase and decrease of gene expression, respectively.

LAMB2 and LAMB3; and other structural genes including vinculin, actin B and actinin 1, indicating changes in expression of genes closely related to the linkage between focal adhesion and the cytoskeleton during cellular adaptation to lr-ECM 3D cell culture conditions. Additionally, the heat map data also revealed up-regulation of integrin ITGB8 in HT29 cells in an ECM-dependent manner.

Figure 3.6B depicts differentially expressed genes involved in the MAPK signaling pathway. In the MAPK category, the expression of 32 genes was altered in CRC cells grown under lr-ECM 3D cell culture conditions compared to those under 2D. Differentially expressed genes included fibroblast growth factors FGF9, FGF19 and FGF20, fibroblast growth factor receptor FGFR3; MAP kinase kinases MAP3K1, MAP3K5, MAP3K8, MAP3K14 and MAP2K3, dual specificity phosphatases DUSP1, DUSP5, DUSP6 and DUSP8; and other kinases TAO kinase 2 (TAOK2) and serine/threonine kinase 4 (STK4). In addition, transcription factor AP1 subunits JUN, FOS and serum response factor (SRF) were significantly down-regulated in HT29 cells in an ECM-dependent manner.

Figure 3.6C shows a heat map from the immune response subset which includes 28 differentially expressed genes involved in chemokine and cytokine-cytokine receptor signaling pathways. A total of 17 inflammatory genes were significantly down-regulated in one or both CRC cells and included chemokines CCL15, CCL16 and CCL26; tumor necrosis factor-related TNFSF15, TNFRSF12a, TNFRSF14 and TNFRSF21; interleukin receptor IL15RA. C-X-C motif chemokine 5 (CXCL5), and chemokine receptor CXCR4 and interleukin receptor IL13RA1 were significantly up-regulated in DLD1 and HT29 cells grown in lr-ECM 3D. In addition, the heat map revealed an opposite expression pattern of five differentially expressed genes including chemokines CCL20, CXCL1, CXCL2, CXCL3 and interleukin IL8 was opposite between CRC cells. These genes were upregulated in DLD1 cells and downregulated in HT29 cells when CRC cells were grown under lr-ECM 3D cell culture conditions.

3.2.9 Microarray data validation

To validate differential expression of genes and miRNAs identified by microarrays, we selected 4 up-regulated genes and miRNAs for qRT-PCR analysis (**Fig 3.7A** and **B;** black columns). The expression of selected Hnf4a (Hepatocyte nuclear factor 4a), Infb1 (Interferon beta-1), Klf8 (Kruppel-like

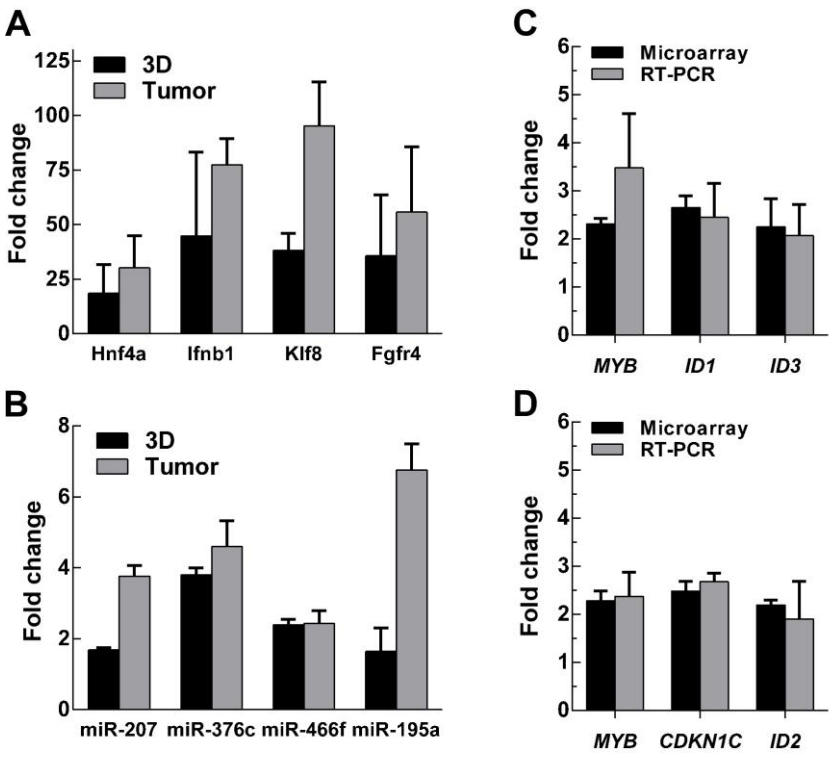

Figure 3.7. Validation of microarray data by RT-qPCR. Graph showing the fold change of A) genes (hnf4a, infb1, klf8 and fgfr4) B) miRNAs (miR-207, miR-376c-3p, miR-466f-3p and miR-195a-5p) in LLC1 cells grown under lr-ECM 3D cell culture conditions or in mouse LLC1 tumors compared to expression levels in cells cultivated in 2D. C) The fold change in levels of selected genes including MYB, ID1 and ID3 in DLD1; and D) the fold change in levels of selected genes including MYB, CDKN1C and ID2 genes in HT29 cells after 48 hours of cultivation under lr-ECM 3D and 2D cell culture conditions are shown. qPCR data analysis was based on $2^{-\Delta\Delta Ct}$. For LLC1, Gpdh or snoRNA-135 were used as housekeeping genes for gene or miRNA qPCR data normalization, respectively. For CRC, HPRT1 was used as housekeeping gene for qPCR data normalization. Results show the mean ±SD (n=3).

factor 8) and Fgfr4 (Fibroblast growth factor receptor 4) genes was significantly up-regulated in LLC1 cells grown under lr-ECM 3D culture conditions compared to expression levels in cells cultured on plastic. All selected miRNAs, miR-207, miR-376c, miR-466f and miR-195a, also showed significant up-regulation by qPCR. Hence, qRT-PCR data confirmed gene and miRNA microarray data.

Additionally, we also compared the expression of selected genes and miRNAs between 2D monolayer and LLC1 tumors (**Fig 3.7A** and **B;** grey columns). qRT-PCR analysis clearly showed that all selected genes and miRNAs likewise observed in 3D cell culture conditions were also significantly up-regulated *in vivo*.

In the present study, we observed that the genes most significantly up-regulated in an ECM-dependent manner were involved in cellular differentiation maintenance. Thus, for microarray data validation, we performed expression analysis of inhibitor of DNA binding ID1, ID2 and ID3; cyclin-dependent kinase inhibitor CDKN1C; and transcriptional activator MYB genes in CRC cells grown under 2D and lr-ECM 3D cell culture by real-time RT-PCR. The RT-PCR data confirmed the microarray data (**Figure 3.7C** and **D**). The expression of most selected genes was up-regulated more than two-fold by RT-PCR.

In summary, the present pathway enrichment results indicated the MAP kinase, cell adhesion and immune response as the most significantly altered functional categories in LLC1, DLD1 and HT29 cells during the switch from 2D to 3D. Global miRNA expression analysis confirmed the involvement of miRNA in the regulation of ECM dependent properties of cancer cells. Comparison of the expression levels of selected genes and miRNA between LLC1 cells grown 3D cell culture and LLC1 tumors implanted in mice indicated correspondence between both model systems. Therefore, the present results indicate the existence of universal regulation for the MAPK, cell adhesion and immune response pathways both in 3D culture and tumor suggesting the most promising directions for translational cancer research using the 3D cell culture models.

3.3 MICROENVIRONMENT AND DOSE DELIVERY DEPENDENT RESPONSE TO IONIZING RADIATION IN HUMAN COLORECTAL CANCER CELL LINES

Our previous observations described in 3.1 as well as studies performed by other researchers suggest that the tumor cell response to irradiation also depends on their microenvironment (Vaupel 2004). Therefore, model systems that better resemble the three-dimensional (3D) organization of tumor tissue have to be considered in current radiobiology. Consequently, 3D cell culture models were introduced to mimic *in vivo* cell microenvironment more accurately than the standard two-dimensional cell monolayer (2D) cultures (Abbott 2003, Yamada and Cukierman 2007). Growing evidence suggest that 2D and 3D cultured cell gene expression pattern discrepancies following irradiation is highly dependent on cell-extracellular matrix (ECM) interactions (Zschenker et al. 2012), therefore different ECM-based models might be the most promising in radiobiology research. In addition, it has been shown that laminin rich extracellular matrix (lr-ECM) used in 3D cultures not only alters cancer cell phenotype and response to external stimuli but also affects cell differentiation, migration and survival (Luca et al. 2013). Hence, a change in these fundamental cell properties also demands us to reconsider data previously collected using 2D *in vitro* models (Benton et al. 2014).

To explore cellular response to IR in ECM enriched microenvironment, in the present study we investigated genome-wide transcriptome changes of human colorectal cancer DLD1 and HT29 cell lines (both bearing distinct P53 mutations) grown in 3D culture following SD of 2 Gy and 10 Gy or FD 5x2 Gy irradiation. All experiments were performed according experimental design described in Methods section 2.2.4.

3.3.1 Clonogenic cell survival

DLD1 and HT29 cells cultured under lr-ECM 3D cell culture conditions showed a significantly higher survival rates after single dose (SD) irradiation than

2D cultured cells (**Figure 3.8A**). The surviving fractions after SD irradiation for 3D and 2D cultured DLD1 cells at 2 - 10 Gy were 0.78 ± 0.05 - 0.068 ± 0.023 and 0.52 ± 0.09 - 0.0036 ± 0.0019, respectively. 3D and 2D cultured HT29 cell surviving fractions at SD were 0.85 ± 0.03 - 0.17 ± 0.04, 0.62 ± 0.04 - 0.0011 ± 0.0005, respectively.

Clonogenic survival following fractionated dose (FD) irradiation was also significantly higher in DLD1 and HT29 cells grown under lr-ECM 3D than in 2D conditions (**Figure 3.8B**). Survival fractions after 5x2 Gy FD irradiation decreased to 0.29 ± 0.03 and 0.055 ± 0.007 for 3D and 2D DLD1 cultured cells, respectively. 3D and 2D cultured HT29 cell surviving fractions at 5x2 Gy were

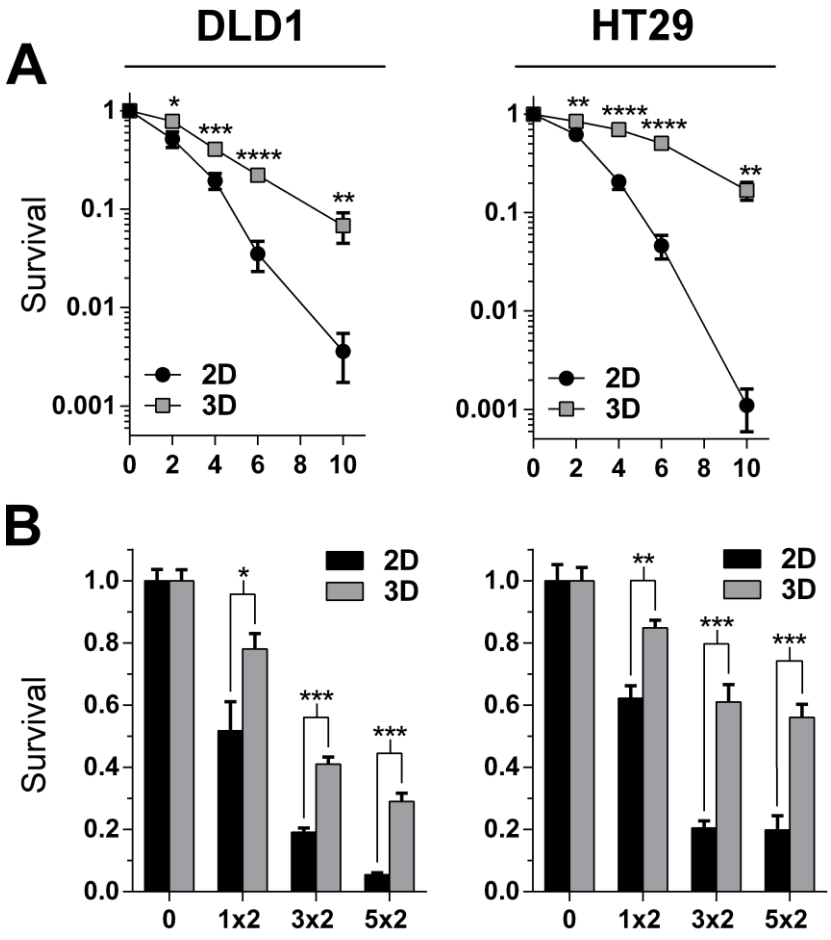

Figure 3.8. Clonogenic survival analysis of colorectal cancer DLD1 and HT29 cells grown under two-dimensional (2D) or three-dimensional (3D) cell culture conditions. Cells were irradiated with a single dose of 2-10 Gy (A) or a fractionated dose of 2 Gy daily up to 5 days (B). Data are ±SD (n=3; t-test; *P<0.05; **P<0.01; ***P<0.001; ****P<0.0001).

0.56 ± 0.04 and 0.20 ± 0.05, respectively. Differences in radiosensitivity between cell lines were most obvious at 3D cell culture conditions.

3.3.2 Genome-wide gene expression

Microarray data analysis revealed that overall 1573 and 935 unique genes in DLD1 and HT29 cells, respectively, were differentially expressed (fold change greater than 1.5; $P < 0.05$) 4 hours following SD of 2 Gy and 10 Gy or FD of 5x2 Gy irradiation compared to non-irradiated cells (**Fig. 3.9**). A significantly higher number of genes were downregulated following each one of irradiation schedules in both cell lines. Of all unique genes, 980 and 620 genes were downregulated in DLD-1 and HT29 cells, respectively. Irradiation of 2 Gy SD altered a similar number of genes in both cell lines (**Table 3.7**). The expression of 468 and 382 genes was altered following 2 Gy in DLD1 and HT29 cells, respectively. Exposure to 10 Gy SD resulted in the highest number of genes that were differentially expressed: 953 and 579 genes in DLD1 and HT29 cells, respectively. Treatment with FD protocol resulted in a higher number of differentially expressed genes in DLD1 than in HT29 cells, 778 and 352 genes, respectively. Venn diagrams (**Fig. 3.9**) also indicated that in both cell lines significantly more common genes amongst all radiation doses were downregulated

Table 3.7. Number of differentially expressed genes after SD or FD irradiation in DLD1 and HT29 cells grown under 3D cell culture conditions compared to untreated cells.

Cell line	Dose	Differentially expressed genes	Up-regulated	Down-regulated
DLD1	2 Gy	468	114	354
	10 Gy	953	275	678
	5x2 Gy	778	302	476
HT29	2 Gy	382	104	278
	10 Gy	579	136	443
	5x2 Gy	352	111	241

Relative gene expression is greater than 1.5, $P<0.05$.

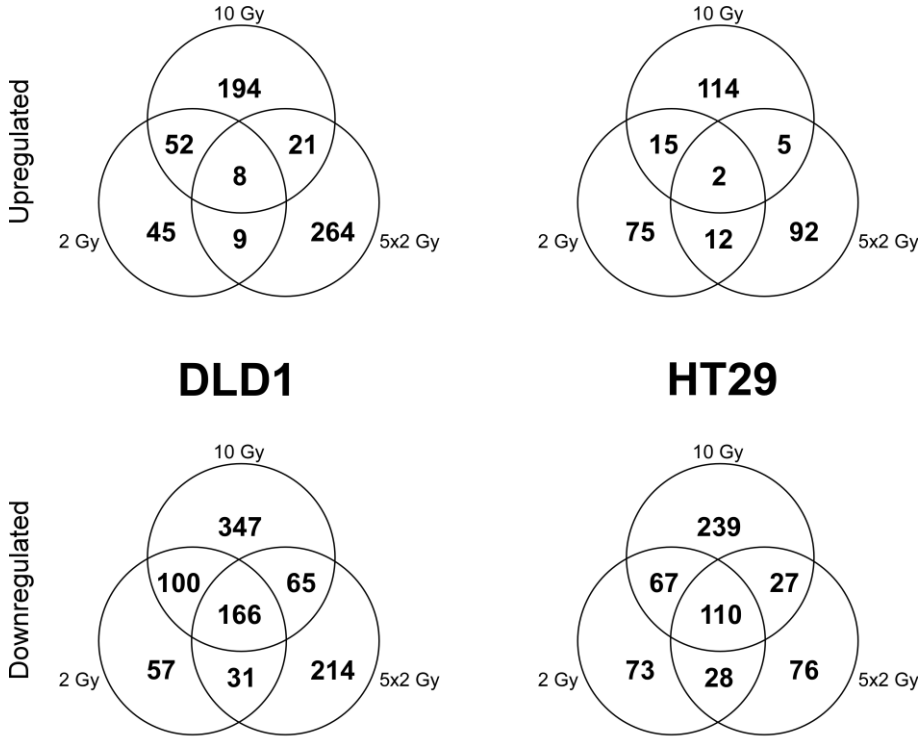

Figure 3.9. Venn diagrams showing the number of up-regulated (upper panel) and down-regulated (lower panel) differently expressed genes (fold change is at least 1.5 and P<0.05) at 4 hours following ionizing radiation exposure to single 2 Gy or 10 Gy or fractionated 5x2 Gy dose in HT29 and DLD1 cells grown under 3D cell culture conditions compared to untreated cells.

(166 and 110 common genes in DLD-1 and HT29 cells) than upregulated (only 8 and 2 common genes, respectively). The highest number of unique differentially expressed genes also predominantly occurred in CRC cells following SD of 10 Gy.

3.3.3 KEGG pathway enrichment analysis

In order to further inspect interactions between genes involved in the response to IR, all differentially expressed genes (fold change >1.5; P<0.05; compared to non-irradiated cells) following both SD and FD irradiation protocols in DLD1 and HT29 cells were classified into KEGG pathway categories (**Table 3.8**). A complete list of categories determined by KEGG pathway enrichment analysis is depicted as Additional files 4 and 5, respectively.

KEGG pathway analysis revealed that in DLD1 cells 5x2 Gy FD irradiation mostly affected the expression of genes involved cell cycle regulatory (P = 2.33 x

10^{-10}), DNA replication ($P = 1.84 \times 10^{-9}$) and P53 ($P = 5.37 \times 10^{-8}$) pathways. DNA repair category related genes were among the second most significantly altered pathway categories in DLD1 cells following FD. By contrast, SD irradiation showed that immune response genes were also significantly altered, whereas no significant changes of immune response gene expression were detected after FD irradiation in DLD1 cells. In addition to immune response, 10 Gy SD triggered BER ($P = 7.18 \times 10^{-5}$), cell cycle regulation ($P = 0.0006$) and P53 ($P = 0.0141$) signaling pathways. No noticeable tendencies of significantly altered gene categories were observed in HT29 cells after SD irradiation. However, unlike DLD1, HT29 cells exposed to FD irradiation expressed a clearly different pattern in immune response gene categories.

Furthermore, all differentially expressed genes (fold change >1.5; $P<0.05$; compared to non-irradiated cells) after exposure to FD in DLD1 and HT29 cells cultured under 3D cell culture conditions irradiation were also associated into gene ontology biological process categories. GO enrichment analysis (**Table 3.8**) further indicated that FD irradiation had the highest impact on an altered expression of genes involved in cell cycle regulation and immune response biological process categories in DLD1 and HT29 cells, respectively.

Table 3.8. KEGG pathway enrichment analysis of genes differentially expressed following irradiation of SD (2 Gy or 10 Gy) or FD (5x2 Gy) in DLD1 and HT29 cells grown under lr-ECM 3D cell culture conditions compared to untreated cells.

Category	DLD1						HT29					
	2 Gy		10 Gy		5x2 Gy		2 Gy		10 Gy		5x2 Gy	
	Genes	p value	Genes	p value	Genes	p value	Genes	p value	Genes	p value	Genes	p value
Cell cycle	0	NS	**10**	**0.0006**	**17**	**2.33E-10**	0	NS	**8**	**0.0004**	0	NS
DNA replication	1	NS	2	NS	**10**	**1.84E-09**	0	NS	2	NS	0	NS
P53 pathway	0	NS	**5**	**0.0141**	**11**	**5.37E-08**	0	NS	4	NS	1	NS
Systemic lupus erythematosus	4	NS	**16**	**2.76E-07**	**13**	**1.18E-06**	4	NS	**5**	**0.0184**	3	NS
Pathways in cancer	8	NS	**14**	**0.0073**	**16**	**0.0002**	6	NS	**9**	**0.0129**	3	NS
Mismatch repair	0	NS	1	NS	**6**	**5.87E-06**	0	NS	1	NS	0	NS
Nucleotide excision repair	0	NS	2	NS	**6**	**0.0002**	0	NS	1	NS	0	NS
Homologous recombination	0	NS	2	NS	**5**	**0.0002**	0	NS	0	NS	0	NS
Base excision repair	1	NS	**7**	**5.18E-05**	**5**	**0.0003**	0	NS	2	NS	0	NS
Tight junction	3	NS	**6**	**0.049**	**8**	**0.0017**	2	NS	3	NS	1	NS

Gap junction	**6**	**0.0004**	**7**	**0.0036**	**5**	**0.0157**	2	NS	1	NS	1	NS
Focal adhesion	**5**	**0.0377**	5	NS	**7**	**0.0393**	3	NS	**7**	**0.0102**	0	NS
Adherens junction	4	NS	**7**	**0.0014**	4	NS	2	NS	**5**	**0.0034**	2	NS
Endocytosis	3	NS	**12**	**0.0014**	**8**	**0.0157**	**6**	**0.0072**	**8**	**0.0044**	3	NS
Hepatitis C	5	NS	5	NS	4	NS	2	NS	2	NS	**7**	**8.16E-6**
RIG-I-like receptor pathway	1	NS	3	NS	0	NS	0	NS	3	NS	**5**	**0.0002**
Antigen processing and presentation	0	NS	3	NS	**6**	**0.0018**	1	NS	2	NS	**6**	**6.04E-5**
Cytokine-cytokine receptor interaction	3	NS	**11**	**0.0175**	5	NS	2	NS	3	NS	**6**	**0.0078**
Chemokine pathway	**6**	**0.0124**	**11**	**0.0026**	3	NS	2	NS	3	NS	4	NS
B cell receptor pathway	**6**	**0.0003**	**8**	**0.0006**	3	NS	4	NS	**6**	**0.0009**	2	NS
T cell receptor pathway	5	NS	**6**	**0.0238**	2	NS	3	NS	**6**	**0.0034**	1	NS

Enrichment significance of KEGG gene categories was calculated by hypergeometric distribution. KEGG categories were assign as significant when associated with at least 5 genes, $p<0.05$. NS, no significance.

3.3.4 Heat Map analysis

Relative changes of gene expression in DLD1 and HT29 cells from selected KEGG pathway categories were depicted to demonstrate the expression profiles of genes within each category following each irradiation regimen (**Fig. 3.10**). The heat maps of each selected pathway category indicated that the expression of most genes associated with cell cycle regulation (**Fig.**

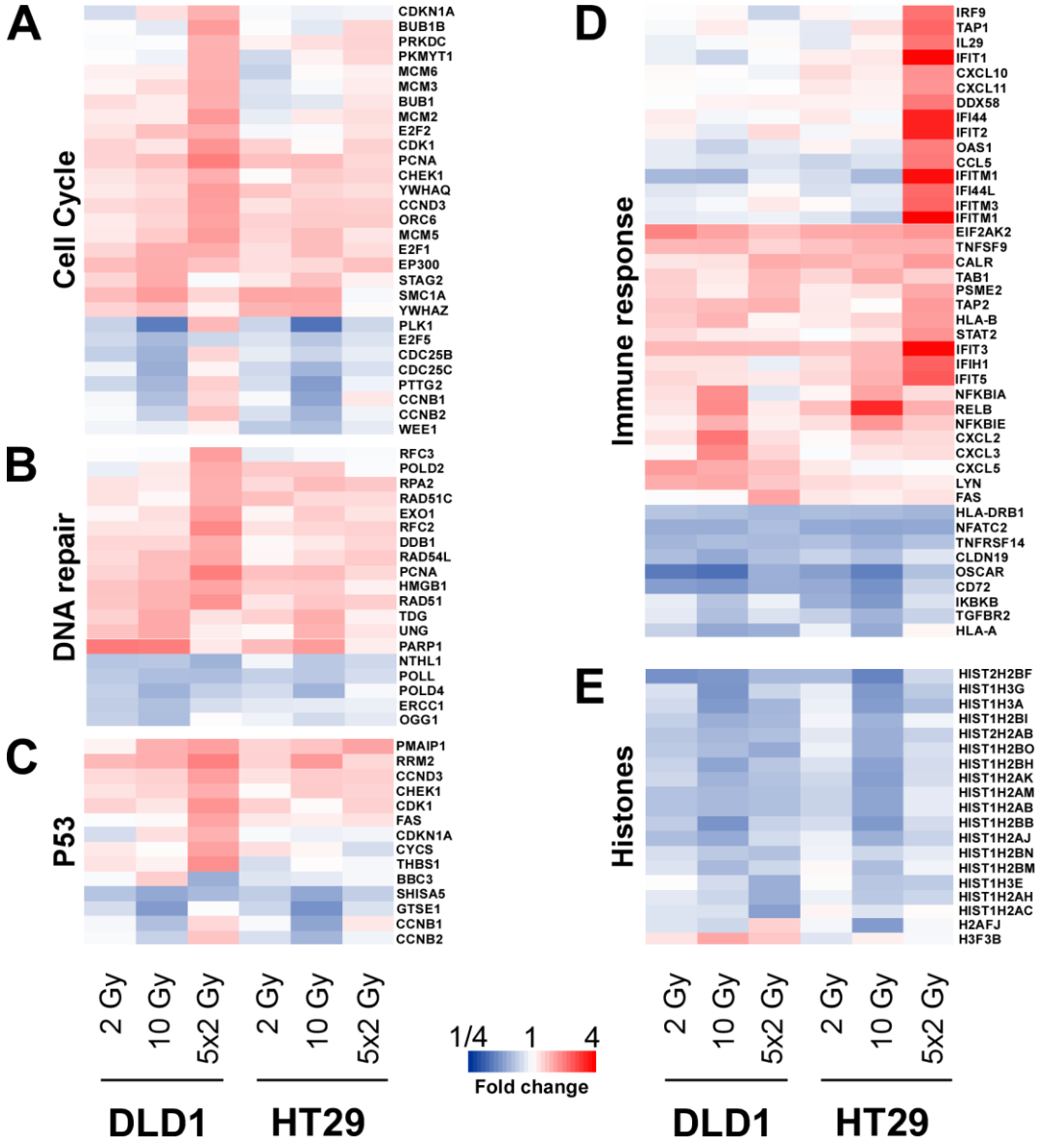

Figure 3.10. Heat maps representing the expression profile for cell cycle regulatory (A), DNA damage repair (B), P53 pathway (C), immune response (D) and histone (E) genes at 4 hours following irradiation of DLD1 and HT29 cells grown under 3D cell culture conditions compared to untreated cells. Cells were exposed to SD 2 Gy (lane 1 and 4),

SD 10 Gy (lane 2 and 5) and FD 5x2 Gy (lane 3 and 5) irradiation. Red and blue colors indicate increase and decrease of gene expression, respectively.

3.10A), DNA damage (**Fig. 3.10B**) and P53 (**Fig. 3.10C**) pathways were upregulated following exposure to both SD and FD irradiation. However the magnitude of expression was significantly higher in DLD1 cells peaking after the exposure to FD. Radiation induced gene expression profile in HT29 cells was similar to DLD1, but the relative expression change of altered genes in HT29 cells in cell cycle regulation, DNA damage and P53 pathways did not pass the cutoff (fold change >1.5; $P<0.05$). Gene expression patterns in these pathways were also very similar between DLD1 and HT29 cells following exposure to SD.

After classification, the highest number of genes fell into immune response category (**Fig. 3.10D**). Heat map visually divided the cluster of inflammatory genes into three different expression pattern subsets. In the first subset the majority of genes were strongly upregulated only in HT29 cells following FD irradiation. Genes depicted in the second subset of immune response genes were generally upregulated in both cell lines following each of radiation regimens with the highest increase in HT29 cells after FD irradiation as well. Expression of inflammatory genes in the third subset were generally downregulated following SD and FD treatment in both cell lines, with a higher magnitude of downregulation after exposure to 10 Gy SD.

Downregulation of histone or histone formation related genes was shown after IR in both DLD1 and HT29 cell lines (**Fig. 3.10E**). Single dose of 10 Gy resulted in the highest magnitude of downregulation.

3.3.5 Microarray Data Validation

Selected differentially expressed genes involved in cell cycle/DNA damage/P53 pathways (CDK1, RAD51 THBS1 and PCNA) or immune response (IL29, IFITM1, IFIT1 and OAS2) from microarray data following FD irradiation were analyzed by qPCR. qPCR data confirmed the relative gene expression levels obtained by microarray data (**Fig. 3.11A**).

In addition, the expression profiles of selected genes in DLD1 and HT29 cells following all irradiation schedules were also compared growing cells under 2D and 3D cell culture conditions (**Fig. 3.11B**). Interestingly, FD irradiation significantly increased expression of CDK1, PCNA and RAD51 in DLD1 cells only under 3D cell culture conditions. qPCR data also indicated that in HT29 cells expression of immune response genes following FD was altered under both cell culture conditions. However, expression of IFITM1, IFIT1 and OAS2 was almost 3 times higher in HT29 cells irradiated under 3D cell culture conditions. It is worth noting that none of the single dose treatments resulted in any significant changes neither in 2D, nor in 3D cultured cells (Supplementary table 9).

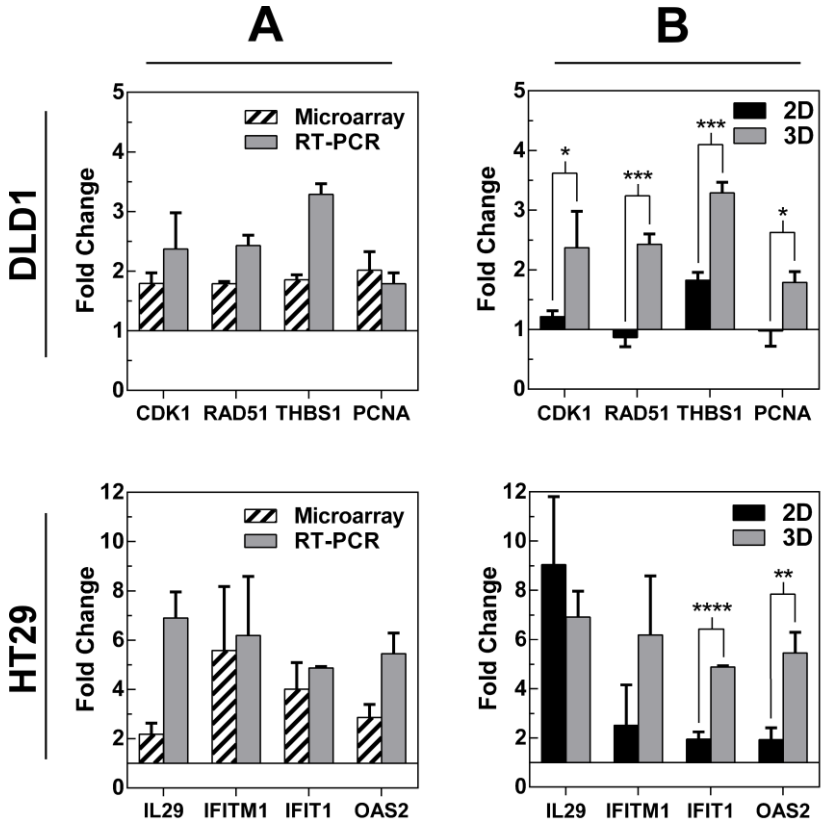

Figure 3.11. Microarray gene expression data validation by qPCR. qPCR was performed as described in Materials and Methods. qPCR data analysis was based on $2^{-\Delta\Delta Ct}$ method and HPRT1 was used as housekeeping gene for gene expression normalization. (A) Relative expression of selected genes identified by microarray data analysis was validated using qPCR. (B) Comparison of relative expression of genes selected from microarray data after FD irradiation in DLD1 and HT29 cells grown in 2D or 3D cell culture conditions compared to untreated cells. Each data point represents mean ±SD (n=3; t-test; *P<0.05; **P<0.01; ***P<0.001; ****P<0.0001).

In summary, fractionated dose irradiation resulted in different genome wide expression profile when compared to single dose treatment in colorectal cancer DLD1 and HT29 cells grown under 3D culture conditions. Despite the fact that a higher number of genes with altered expression were down-regulated in both cell lines after irradiation, cell cycle/DNA damage or immune response genes have been most significantly up-regulated following irradiation in 3D conditions cultured DLD1 and HT29 cell lines, respectively. Furthermore, the expression signature of selected genes following FD treatment was dependent on cell culture conditions and resulted in higher expression in cells grown under 3D conditions. In addition, we demonstrated higher radiotolerance in both cell lines under 3D cell culture conditions if compared to 2D. These results indicate that cancer cell survival after IR treatment in addition to cellular P53 status is ECM dependent. Therefore, the data in the present study suggest that ECM based 3D cell culture models in combination with the fractionated dose treatment of ionizing radiation could accelerate the understanding of molecular mechanisms associated with therapy dependent radioresistance in tumors and promote the development of more efficient radiotherapy.

4 DISCUSSION

4.1 Gene and miRNA expression profiles of mouse Lewis lung carcinoma LLC1 cells following single or fractionated dose irradiation

In the first part of the study we have investigated the changes in gene and miRNA expression signature after irradiation of single dose of 2 Gy or 10 Gy and fractionated dose of 5x2 Gy in mouse lung carcinoma LLC1 cells and syngeneic LLC1 tumors. The obtained data revealed that gene expression profiles of LLC1 cells were irradiation dose delivery dependent. In addition, we demonstrated by KEGG pathway enrichment analysis that P53 signaling, cell cycle, apoptosis and inflammatory response pathways were the most significantly altered functional categories in LLC1 cells following irradiation. The extent of differentially expressed genes was also irradiation dose delivery dependent. The miRNA microarray data indicated that fractionated irradiation induced a significantly different miRNA expression pattern compared to SD irradiation. Furthermore, the miRNA-target filter analysis revealed a significant correlation between mRNA and miRNA expression signatures in LLC1 cells after exposure to irradiation. Nevertheless, the RT-qPCR analysis showed that LLC1 tumors exhibited no significant changes in the expression of selected genes and miRNAs following a fractionated irradiation regimen.

The microarray data revealed that FD irradiation induced differential expression in the highest number genes. In addition, only a total of 145 genes were commonly expressed between all irradiation regimens demonstrating a significantly different gene expression pattern in LLC1 cells following exposure to single or fractionated dose irradiation. These results are supported by previous reports (Tsai et al. 2007, Simone et al. 2013, Palayoor et al. 2014) that also indicated that different gene expression profiles in human carcinoma cell lines were irradiation dose delivery dependent. In addition, Coleman's group previously identified potential therapeutic targets in human prostate carcinoma cells exposed to fractionated irradiation (John-Aryankalayil et al. 2010).

Therefore, with regard to these observations, our findings also suggest that fractionated dose irradiation could be a more relevant approach in identifying genes and molecular pathways clinically important to the improvement of radiotherapy.

In the present study we have demonstrated that the most significantly altered functional categories in LLC1 cells following all irradiation regimens were cell cycle regulation and P53 signaling pathways. In addition, the most significant pathway enrichment was identified in cells exposed to FD.

Previous studies suggested that the tumor suppressor P53 plays a central role in cellular response to irradiation in P53 wild type cell lines (Fei and El-Deiry 0000, Gudkov and Komarova 2003, Rashi-Elkeles et al. 2011). The radiation-induced activation of P53 results in temporary cell cycle arrest to facilitate damaged DNA repair as well as apoptosis if the DNA damage is too severe (Fei and El-Deiry 0000, Mirzayans et al. 2012). In this study we found that the majority of cell cycle genes were downregulated in LLC1 cells following SD and FD regimens including genes promoting G1-S and G2-M transition. Interestingly, the expression of kinases Atr and Chek1, which are implicated in S-phase DNA damage checkpoint (Willis and Rhind 2009), was also downregulated in LLC1 cells exposed to irradiation. In addition, treatment with irradiation resulted in a significant upregulation of cyclin dependent kinase inhibitor P21 which is a master regulator of cell cycle checkpoints (Cazzalini et al. 2010). However, the deregulation of gene expression was more robust in cells exposed to FD. These included differentially expressed genes associated with the progression of DNA replication and mitosis. For instance, the expression of anaphase-promoting APC/C complex encoding genes including Cdc26, Cdc27, Anapc2 and Anapc11 was altered in cells exposed to FD. In addition, FD irradiation deregulated the expression of Bub1 and Bub3 which are involved strictly in the spindle assembly checkpoint and the regulation of APC/C catalytic activity (Shepperd et al. 2012). In addition, the irradiated LLC1 cells demonstrated a significantly upregulated expression of genes involved in the

regulation of apoptosis. However, microarray data indicated that the deregulation of gene expression associated with pro-apoptotic process peaked in cells exposed to SD10. The expression levels of anti-apoptotic genes including Bcl2l1 and Akt2 were more elevated in cells after the exposure to FD compared to SD. These data correlated with the finding that the survival fractions of LLC1 cells were significantly higher after exposure to FD compared to SD10. Therefore, together these results indicate that the final prosurvival outcome of radiation-induced DNA damage response of LLC1 cells treated with FD is dependent on the cumulative effect of the differential expression of genes.

The present study revealed that the expression of genes involved in the immune response was significantly altered in LLC1 cells following all irradiation regimens. Despite that, the extent of differentially expressed genes was similar in cells exposed to SD10 and FD, but the set of differentially expressed inflammatory genes was significantly different between these irradiation protocols. This is in accordance with previous reports that indicated a distinct expression profile of immune response genes in cells exposed to SD or FD (John-Aryankalayil et al. 2010, Palayoor et al. 2014). The microarray analysis also demonstrated that genes from the immune response category differently expressed in the irradiated LLC1 cells included genes encoding chemokines, cytokines and cytokine receptors, tumor necrosis factors and other proteins involved in the regulation of immune response signaling. Our results are consistent with previous studies demonstrating that RT can promote the immune recognition of tumor cells by increasing the expression of antigen presenting molecules, pro-inflammatory cytokines and the release of "danger signals" leading to the attraction of the immune cells to the irradiated tumor site (Formenti and Demaria 2013). Moreover, the expression of transcription factors including Nfatc1 and Stat1 was upregulated in cells exposed to SD and FD irradiation. Members of the STAT family have been shown to activate the transcription of genes involved in cancer cell survival, proliferation and angiogenesis (O'Shea et al. 2015). In addition, it was shown that the overexpression of Stat1 in tumor cells

is associated with in an increased resistance to irradiation (Khodarev et al. 2004, Zhan et al. 2011). Furthermore, the treatment with FD elevated the expression of Stat5a suggesting that other Stat family members could be involved in the resistance to radiotherapy. This is further supported by a previous study that demonstrated a correlation between the expression levels of Stat5a and the radiosensitivity in HNSCC cancer cells (Stegeman et al. 2013). Therefore, these findings suggest that radiation-induced immune response in the irradiated LLC1 cells may contribute to the outcome of tumor development in a dose delivery dependent manner. Furthermore, radiation-induced changes in the expression of inflammatory genes in tumor cells and the tumor microenvironment are considered to be pro-imunogenic, increasing the ability to combine RT with immunotherapy for cancer treatment (Kalbasi et al. , Frey et al. 2014). Preclinical data also indicates that the promotion of antitumor immune response is irradiation delivery type dependent since RT delivered as single dose is not sufficient to induce antitumor immunity (Dewan et al. 2009, Schaue et al. 2012, Kulzer et al. 2014). Together these findings suggest possible directions for the development of more efficient anticancer irradiation treatment strategies, based on exploiting the prosurvival and immunogenic tumor inflammatory pathway alterations during FD irradiation.

Several previous studies have shown that exposure to single dose irradiation results in differential expression of miRNAs in various cancer and normal cells (reviewed in (Metheetrairut and Slack 2013)). In the present study, the expression of a total of 18 miRNAs was significantly altered in LLC1 cells exposed to IR. The microarray analysis also identified that the expression of miR-34 cluster miRNAs including miR-34b and miR-34c was significantly up-regulated in cells exposed to both irradiation regimens. Previous reports have shown that members of the miR-34 family are regulated by P53 and are involved in the regulation of cell cycle arrest, proliferation inhibition and apoptosis (Hermeking). miR-34 family miRNAs were also shown to be up-regulated in different human cancer cells exposed to IR (Josson et al. 2008, Girardi et al.

2012). These observations suggest that miR-34 family miRNAs play a key role in the response to IR in LLC1 cells. The microarray data analysis demonstrated that fractionated irradiation induced the most robust deregulation of miRNA expression, indicating that the expression of miRNA is also altered in an irradiation delivery dependent manner. Similar results were shown in previous reports that demonstrated a higher magnitude of changes in the expression of miRNA in prostate cancer and endothelium cells following FD (John-Aryankalayil et al. 2012, Palayoor et al. 2014). In addition, Leung et al. (Leung et al. 2014) reported that only a small number of miRNAs differentially expressed in breast cancer cells exposed to SD or FD were the same, suggesting that FD induces a distinct miRNA signature compared to SD treatment.

To further extend the understanding of the role miRNAs play in the cellular response to IR, we performed miRNA target filter analysis to identify potential functional relations between differentially expressed mRNA and miRNA in LLC1 cells exposed to radiation. However, the identification of regulatory miRNAs and their target mRNAs is a major challenge since a single miRNA may regulate multiple mRNAs and vice versa. In addition, statistical methods which are able to identify these miRNA controlled regulations may result in thousands of putative miRNA-mRNA pairs leading to the inability to extract biologically relevant understanding of the collective function of differentially expressed miRNAs. Therefore, in the present study we focused on the negative correlation between the expression of miRNA and genes associated with P53, cell cycle, apoptosis and immune response pathways which were shown to be the most prominently altered in LLC1 cells following SD and FD irradiation.

It has been shown that the transcription factor P53 plays an important role in the regulation of the transcription of several miRNAs which in turn control the expression of P53-regulated genes mediating cell cycle arrest and apoptosis (Hermeking , Hermeking 2012). The present miRNA target analysis revealed an inverse correlation between miR-34c and differentially expressed E2f3, E2f5 and

Ccne2 suggesting that the up-regulation of miR-34c could be associated with G1 phase control in LLC1 cells exposed to radiation. This is also supported by previous reports that have pointed out the role of miR-34c in the induction of G1 as well as G2/M cell cycle arrest (Cannell et al. 2010, Achari et al. 2014). In addition, Li et al. (Li et al. 2015) have shown that the expression of E2F3 was also reduced after the up-regulation of miR-34c in endometrial carcinoma cells indicating that E2F3 could be a target of miR-34c. Furthermore, our results identified a negative correlation between several miRNAs and genes differentially expressed in cells exposed to FD. For instance, the upregulation of miR-30c correlated with the downregulation of Ccne2, Stag1, Orc4 and Skp2. In addition, the expression of Stag1 and Orc4 inversely correlated with the differential expression of miR-129, miR-145a and miR-186. Taken together, our observations suggest that these miRNAs may play an important role in cell cycle arrest in LLC1 cells in an irradiation dose delivery dependent manner. However, we did not observe any significant correlation between differentially expressed miRNAs and genes involved in apoptosis with the exception of a negative correlation between the expression of miR-30c and Ppp3cb. Nevertheless, several miRNAs differentially expressed after irradiation were previously shown to be associated with the regulation of apoptosis implying their potential role in irradiated LLC1 cells. For instance, the overexpression of miR-129 promoted cellular death of irradiated breast cancer cells by targeting HMGB1 (Luo et al. 2015). miR-30c was also demonstrated as a key player in radiation-induced hematopoietic cell damage response (Li et al. 2012).

There is emerging evidence that miRNAs are involved in radiation-induced regulation of the inflammatory responses (John-Aryankalayil et al. 2012, Zhao et al. 2013, Palayoor et al. 2014). Target filter analysis revealed that almost all miRNAs differentially expressed in LLC1 cells exposed to SD and FD showed inverse correlations with several genes associated with immune response underlining the role of miRNA in the inflammatory response to irradiation. Target enrichment data also indicated that the regulation of miRNA and

inflammatory gene network in LLC1 cells treated with fractionated irradiation was significantly different. In addition, the upregulation of Stat1 correlated with miR-710 and miR-105 which were downregulated in cells exposed to SD or FD, respectively. The data present reveals, that treatment with FD also upregulated the expression of miR-145-5p which was identified previously to target Stat1 (Gregersen et al. 2010) indicating that some differentially expressed genes could be regulated by distinct miRNAs in cells irradiated with SD or FD. Therefore, these data suggest that the regulation of immune response by miRNAs in irradiated LLC1 cells might be irradiation dose delivery dependent.

However, the present study also clearly demonstrated that the expression of genes and miRNAs induced in LLC1 cells after the exposure to irradiation did not elevate in cells irradiated *in vivo*. Despite the fact that treatment with SD10 increased the expression of genes involved in P53 pathway in LLC1 tumors, no significant changes in the expression of selected genes and miRNAs were observed *in vivo* following the exposure to fractionated irradiation, suggesting that radiation-induced changes in gene and miRNA expression might be differently modulated by the tumor microenvironment. In fact, similar results were obtained by previous studies which have applied different strategies to validate *in vitro* data. Camphausen et al. (Camphausen et al. 2005) reported that glioblastoma U87 and U251 cells exposed to single dose of 6 Gy *in vivo* exerted a different set of differentially expressed genes compared to cells grown in tissue culture. Moreover, Tsai et al. (Tsai et al. 2007) demonstrated that prostate cancer DU145 cell xenografts exhibited a completely different profile of genes induced by both SD and FD compared to the same cells exposed to irradiation *in vitro* indicating that a 10 Gy exposure *in vivo* could only reach an effect of up to 3 Gy exposure under *in vitro* growth conditions. Therefore, these data suggest that the investigations on the functional consequences of gene and miRNA expression will require considering to more biologically relevant experimental conditions.

In summary, our results indicated that the gene and miRNA expression profiles in LLC1 cells exposed to irradiation were dose delivery type dependent.

Data analysis also revealed mRNAs possibly regulated by miRNAs in a radiation dependent manner, suggesting those mRNAs and miRNAS as potential targets to modulate radiation-induced cell response after the exposure to SD or FD irradiation. The tumor response to fractionated irradiation was different compared to irradiated cells *in vitro*, suggesting that experimental *in vitro* conditions, especially the tumor microenvironment, should be reconsidered in more detail to promote the development of more efficient radiotherapy. Nevertheless, the present study points out the key pathways involved in radiation induced response of murine cancer cells exposed to irradiation. Our data obtained utilizing LLC1 cells in monolayer cell culture and syngeneic LLC1 tumors can be further applied to improve the outcome and the development of radiotherapy in preclinical animal model settings.

4.2 The regulation of gene expression in an ECM dependent manner

The loss of numerous physiological features was noted in cancer cells cultivated in 2D cell cultures, leading to a poor representation of molecular events occurring in tumor tissue (Ross et al. 2000, Irish et al. 2004). Nevertheless, restoration of cell characteristics physiologically more representative of tumor tissue, including cellular phenotype, gene expression and signaling patterns, is expected when cells are cultured in 3D (Storch et al. 2010). Observations that cancer cells grown under 3D cell culture conditions are less susceptible to agents of anticancer treatment suggest that differential gene expression profiles in cancer cells grown in 2D compared with 3D cell culture provide a therapeutic window for molecular targeting and prognostic strategies that could be used in the development of anticancer therapy. Therefore, in the present study we compared cellular morphology, genome-wide gene and miRNA expression changes in murine Lewis lung carcinoma cells and genome-wide expression changes in two human colon carcinoma cell lines DLD1 and HT29 grown in lr-ECM 3D cell culture to cells grown on plastic. The present results indicate the most significantly altered functional pathway categories in cells cultured under 3D cell culture conditions.

In the second part of the study, we observed that cells grown under lr-ECM 3D cell culture conditions compared to 2D displayed specific morphological changes as LLC1, DLD1 and HT29 cells formed 3D spheroids. These observations are consistent with a previous report that demonstrated similarly altered cellular morphology of CRC cells cultured in “ECM on top” 3D model (Luca et al. 2013). In addition, Kenny et al. also indicated that distinct 3D cell culture phenotypes of breast cancer cells reflected distinct gene-expression profiles correlated with invasiveness of tumor cell lines obtained from metastases (Kenny et al. 2007). These observations suggest that the ECM provides a more reliable microenvironment than plastic and is markedly mare similar to the microenvironment in tumor tissue. Hence, further investigation of differential

gene expression profiles using 3D cell culture models could uncover molecular characteristics of CRC cells closely related to tumors *in vivo*, which cannot be well established in 2D cell cultures.

Our findings demonstrated a markedly altered gene expression signature of LLC1 and CRC cells grown lr-ECM 3D cell culture conditions compared to 2D. The differences in cell culture conditions resulted in 1884 differently expressed genes in LLC1 cells demonstrating the broad influence of the ECM environment in gene expression regulation. In addition, we also found that the expression of selected hnf4a, infb1, klf8 and fgfr4 genes was significantly increased in LLC1 tumors likewise in LLC1 cells cultured under 3D cell culture conditions compared to gene expression levels in cells grown on plastic. Our microarray data also demonstrated significantly altered expression signatures in CRC cells between the two cell culture models. We found that changes in cell culture conditions resulted in a significantly altered expression of a total 841 and 1190 genes in DLD1 and HT29 cells, respectively. Furthermore, our results revealed that a higher number of genes were down-regulated in an ECM-dependent manner compared to 2D. In addition, microarray data also indicated 383 common genes differentially expressed in both cell lines, and most of these genes were also down-regulated in an ECM-dependent manner. Together these findings are consistent with previous reports that noted significantly altered gene-expression profiles in numerous cancer cell types between 2D and 3D cell culture models (Fournier and Martin 2006, Härmä et al. 2010, Zschenker et al. 2012, Luca et al. 2013). Furthermore, KEGG pathway enrichment results revealed significant ECM-dependent alterations in gene functional categories in LLC1 and CRC cells grown in 3D. We found that MAP kinase, cell adhesion and immune response functional pathway categories were most significantly altered in LLC1, DLD1 and HT29 cells between 2D and 3D culture conditions, suggesting the existence of common molecular mechanisms controlled in an ECM-dependent manner.

Our findings are in agreement with a previous reports also indicating that cellular adaptation to a 3D culture environment significantly alters the expression of genes involved in ECM and cell adhesion (Frith et al. 2010, Zschenker et al. 2012). In addition, our results indicate that functional categories associated with cell–ECM and cell–cell interactions were most significantly altered in CRC cells. In addition, microarray data revealed significantly altered expression of numerous integrins (ITGA3, ITGB4/5/7/8) in CRC cells grown under 3D and 2D cell culture conditions. These findings are in accordance with a previous report that also showed a differential expression of genes involved in the regulation of integrin signaling and cell–cell interaction, leading to different cellular response to radio- and chemotherapy (Zschenker et al. 2012). In addition, Bissel et al.'s group also demonstrated that the inhibition of the integrin signaling cascade remarkably influenced the cellular phenotype and behavior of breast cancer cells cultured in 3D, indicating the key role of the ECM–integrin signaling cascade during cellular adaptation to a 3D cell culture microenvironment (Weaver et al. 1997).

Two previous studies demonstrated differential expression of MAPK pathway genes in CRC cells cultured under ECM 3D cell culture compared with 2D using genome-wide transcriptome approach. Tsunoda et al. revealed that activated V-Ki-ras2 Kristen rat sarcoma viral oncogene homolog (KRAS) in colon carcinoma HCT116 cells markedly suppressed DNA repair genes and apoptosis in a 3D cell culture but not in 2D, suggesting a critical role of MAPK pathway in accumulation of genetic mutations through inhibition of tumor-suppressor genes (Tsunoda et al. 2010). Luca et al. also demonstrated altered epidermis growth factor receptor (EGFR) protein levels and a switch between rat sarcoma oncogene RAS-MAPK pathway activation between 2D and lr-ECM 3D models, suggesting that cellular adaptation to a 3D microenvironment might promote essential reorganization of molecular mechanisms to acquire resistance to targeted therapy during cancer progression (Luca et al. 2013). In keeping with previous considerations, The MAP kinase signaling pathway was the one of the

most significantly altered KEGG categories and resulted in 25 genes differently expressed in LLC1 cells cultured under lr-ECM 3D culture conditions compared to 2D. Furthermore, our microarray results indicated altered expression of fibroblast growth factor-related FGFR3, FGF9/19/20 and MAPK kinases MAP2K3, MAP3K1, MAP3K5, MAP3K8 and MAP3K14 genes in CRC cells grown under 3D and 2D cell culture conditions. Together these observations suggest that the ECM plays crucial role in regulation of MAPK pathway-related genes. Thus, 3D culture model as a useful approach could promote the investigation of MAPK-driven molecular mechanisms in CRC development and might also be exploited for the development of targeted cancer therapy.

Additionally, microarray data also revealed differential expression of genes associated with inflammatory response in LLC1 and CRC cells grown under lr-ECM 3D and 2D conditions. We found that the expression of genes related to cytokine (e.g. IL8) and chemokine (e.g. CXCL1-3) signaling pathways were markedly altered in CRC cells an ECM-dependent manner. In addition, our results also depicted the differential expression of cytokine receptors (il2ra, il12rb2, il21r and il22ra), chemokine receptors (ccr3, xrc1 and cxcr7) and tumor necrosis factor receptors (tnfrsf1b, 9, 11a and 25) supporting further modulation of cross-talk between cancer and their microenvironment in ECM dependent manner, which cannot be established in 2D cultures. Chemokines and cytokines play the key roles in the initiation of immune response during tumor development (Burkholder et al. 2014). Chemokines attract lymphocytic migration, whereas cytokines can direct the polarization and activation of antigen-presenting cells (e.g. macrophages) and T-cells. Nevertheless, deregulated signaling of cytokines and chemokines in a tumor microenvironment promotes tumor progression (Zamarron and Chen 2011). Furthermore, interferon 1 beta (infb1) was the most significantly up-regulated inflammatory gene in LLC1 cells under 3D conditions. Interferons have been shown to promote anti-proliferative, anti-angiogenic and immunoregulatory effects on many tumor types (Wilderman et al. 2005, Trinchieri 2010). Nevertheless, we also observed increased ifnb1 levels in mouse

LLC1 tumors suggesting that the primary role of elevated basal ifnb1 levels could be more associated with regulation of tumor immuno-surveillance, but not necessarily with tumor suppression. Our results also indicated increased expression of NFAT family nfatc2 and nfatc4 genes in LLC1 cells grown under lr-ECM 3D culture conditions as compared to 2D. As NFAT transcription factor family was originally identified to mediate the response of immune cells, recent studies have demonstrated that NFATs also perform important roles in formation of tumor microenvironment. Activation of NFAT signaling in cancer cells results in inflammatory chemokine production eventually leading to recruitment of inflammatory cells to the tumor (Grivennikov et al. 2010). Interestingly, a recent report suggested that NFAT2 constitutive activation in transgenic mice also linked the microenvironment and the neighboring cells, as both tumor cells expressing NFAT2 and neighboring wild-type cells up-regulated c-Myc and STAT3 in spontaneous skin and ovary tumors (Tripathi et al. 2014). On the other hand, previous reports also associated NFAT signaling axis to VEGF driven tumor angiogenesis regulation indicating complex nature of NFAT in metastatic niche formation (Minami et al. 2013). Therefore, we suggest that the 3D cell culture model should be considered as an essential tool for the investigation of genes involved in tumor cell–immune system interactions. A better understanding of the cross-talk between tumor and immune cells in an ECM-dependent manner could also notably promote development of preclinical targeted immunotherapy which cannot be properly established under 2D culture conditions.

While it has been well observed that miRNAs regulate the expression of ECM molecules, emerging evidence shows that miRNA expression and function could be significantly affected by the ECM (Rutnam et al. 2013, Soon and Kiaris 2013). Consistent with these observations, in the present study microarray data demonstrated a signature of significantly altered expression of 77 miRNAs in LLC1 cells grown under 2D and lr-ECM 3D cell culture conditions compared to cells cultured on plastic. Interestingly, our results showed that ECM strongly induced the up-regulation of miRNA in LLC1 cells grown under 3D culture

conditions. This is in accordance with a previous report which suggested that global upregulation of miRNA expression may be linked with the changes in cellular density (Hwang et al. 2009). Furthermore, our results also indicated that the ECM induced upregulation of miR-466~467~669 (e.g. miR-466b,c,d), miR-376 (miR-376a, miR-376b, miR-376c), and miR-34 (miR-34b and miR-34c) clusters. The miR-466~467~669 cluster is known as one of the largest miRNA clusters in mouse genome containing 71 miRNAs. A previous report (Zheng et al. 2011) suggested that members of this cluster are abundantly expressed during mouse embryo development and might regulate growth and survival of embryonic stem cells. On the other hand, it has been shown that miR-376 cluster miRNAs are associated with tumorigenesis. For example, elevated expression of miR-376a promoted tumor cell migration and invasion and also positively correlated with advanced tumor metastasis and shorter patient survival (Choudhury et al. , Mo et al. 2014). In addition, overexpression of miR-376c increased ovarian cancer cell survival and was associated with a poor response to chemotherapy (Ye et al. 2011). Moreover, elevated levels of miR-376c were shown in plasma of early stage breast cancer patients (Cuk et al. 2013). By contrast, miR-34 cluster encodes miRNAs possessing tumor suppressive properties mediating apoptosis, cell cycle arrest and senescence (Hermeking 2009). Our miRNA microarray data were consistent with previous reports indicating that human cancer cells cultured on ECM 3D cell culture conditions have also exhibited a significantly altered miRNA expression profile compared to cells cultured on plastic (Li et al. 2012, Nguyen et al. 2012, Price et al. 2012). ECM 3D cell culture associated miRNA profiles demonstrated altered expression of tumor suppressive and oncogenic miRNAs and also correlated with distinct cellular morphogenesis under 3D culture conditions highlighting the regulation of miRNA expression in an ECM dependent manner. Additionally, we also showed that the expression of selected miR-195a, miR-207, miR-376c and miR-466f miRNAs was also significantly increased in mouse LLC1 tumors as compared to miRNA expression levels in 2D indicating the potential role of these miRNAs in

tumor progression *in vivo*. Altogether, these findings suggest that the 3D cell culture should be considered as a critical experimental approach for essential understanding of the miRNA biology associated with tumor microenvironment. Indeed, the gene expression signature of 3D culture of breast cancer cells has been found to define prognostic value for patients with breast cancer (Martin et al. 2008). Understanding how ECM regulates miRNA expression will also further elucidate how miRNAs determine tumor development and reveal potential prognostic and therapeutic opportunities.

Further on we also investigated potential relations between 77 differently expressed miRNAs and their target genes to depict possible miRNA-mRNA interactions in LLC1 cells regulated by ECM microenvironment under 3D cell culture conditions. We found that 8629 unique target genes could be regulated by these differently expressed miRNAs. Pathway enrichment analysis also revealed that 69 KEGG pathways were enriched in target genes related to these miRNAs including pathways involved in tumor development. However, as it is known that miRNA targets multiple mRNAs, the ability to find the key pathways by computational approaches is highly dependent on size of miRNA profile. In addition, the statistical target analysis approach could be successful if the miRNA of interest has an effect on the abundance of expressed target gene, but not if expression of target gene is regulated only by translational inhibition. Hence, we focused on negative correlation analysis between differently expressed miRNA and genes associated with MAPK, cell adhesion and immune response pathways in LLC1 cells grown under 2D and 3D cell culture conditions. Indeed, we found that differently expressed genes associated to these pathways could be potentially regulated by miRNAs differently expressed in LLC1 cells.

In the present study, the miRNA target filter analysis identified that the expression of kras, mknk1 and pak2 kinases involved in the MAP kinase pathway negatively correlated with the expression of miR-761, mir-195 and miR-297a, respectively. The target correlation analysis also depicted miR-34b, miR-34c, miR-466f and miR-500 miRNAs as potential negative regulators of sos2 gene

expression. However, the evidence implicating miRNAs role in MAP kinase pathway is still emerging. Previous report suggested that miR-34c may suppress proliferation of lung cancer cells by inhibition of MAPK pathway (Zhou et al. 2015). In addition, previous data also associated regulation of miRNAs with MAP kinases in pancreatic cancer cells showing that expression of miR34a inversely correlated with MAPK pathway activity (Ikeda et al. 2012). Ichimura et al. also demonstrated that miR-34a suppressed the expression of MEK1 leading to repression of the MEK-ERK signaling axis (Ichimura et al. 2010). In the present study we also observed a significant link between deregulated expression of miRNA and cell adhesion molecules. For example, our results indicated a negative correlation between expression of col1a1 and miR-135a, miR-137 and miR-590. In addition, decreased flna expression might be influenced by miR-328 and miR-761. These findings are consistent with a previous report indicating the presence of feedback mechanisms that promote ECM molecules, which are downstream targets of specific miRNA, to regulate expression of these miRNAs (Price et al. 2012). A similar target enrichment analysis also revealed that increased expression of miRNAs might be connected with the regulation of immune response pathway genes. For example, our results depicted a negative correlation between expression of chemokine receptor xcr1 and miR-669b. Additionally, we also noted that decreased expression of oas3 might be affected by numerous miRNAs. Thus, taken together these findings suggest that metabolic, MAP kinase, cell adhesion and immune response pathway genes might be regulated by miRNAs altered in ECM dependent manner. Therefore, the 3D cell culture model could be applied not only for further investigation of common cancer pathways altered in ECM dependent manner but also for the study of specific miRNAs involved in ECM-mediated cancer signaling networks. Further understanding of complex ECM dependent signaling networks in tumors could direct to novel cancer treatment strategies.

In summary, our results indicated the MAP kinase, cell adhesion and immune response as the most significantly altered functional categories in LLC1,

DLD1 and HT29 cells during the switch from 2D to 3D. Global miRNA expression analysis confirmed the involvement of miRNA in the regulation of ECM dependent properties of cancer cells. Comparison of the expression levels of selected genes and miRNA between LLC1 cells grown in 3D cell culture or LLC1 tumors implanted in mice indicated correspondence between both model systems. Therefore, the present results indicate the existence of universal regulation for the key pathways both in 3D culture and tumor suggesting the most promising directions for translational cancer research using the 3D cell culture models.

4.3 Microenvironment and dose delivery dependent response to ionizing radiation in human colorectal cancer cell lines

As discussed previously, the extracellular matrix plays an important role in cancer cell development and other cancer related molecular processes (Hanahan and Weinberg). Moreover, cells cultured under ECM based 3D cell culture conditions maintain an increased resistance to common cancer therapies and could be employed to identify gene signatures for the prediction of clinical outcome (Fournier and Martin 2006, Fernandez-Fuente et al. 2014). Therefore, in the third part of the study, we focused on genome-wide transcriptome changes of human colorectal cancer DLD1 and HT29 cell lines (both bearing distinct P53 mutations) grown in 3D culture following SD of 2 Gy and 10 Gy or FD 5x2 Gy irradiation to indicate possible molecular mechanisms promoting tumor cell resistance to irradiation.

In the present study, both DLD1 and HT29 cells showed significantly enhanced cell survival under 3D culture conditions following both irradiation protocols compared to cells grown in 2D. In addition, exposure to FD resulted in an increase of clonogenic survival under 3D cell culture conditions in both cell lines, compared to SD. These results correlated with previous data that indicated an increase of cell adaptation to irradiation following FD regimen under 2D cell culture conditions (John-Aryankalayil et al. 2010, John-Aryankalayil et al. 2012). In addition, other studies have clearly demonstrated an increase in cell survival after SD treatment in a cell-cell and cell-ECM interaction dependent manner leading to increased DNA repair rate, chromatin remodeling or maintenance of cell survival in association to the activation of the integrin signaling cascade (Hehlgans et al. 2007, Storch et al. 2010). Therefore, together these findings suggest that that fractionated dose irradiation could be a more relevant approach to further predict and identify genes potentially involved in cancer cell response to radiation treatment and cell survival when cells are exposed to irradiation under lr-ECM 3D cell culture conditions.

In the present study, the microarray data demonstrated significantly different gene expression patterns in response to SD or FD treatment in CRC cells under lr-ECM 3D cell culture conditions compared to non-irradiated cells. Most of these genes were downregulated in both DLD1 and HT29 cell lines and a significantly higher number of downregulated genes were common amongst all radiation doses, thus implying that decreased gene expression is a general result of the cellular response to IR. This study also demonstrated that altered gene expression patterns significantly differed between CRC cell lines. The differential expression of P53 target genes involved in cell cycle control, DNA replication and DNA damage repair was clearly evident in DLD1 cells in an irradiation dose delivery dependent manner. In addition, the qPCR analysis indicated that the expression of genes involved in P53 signaling pathway in DLD1 cells could be induced in a cell-ECM interaction dependent manner.

The function of P53 is frequently altered or impaired in human tumors and a major variety of P53 mutants exhibit gain of function properties that further could be involved in prosurvival signaling and tumor progression (Oren and Rotter 2010). Consequently, the cellular response to irradiation may also depend on the variety of mutations occurring in P53 (OKAICHI et al. 2008). If such mutations facilitate the activation of the cell cycle and DNA repair pathways but not apoptosis, gain of function would increase cellular survival following irradiation. Therefore, the activation of the P53 related pathways could increase radiation survival in DLD1 cells exposed to irradiation.

Radiation induced DNA damage mediated activation of cell cycle checkpoints results in the arrest of cell cycle to allow the repair of damaged DNA, if the damage is not too severe. Previous studies have also suggested that the regulation of DNA repair pathways may be induced at early time points following irradiation and may be involved in the adaptive response to irradiation inflicted stress (Sharp et al. 2007, Short et al. 2007). In the present study we demonstrated that cell cycle and DNA replication/DNA damage repair pathways were the most significantly enriched KEGG categories altered in DLD1 cells in

an irradiation dose delivery dependent manner. Microarray results also demonstrated that the expression of genes promoting G1/S or G2/M cell cycle transition was significantly increased in DLD1 cells following FD. On the contrary, previous studies have demonstrated that the expression of genes promoting cell cycle transition was significantly downregulated in P53 wt cells grown in a 2D culture following irradiation with SD or FD (John-Aryankalayil et al. 2010, John-Aryankalayil et al. 2012, Palayoor et al. 2014). Moreover, a study of NCI-60 cell line panel irradiated with SD of 8 Gy indicated a similar set of downregulated genes involved in G2/M transition in cell lines carrying wt P53 (Amundson et al. 2008). Therefore, considering these findings, our observations suggest that the activation of the expression of cell cycle progression genes in DLD1 cells in an ECM dependent manner might be associated with the increased survival of tumor cells during the course of radiotherapy. This is further supported by the previous observations indicating that genes involved in the cell cycle progression could also directly contribute to the maintenance of DNA damage repair (Enserink and Kolodner 2010, Chen et al. 2011, Chen et al. 2016). In addition, Storch and Cordes indicated that the over-expression of CDK9 mediated radioprotection of HNSCC cell lines grown in lr-ECM 3D cell culture conditions (Storch and Cordes 2016). Furthermore, our data demonstrated that the expression of DNA repair genes peaked in DLD1 cells exposed to FD. On the contrary to this finding, previous genome-wide studies showed no significant changes in expression of DNA damage repair genes in cells after SD and FD irradiation (John-Aryankalayil et al. 2010, Simone et al. 2013) or the expression of DNA repair genes was significantly downregulated in exposed cells grown in 2D (Tsai et al. 2007, Palayoor et al. 2014). However, it was previously demonstrated that an increased DNA damage repair in tumors cells exposed to irradiation under lr-ECM 3D cell culture conditions could be ECM signaling dependent (Eke et al. 2012, Hennig et al. 2014, Eke and Cordes 2015). These findings suggest that DNA repair genes could be involved in resistance to IR in DLD1 cells grown under 3D cell culture conditions. Therefore, the inhibition of

these pathways could be employed for the modulation of cellular radiosensitivity during the radiotherapy treatment.

This study revealed that the expression of a relatively high number of immune response genes was altered in both CRC cell lines in an irradiation delivery dependent manner. Nevertheless, fold change levels of differentially expressed genes peaked in HT29 cells exposed to FD irradiation. The most significantly up-regulated genes included those encoding for interferon stimulated gene (ISG) family proteins, which have been shown to activate several immune system components in response to viral infection and regulate pro-inflammatory processes (Melchjorsen et al. 2009, Diamond and Farzan 2013). In addition, the expression of interferon λ (IL29, type III interferon) was significantly induced in HT29 cells following the FD regimen. IL29 have been reported to possess antiviral, anti-proliferative and *in vivo* antitumor activities (Uze and Monneron 2007). This is in accordance with previous reports, indicating that response to IR is dependent on interferon (INF) cytokines (Tsai et al. 2007, Simone et al. 2013). It was also shown that irradiated cells harboring elevated expression of ISGs were significantly more radioresistant, indicating that the modulation of the interferon signaling pathway could be applied in immunoradiotherapy (Kita et al. 2003). Therefore, these observations suggest that INF inducible genes also could be linked to ECM-cell interaction dependent radioresistance. In addition, one of the key mediators of the type I and type III interferon JAK-STAT signaling pathway, STAT2 was upregulated in a fashion described above. STAT1 and STAT2 associate with IFN regulatory factor 9 (IRF9) to form transcription factor complex ISGF3, which further drives transcription of various INF related genes (Au-Yeung et al. 2013). Previous data also demonstrated that elevated levels of STAT2 in cells leads to more resistant response to DNA damage (Cheon et al. 2013). Therefore, together these observations highlight the possible link between cell immune response and tumor cell niche formation via inflammatory processes in cancer cells exposed to ionizing radiation. In addition, the expression patterns of many immune response

genes are used as biomarkers for *in vivo* chemotherapeutic agent activity screening (Cairo et al. 2012), thus results obtained in our present study under ECM based 3D cell culture conditions may help to further improve targeted radiation therapy.

A minority of differentially expressed genes were similarly upregulated or downregulated in CRC cell lines following irradiation. Several immune response genes were upregulated in CRC cells exposed to SD of 10 Gy including RELB, NFKBIA, NFKBIE. The NF-κB pathway has been reported to play an important role in the formation of an inflammatory microenvironment during malignant progression and it is also involved in the development of tumor radioresistance (Karin 2009, Li and Sethi 2010). Treatment with SD in CRC cells also resulted in downregulation of genes involved in the cell cycle progression including AURKA, PLK1, CCNB1, CDC25C and PTTG2. In addition, the expression of HIST2H2BF and HIST1H3A which are the key components of nucleosome structure was downregulated in CRC cells exposed to SD of 10 Gy or FD, respectively. The pathway enrichment analysis revealed that the expression of genes encoding histones was significantly downregulated in DLD1 cells exposed to irradiation. This finding indicates that treatment with irradiation could induce the rearrangement of chromatin in CRC cells. This is supported by the recent evidence suggesting that the chromatin organization could mediate the cellular response to DNA damage (Costes et al. 2010). Chromatin decondensation around the DSB was associated with subsequent activation of ATM (Kim et al. 2009). Previous findings also showed a connection between heterochromatin factors, heterochromatin protein 1α and ATM dependent radiation-induced DNA damage repair (Goodarzi et al. 2008). In addition, Cordes group evaluated the role of chromatin condensation for the radiation survival of cells grown in 2D and 3D culture (Storch et al. 2010). They indicated that increased levels of heterochromatin in cells cultured in 3D resulted in increased cellular survival, decreased number of DSBs and chromosome aberrations. Furthermore, it was shown that cellular radiosensitivity in 3D cell culture conditions might be

modulated by the specific inhibitors of chromatin factors HDACs (Storch et al. 2010, Hehlgans et al. 2013). However, the mechanism by which chromatin architecture mediates DNA lesions remains unclear. Therefore, a further assessment of this association is needed for the development of targeted therapeutic approaches in radiotherapy.

In summary, fractionated dose irradiation resulted in different genome-wide gene expression profiles compared to a single dose treatment in colorectal cancer DLD1 and HT29 cells grown under 3D culture conditions. Despite the fact that a higher number of genes were down-regulated in both CRC cell lines exposed to irradiation, cell cycle/DNA damage or immune response genes being the most significantly up-regulated following irradiation in 3D conditions DLD1 and HT29 cells cultured in 3D, respectively. In addition, we demonstrated a higher radiotolerance in both CRC cells grown under 3D cell culture conditions compared to 2D. Furthermore, the expression signature of selected genes following FD treatment was dependent on cell culture conditions and resulted in higher expression in cells under 3D conditions. In addition, we demonstrated higher radiotolerance in both cell lines under 3D cell culture conditions compared to 2D. Therefore, the data in the present study suggest that ECM based 3D cell culture models in combination with the fractionated dose treatment of ionizing radiation could accelerate the understanding of molecular mechanisms associated with therapy dependent radioresistance in tumors and promote the development of more efficient radiotherapy.

CONCLUSIONS

1. Global gene and miRNA expression profiles of Lewis lung carcinoma LLC1 cells exposed to irradiation is irradiation dose delivery dependent. However, the expression of genes and miRNAs between 2D cell culture and tumors do not correspond after the exposure to fractionated dose irradiation;

2. The expression of genes and miRNAs in Lewis lung carcinoma LLC1 cells as well as the expression of genes in human colorectal carcinoma DLD1 and HT29 cells is significantly altered in an ECM dependent manner;

3. Common pathways including MAP kinase, cell adhesion and immune response are significantly altered in cancer cells of different origin in an ECM microenvironment dependent manner;

4. Cellular response to fractionated dose irradiation in human colorectal carcinoma DLD1 and HT29 cells is ECM-dependent. Differentially expressed genes involved in cell cycle/DNA damage repair or immune response pathways are considered as potential target candidates for the further improvement of radiotherapy.

LIST OF PUBLICATIONS

1. Stankevicius V, Vasauskas G, Bulotiene D, Butkyte S, Jarmalaite S, Rotomskis R, Suziedelis K. (2016) Gene and miRNA expression signature of Lewis lung carcinoma LLC1 cells in extracellular matrix enriched microenvironment. BMC Cancer. 2016 Oct 11;16(1):769.

2. Stankevicius V, Vasauskas G, Noreikiene R, Kuodyte K, Valius M, Suziedelis K (2016) Extracellular matrix-dependent pathways in colorectal cancer cells lines reveal targets for anticancer therapies. Anticancer Research. 36(9):4559-67.

3. Stankevicius V, Kuodyte K, Schveigert D, Bulotiene D, Paulauskas T, Daniunaite K, Suziedelis K. Gene and miRNA expression profiles of mouse Lewis lung carcinoma LLC1 cells following single or fractionated dose irradiation. Oncology letters. **Accepted.**

CONFERENCE PRESENTATIONS

1. Stankevicius V, Ceponyte R, Suziedelis K. Gene and miRNA expression regulation during cell growth in laminin rich ECM microenvironment. 21st century genetics: Genes at work, Cold Spring Harbor Laboratory, New York, USA, 2015.05.26-31;

2. Stankevicius V, Ceponyte R, Schveigert D, Venius J, Valuckas KP, Aleknavicius E, Rotomskis R, Suziedelis. Cellular Response To Ionizing Radiation: application of different murine models. 9th International scientific conference: The Vital Nature Sign, Kaunas, Lithuania, 2015.05.14-16;

3. Stankevicius V, Ceponyte R, Strainiene E, Laurinavicius S, Aleknavicius E, Suziedelis K. Cellular response to ionizing radiation in different murine cell culture models. EMBO/EMBL Symposium: Tumour microenvironment and signalling, Heidelberg, Germany, 2014.05.07-10.

4. Ceponyte R, **Stankevicius V.** Cell culture model to investigate cellular response to ionizing radiation. XIIIth International Conference of Lithuanian Biochemical Society, Birstonas, Lithuania 2014.06.17-20

ACKNOWLEDGMENTS

Firstly, I would like to express my sincere gratitude to my supervisor Dr. Kestutis Suziedelis for the opportunity to work in his lab and help preparing the manuscripts and doctoral thesis. His never-ending positive attitude has been the major driving force to further evolve my carrier. In addition, I would like to thank to all my colleagues for the advice, suggestions, warm discussions and help with experiments.

I am greatly thankful to professor Nils Cordes (OncoRay Center, Dresden) and his team for the guidance on maintaining 3D cell cultures.

I am also grateful to professor Sonata Jarmalaite and Kristina Daniunaite for miRNA microarray hybridization experiments, dr. Mindaugas Valius for the help in confocal microscopy and Stasele Butkyte for great advices working on miRNA qPCR.

Very special thanks to my parents, Simona, Hese, Karolina, Gintautas and Tomas for the great support preparing the doctoral thesis and endless patience. I thank you a lot.

SUPPLEMENTARY MATERIAL

Supplementary table 1. List of primer sequences used for miRNA cDNA synthesis.

miRNAs	Stem-loop sequence
mir-207	5'-GTCGTATCCAGTGCAGGGTCCGAGGTATTCGCACTGGATACGACGAGGGA-3'
miR-376c-3p	5'-GTCGTATCCAGTGCAGGGTCCGAGGTATTCGCACTGGATACGACACGTGA-3'
miR-466f-3p	5'-GTCGTATCCAGTGCAGGGTCCGAGGTATTCGCACTGGATACGACGTGTGT-3'
miR-195a-5p	5'-GTCGTATCCAGTGCAGGGTCCGAGGTATTCGCACTGGATACGACGCCAAT-3'
miR-34b-3p	5'-GTCGTATCCAGTGCAGGGTCCGAGGTATTCGCACTGGATACGACGATGGC-3'
miR-34c-5p	5'-GTCGTATCCAGTGCAGGGTCCGAGGTATTCGCACTGGATACGACGCAATC-3'
miR-186-5p	5'-GTCGTATCCAGTGCAGGGTCCGAGGTATTCGCACTGGATACGACAGCCCA-3'
miR-145a-5p	5'-GTCGTATCCAGTGCAGGGTCCGAGGTATTCGCACTGGATACGACAGGGAT-3'
Sno135	5'-GTCGTATCCAGTGCAGGGTCCGAGGTATTCGCACTGGATACGACCTTCAG-3'

Supplementary table 2. List of primer sequences used for mRNA RT-qPCR.

Gene	Forward sequence	Reverse sequence
Hnf4a	5'-CACGCGGAGGTCAAGCTAC-3'	5'-CCCAGAGATGGGAGAGGTGAT-3'
Ifnb1	5'-CCGAGCAGAGATCTTCAGGAA-3'	5'-CCTGCAACCACCACTCATTCT-3'
Klf8	5'-TCAGAAAGTGGTTCGATGCAG-3'	5'-AACAGAGCTGGGTTCTCCATT-3'
Fgfr4	5'-GCTCGGAGGTAGAGGTCTTGT-3'	5'-CCACGCTGACTGGTAGGAA-3'
Hprt1	5'-CCTAAGATGAGCGCAAGTTGAA-3'	5'-CCACAGGACTAGAACACCTGCTAA-3'
CDK1	5'-AAACTACAGGTCAAGTGGTAGCC-3'	5'-TCCTGCATAAGCACATCCTGA-3'
RAD51	5'-CAACCCATTTCACGGTTAGAGC-3'	5'-TTCTTTGGCGCATAGGCAACA-3'
THBS1	5'-TGCTATCACAACGGAGTTCAGT-3'	5'-GCAGGACACCTTTTTGCAGATG-3'
PCNA	5'-AGGCACTCAAGGACCTCATCA-3'	5'-GAGTCCATGCTCTGCAGGTTT-3'
IL29	5'-GGACGCCTTGGAAGAGTCAC-3'	5'-AGCTGGGAGAGGATGTGGT-3'
IFITM1	5'-ACGTGACATCCTCGATAAAACTG-3'	5'-GAACCCATCAAGGGACTTCTG-3'
IFIT1	5'-CCAAGGTCCACCGTGATTAAC-3'	5'-ACCAGTTCAAGAAGAGGGTGTT-3'
OAS2	5'-TCATCAGGTCAAGGATAGTCTG-3'	5'-GGTGTTTCACATAGGCTAGTAG-3'
HPRT	5'-TGCAGACTTTGCTTTCCTTGGTC-3'	5'-CCAACACTTCGTGGGGTCCTT-3'

Supplementary table 3. List of primer sequences used for miRNA RT-qPCR.

miRNAs	Forward sequence	Reverse sequence
miR-207	5'-CGGCTTCTCCTGGCTCTCC-3	5'-CAGTGCAGGGTCCGAGGT-3'
miR-376c-3p	5'-CGGCGAACATAGAGGAAATT-3	5'-CAGTGCAGGGTCCGAGGT-3'
miR-466f-3p	5'-GGCGCATACACACACACAT-3	5'-CAGTGCAGGGTCCGAGGT-3'
miR-195a-5p	5'-GGCGTAGGTAGTTTCATGTT-3	5'-CAGTGCAGGGTCCGAGGT-3'
miR-34b-3p	5'-CGGCGAATCACTAACTCCACT-3'	5'-CAGTGCAGGGTCCGAGGT-3'
miR-34c-5p	5'-GGCGAGGCAGTGTAGTTAGCT-3'	5'-CAGTGCAGGGTCCGAGGT-3'
miR-186-5p	5'-GGCGCAAAGAATTCTCCTTT-3'	5'-CAGTGCAGGGTCCGAGGT-3'
miR-145a-5p	5'-CGGTCCAGTTTTCCCAGGA-3'	5'-CAGTGCAGGGTCCGAGGT-3'
SnoRNA-135	5'-GTAGTGGTGAGCCTATGGTTTT-3	5'-CAGTGCAGGGTCCGAGGT-3'

Supplementary table 4. Survival fractions of LLC1 cells exposed to a single dose or a fractionated dose irradiation.

IR treatment		Survival (n=3)
Single dose treatment	2 Gy	62,2% ± 4,1%
	4 Gy	20,8% ± 3,6%
	6 Gy	4,6% ± 1,3%
	10 Gy	0,1% ± 0,5%
Fractioned dose treatment	3x2 Gy	20,5% ± 2,3%
	5x2 Gy	19,8% ± 4,7%

Supplementary table 5. The relative expression of miRNAs differentially expressed in LLC1 cells after exposure to SD (2Gy or 10 Gy) or FD (5x2 Gy) irradiation.

miRNA	miRbase ID	Irradiation dose		
		2 Gy	10 Gy	5x2 Gy
miR-34c-5p	MIMAT0000381	**2.19**	**2.79**	**5.30**
miR-145a-3p	MIMAT0004534	**-2.46**	**-2.08**	**-2.94**
miR-878-5p	MIMAT0004932	**-2.20**	**-2.74**	-2.43
miR-126a-5p	MIMAT0000137	**-2.16**	-1.6	-2.15
miR-338-5p	MIMAT0004647	**-2.03**	1.10	-1.89
miR-26b-3p	MIMAT0004630	-1.31	**-2.32**	-1.33
miR-136-5p	MIMAT0000148	-1.28	**2.17**	-1.43
miR-466a-5p	MIMAT0004759	-1.73	**-2.58**	-3.28
miR-710	MIMAT0003500	-1.71	**-2.45**	-3.11
miR-34b-3p	MIMAT0004581	2.18	**4.07**	**14.78**
miR-34c-3p	MIMAT0004580	2.32	**4.77**	**24.93**
miR-30c-5p	MIMAT0000514	-1.10	1.11	**5.50**
miR-105	MIMAT0004856	-1.54	-1.31	**-3.65**
miR-129-5p	MIMAT0000209	1.27	2.07	**4.26**
miR-129-2-3p	MIMAT0000544	-1.09	1.35	**8.10**
miR-145a-5p	MIMAT0000157	1.12	1.12	**6.99**
miR-186-5p	MIMAT0000215	1.46	1.55	**3.55**
miR-192-5p	MIMAT0000517	1.55	1.36	**2.62**

Relative miRNA expression greater than 2 and $p<0.05$ is shown in bold.

Supplementary table 6. Validation of mRNA and miRNA microarray data by RT-qPCR.

Gene		10 Gy	5x2 Gy
Btg2	RT-qPCR	5.09±0.34	4.51±0.73
	Microarrays	5.38±1.55	2.74±0.09
Ccng1	RT-qPCR	4.02±0.57	3.2±0.47
	Microarrays	2.06±0.47	2.30±0.45
P21	RT-qPCR	2.64±0.06	2.6±0.49
	Microarrays	5.96±1.28	2.43±0.16
Thbs2	RT-qPCR	1.30±0.10	2.76±0.67
	Microarrays	1.29±0.18	2.26±0.11
miRNA			
miR-34b-3p	RT-qPCR	2.76±0.48	3.6±0.58
	Microarrays	4.07±1.53	14.78±4.75
miR-34c-5p	RT-qPCR	2.67±0.66	2.32±0.34
	Microarrays	2.79±0.33	5.3±0.90
miR-186-5p	RT-qPCR	1.62±0.48	2.28±0.06
	Microarrays	1.55±0.59	3.55±0.81
miR-145a-5p	RT-qPCR	1.41±0.46	3.44±0.49
	Microarrays	1.12±0.88	6.99±1.41

Supplementary table 7. Full list of differentially expressed genes associated with MAP kinase, cell adhesion and immune response functional categories in LLC cells cultured in lr-ECM 3D versus 2D.

Category	Number of genes	Genes	P-value
MAPK signaling pathway	25	Elk4, Fgfr4, Cacng5, Pla2g3, Ppp3cc, Fgf20, Nfatc4, Ecsit, Cacna1d, Kras, Mapk8ip3, Rasgrp4, Pak2, Gng12, Flnc, Stmn1, Map3k14, Traf6, Sos2, Mknk1, Flna, Fgfr3, Pla2g12a, Pla2g2c, Ikbkg	6.23e-08
Regulation of actin cytoskeleton	20	Fgfr4, Diap3, Fgf20, Pik3r2, Pak3, Kras, Itgb7, Pak2, Ppp1cb, Gng12, Myh10, Slc9a1, Sos2, Arhgef4, Ssh1, Fgfr3, Tmsb4x, RhoaItgal Ssh3	1.35e-06
Focal adhesion	17	Lamb3, Vasp, Pdpk1, Pik3r2, Pak3, Vegfa, Itgb7, Pak2, Ppp1cb, Chad, Flnc, Sos2, Flna, Col3a1, Rhoa, Col1a1, Cav3	3.33e-05
Cell adhesion molecules (CAMs)	10	Cldn16, 4930412D23Rik, Cdh4, H2-Bl, Cadm1, Nrcam, Itgal, Itgb7, Cd8a, Cntn2	0.0062
Gap junction	7	Grm1, Tubb2a, Gnas, Kras, Htr2c, Sos2, Itpr1	0.0103
Tight junction	9	Ppp2r1b, Myh10, Cldn16, 4930412D23Rik, Pard3, Ppp2r2b, Kras, Rhoa, Inadl	0.0103
ECM-receptor interaction	6	Lamb3, Itgb7, Col1a1, Chad, Col3a1, Agrn	0.0237
Cytokine-cytokine receptor interaction	18	Ltb, Xcr1, Il12rb2, Tnfrsf11a, Cxcr7, Ifnb1, Acvr2a, Vegfa, Tnfrsf1b, Epo, Tnfrsf9, Il22ra1, Il21r, Tnfrsf25, Ccr3, Bmpr1a, Cntfr, Il2ra	0.0001
T cell receptor signaling pathway	11	Map3k14, Sos2, Ppp3cc, Pik3r2, Pak3, Nfatc4, Kras, Rhoa, Ikbkg, Cd8a, Pak2	0.0003
VEGF signaling pathway	9	Nfatc4, Pla2g3, Kras, Vegfa, Sphk1, Pla2g2c, Ppp3cc, Pla2g12a, Pik3r2	0.0004
Cytosolic DNA-sensing pathway	7	Polr3k, Tbk1, Ifnb1, Ddx58, Irf3, Ikbkg, Polr3g	0.0013
B cell receptor signaling pathway	7	Nfatc4, Lilrb3, Kras, Sos2, Ppp3cc, Ikbkg, Pik3r2	0.0058
RIG-I-like receptor signaling pathway	6	Tbk1, Ifnb1, Ddx58, Irf3, Traf6, Ikbkg	0.0121
Natural killer cell mediated cytotoxicity	8	Klra7, Sos2, Ppp3cc, Pik3r2, Nfatc4, Ifnb1, Kras, Itgal	0.0153
Jak-STAT signaling pathway	9	Cntfr, Ifnb1, Il2ra, Sos2, Epo, Il12rb2, Il21r, Pik3r2, Il22ra1	0.0159
Fc epsilon RI signaling pathway	6	Pla2g3, Kras, Pla2g2c, Sos2, Pla2g12a, Pik3r2	0.0186
Chemokine signaling pathway	9	Ccr3, Xcr1, Sos2, Pik3r2, Pard3, Kras, Rhoa, Ikbkg, Gng12	0.0362
Toll-like receptor signaling pathway	5	Tbk1, Ifnb1, Ifnb1, Traf6, Ikbkg, Pik3r2	0.0401

Supplementary table 8. List of differentially expressed miRNA clusters in LLC cells grown under lr-ECM 3D cell culture conditions as compared to 2D.

miRNA	Location	Fold change	P-value
miR-297b-5p	chr2	-2.1	0.0348
miR-466b-3p	chr2	20.4	0.0026
miR-466b-5p	chr2	-2.6	0.0116
miR-466c-5p	chr2	5.4	0.0129
miR-466d-3p	chr2	28.1	0.0022
miR-466f-3p	chr2	216.5	4.9e-4
miR-466g	chr2	183.3	8.8e-4
miR-466h-5p	chr2	8.9	0.0181
miR-467b-3p	chr2	128.5	9.26e-4
miR-467d-3p	chr2	130.8	0.0011
miR-467e-3p	chr2	94.7	9.21e-4
miR-699b-5p	chr2	5.34	0.0224
miR-34b-3p	chr9	7.1	0.0365
miR-34c-3p	chr9	4.4	0.0372
miR-376a-3p	chr12	17.3	0.0015
miR-376b-3p	chr12	12.2	0.0015
miR-376c-3p	chr12	217.4	0.0018
miR-376c-5p	chr12	-3.8	0.0184
miR-459-3p	chr12	-2.3	0.0173
miR-485-3p	chr12	30.4	0.0016
miR-544-3p	chr12	-2.2	0.0291
miR-743b-3p	chrX	-2.0	0.0199
miR-883a-5p	chrX	-2.1	0.0474
miR-883b-5p	chrX	-2.2	0.0348
miR-471-5p	chrX	-2.2	0.0488
miR-881-3p	chrX	-3.3	0.0447

Supplementary table 9. Validation of microarray data by qPCR. The table shows fold change of gene expression following exposure to SD and FD irradiation in DLD1 and HT29 cells cultured under 2D or 3D and microarray analysis.

DLD-1		**2 Gy**	**10 Gy**	**5x2 Gy**
	2D qPCR	1.31 ± 0.09	0.99 ± 0.16	1.21 ± 0.10
CDK1	3D qPCR	1.10 ± 0.12	0.92 ± 0.12	2.37 ± 0.61
	3D microarray	1.27±0.07	1.14±0.04	1.79±0.18
	2D qPCR	1.02 ± 0.04	1.05 ± 0.06	0.87 ± 0.15
RAD51	3D qPCR	1.12 ± 0.13	1.10 ± 0.13	2.43 ± 0.17
	3D microarray	1.36±0.04	1.51±0.20	1.79±0.04
	2D qPCR	1.34 ± 0.14	1.08 ± 0.08	1.83 ± 0.13
THBS1	3D qPCR	1.31 ± 0.13	1.16 ± 0.14	3.29 ± 0.18
	3D microarray	0.82±0.04	0.92±0.03	1.86±0.08
	2D qPCR	1.25 ± 0.04	1.03 ± 0.11	0.98 ± 0.26
PCNA	3D qPCR	0.95 ± 0.07	0.98 ± 0.10	1.79 ± 0.18
	3D microarray	1.23±0.03	1.37±0.042	2.06±0.31
	2D qPCR	0.50±0.20	0.69±0.13	0.97±0.16
IL29	3D qPCR	1.01±0.02	0.77±0.10	0.45±0.15
	3D microarray	0.91±0.16	0.97±0.08	1.03±0.07
	2D qPCR	0.57±0.15	0.83±0.14	0.91±0.39
IFITM1	3D qPCR	1.08±0.26	1.05±0.13	1.30±0.10
	3D microarray	0.89±0.24	0.90±0.15	0.92±0.09
	2D qPCR	0.89±0.22	0.86±0.08	0.94±0.06
IFIT1	3D qPCR	0.92±0.13	0.80±0.11	0.60±0.14
	3D microarray	0.93±0.22	0.77±0.11	0.99±0.15
	2D qPCR	0.77±0.30	1.23±0.09	0.99±0.03
OAS2	3D qPCR	1.28±0.29	1.10±0.13	0.49±0.19
	3D microarray	1.17±0.17	0.92±0.08	1.12±0.02
HT29		**2 Gy**	**10 Gy**	**5x2 Gy**
	2D qPCR	1.17±0.16	0.83±0.13	0.94±0.07
CDK1	3D qPCR	0.99±0.15	0.79±0.1	1.22±0.41
	3D microarray	1.28±0.01	1.02±0.02	1.28±0.05
	2D qPCR	1.11±0.1	1.04±0.36	1.92±0.07
RAD51	3D qPCR	0.89±0.12	0.99±0.1	1.16±0.31
	3D microarray	1.15±0.08	1.37±0.25	1.29±0.10
	2D qPCR	1.13±0.13	1.15 ± 0.39	0.79 ±0.07
THBS1	3D qPCR	0.76±0.06	0.99±0.08	1.33±0.91
	3D microarray	0.77±0.06	0.74±0.06	0.96±0.06
	2D qPCR	0.98±0.09	0.97±0.24	0.74±0.14
PCNA	3D qPCR	0.8±0.16	0.94±0.15	0.85±0.46
	3D microarray	1.17±0.03	1.27±0.04	1.24±0.18
	2D qPCR	1.23 ± 0.17	1.20 ± 0.27	9.04 ± 2.77
IL29	3D qPCR	1.01 ± 0.82	0.93 ± 0.27	6.91 ± 1.05
	3D microarray	0.87±0.07	1.06±0.18	2.18±0.44
	2D qPCR	1.16 ± 0.26	0.93 ± 0.33	2.51 ± 1.64
IFITM1	3D qPCR	0.88 ± 0.76	0.58 ± 0.33	6.19 ± 2.39
	3D microarray	0.88±0.30	0.74±0.35	5.58±2.59
	2D qPCR	1.01 ± 0.15	0.84 ± 0.11	1.95 ± 0.30
IFIT1	3D qPCR	0.95 ± 0.41	0.83 ± 0.11	4.88 ± 0.05
	3D microarray	1.10±0.18	1.14±0.16	4.02±1.08
	2D qPCR	1.07 ± 0.09	0.96 ± 0.27	1.93 ± 0.48
OAS2	3D qPCR	0.69 ± 0.48	0.67 ± 0.27	5.46 ± 0.84
	3D microarray	0.99±0.21	0.73±0.17	2.87±0.53

REFERENCES

1. Abbott, A. (2003). "Cell culture: biology's new dimension." Nature **424**(6951): 870-872.

2. Achari, C., S. Winslow, Y. Ceder and C. Larsson (2014). "Expression of miR-34c induces G2/M cell cycle arrest in breast cancer cells." BMC Cancer **14**(1): 1-9.

3. Albini, A. and M. B. Sporn (2007). "The tumour microenvironment as a target for chemoprevention." Nat Rev Cancer **7**(2): 139-147.

4. Amundson, S. A., K. T. Do, L. C. Vinikoor, R. A. Lee, C. A. Koch-Paiz, J. Ahn, M. Reimers, Y. Chen, D. A. Scudiero, J. N. Weinstein, J. M. Trent, M. L. Bittner, P. S. Meltzer and A. J. Fornace, Jr. (2008). "Integrating global gene expression and radiation survival parameters across the 60 cell lines of the National Cancer Institute Anticancer Drug Screen." Cancer Res **68**(2): 415-424.

5. Appella, E. and C. W. Anderson (2000). "Signaling to p53: breaking the posttranslational modification code." Pathol Biol (Paris) **48**(3): 227-245.

6. Armulik, A., A. Abramsson and C. Betsholtz (2005). "Endothelial/pericyte interactions." Circ Res **97**(6): 512-523.

7. Au-Yeung, N., R. Mandhana and C. M. Horvath (2013). "Transcriptional regulation by STAT1 and STAT2 in the interferon JAK-STAT pathway." JAKSTAT **2**(3): e23931.

8. Aumailley, M., A. El Khal, N. Knoss and L. Tunggal (2003). "Laminin 5 processing and its integration into the ECM." Matrix Biol **22**(1): 49-54.

9. BALÇA-SILVA, J., S. S. NEVES, A. C. GONÇALVES, A. M. ABRANTES, J. CASALTA-LOPES, M. F. BOTELHO, A. B. SARMENTO-RIBEIRO and H. C. SILVA (2012). "Effect of miR-34b Overexpression on the Radiosensitivity of Non-small Cell Lung Cancer Cell Lines." Anticancer Research **32**(5): 1603-1609.

10. Barcellos-Hoff, M. H., C. Park and E. G. Wright (2005). "Radiation and the microenvironment - tumorigenesis and therapy." Nat Rev Cancer **5**(11): 867-875.

11. Baskar, R., K. A. Lee, R. Yeo and K. W. Yeoh (2012). "Cancer and radiation therapy: current advances and future directions." Int J Med Sci **9**(3): 193-199.

12. Begg, A. C., F. A. Stewart and C. Vens (2011). "Strategies to improve radiotherapy with targeted drugs." Nat Rev Cancer **11**(4): 239-253.

13. Benton, G., I. Arnaoutova, J. George, H. K. Kleinman and J. Koblinski (2014). "Matrigel: From discovery and ECM mimicry to assays and models for cancer research." Advanced Drug Delivery Reviews **79–80**: 3-18.

14. Berrier, A. L. and K. M. Yamada (2007). "Cell–matrix adhesion." Journal of Cellular Physiology **213**(3): 565-573.

15. Bissell, M. J., D. C. Radisky, A. Rizki, V. M. Weaver and O. W. Petersen (2002). "The organizing principle: microenvironmental influences in the normal and malignant breast." Differentiation **70**(9-10): 537-546.

16. Brady, C. A. and L. D. Attardi (2010). "p53 at a glance." Journal of Cell Science **123**(15): 2527-2532.

17. Brooks, C. L. and W. Gu (2006). "p53 Ubiquitination: Mdm2 and Beyond." Molecular cell **21**(3): 307-315.
18. Brown, E. J. and D. Baltimore (2003). "Essential and dispensable roles of ATR in cell cycle arrest and genome maintenance." Genes Dev **17**(5): 615-628.
19. Buch, K., T. Peters, T. Nawroth, M. Sänger, H. Schmidberger and P. Langguth (2012). "Determination of cell survival after irradiation via clonogenic assay versus multiple MTT Assay - A comparative study." Radiation Oncology **7**(1): 1-6.
20. Burkholder, B., R.-Y. Huang, R. Burgess, S. Luo, V. S. Jones, W. Zhang, Z.-Q. Lv, C.-Y. Gao, B.-L. Wang, Y.-M. Zhang and R.-P. Huang (2014). "Tumor-induced perturbations of cytokines and immune cell networks." Biochimica et Biophysica Acta (BBA) - Reviews on Cancer **1845**(2): 182-201.
21. Butcher, D. T., T. Alliston and V. M. Weaver (2009). "A tense situation: forcing tumour progression." Nature reviews. Cancer **9**(2): 108-122.
22. Cairo, S., J. G. Judde and M. E. LEGRIER (2012). Markers for cancer prognosis and therapy and methods of use, Google Patents.
23. Camphausen, K., B. Purow, M. Sproull, T. Scott, T. Ozawa, D. F. Deen and P. J. Tofilon (2005). "Orthotopic Growth of Human Glioma Cells Quantitatively and Qualitatively Influences Radiation-Induced Changes in Gene Expression." Cancer Research **65**(22): 10389.
24. Campisi, J. (2013). "Aging, Cellular Senescence, and Cancer." Annual review of physiology **75**: 685-705.
25. Campisi, J. and F. d'Adda di Fagagna (2007). "Cellular senescence: when bad things happen to good cells." Nat Rev Mol Cell Biol **8**(9): 729-740.
26. Cannell, I. G., Y. W. Kong, S. J. Johnston, M. L. Chen, H. M. Collins, H. C. Dobbyn, A. Elia, T. R. Kress, M. Dickens, M. J. Clemens, D. M. Heery, M. Gaestel, M. Eilers, A. E. Willis and M. Bushell (2010). "p38 MAPK/MK2-mediated induction of miR-34c following DNA damage prevents Myc-dependent DNA replication." Proceedings of the National Academy of Sciences of the United States of America **107**(12): 5375-5380.
27. Castedo, M. and G. Kroemer (2004). "[Mitotic catastrophe: a special case of apoptosis]." J Soc Biol **198**(2): 97-103.
28. Castedo, M., J. L. Perfettini, T. Roumier, K. Yakushijin, D. Horne, R. Medema and G. Kroemer (2004). "The cell cycle checkpoint kinase Chk2 is a negative regulator of mitotic catastrophe." Oncogene **23**(25): 4353-4361.
29. Cazzalini, O., A. I. Scovassi, M. Savio, L. A. Stivala and E. Prosperi (2010). "Multiple roles of the cell cycle inhibitor p21CDKN1A in the DNA damage response." Mutation Research/Reviews in Mutation Research **704**(1–3): 12-20.
30. Chen, J., F. Zhu, R. L. Weaks, A. K. Biswas, R. Guo, Y. Li and D. G. Johnson (2011). "E2F1 promotes the recruitment of DNA repair factors to sites of DNA double-strand breaks." Cell Cycle **10**(8): 1287-1294.
31. Chen, X., H. Niu, Y. Yu, J. Wang, S. Zhu, J. Zhou, A. Papusha, D. Cui, X. Pan, Y. Kwon, P. Sung and G. Ira (2016). "Enrichment of Cdk1-cyclins at DNA double-strand breaks stimulates Fun30 phosphorylation and DNA end resection." Nucleic Acids Research.

32. Chen, Z., C. M. Fillmore, P. S. Hammerman, C. F. Kim and K.-K. Wong (2014). "Non-small-cell lung cancers: a heterogeneous set of diseases." Nat Rev Cancer **14**(8): 535-546.
33. Cheon, H., E. G. Holvey-Bates, J. W. Schoggins, S. Forster, P. Hertzog, N. Imanaka, C. M. Rice, M. W. Jackson, D. J. Junk and G. R. Stark (2013). "IFNβ-dependent increases in STAT1, STAT2, and IRF9 mediate resistance to viruses and DNA damage." The EMBO Journal **32**(20): 2751-2763.
34. Choudhury, Y., F. C. Tay, D. H. Lam, E. Sandanaraj, C. Tang, B.-T. Ang and S. Wang "Attenuated adenosine-to-inosine editing of microRNA-376a* promotes invasiveness of glioblastoma cells." The Journal of Clinical Investigation **122**(11): 4059-4076.
35. Ciccia, A. and S. J. Elledge (2010). "The DNA damage response: making it safe to play with knives." Mol Cell **40**(2): 179-204.
36. Ciccia, A. and S. J. Elledge (2010). "The DNA Damage Response: Making it safe to play with knives." Molecular cell **40**(2): 179-204.
37. Costes, S. V., I. Chiolo, J. M. Pluth, M. H. Barcellos-Hoff and B. Jakob (2010). "Spatiotemporal characterization of ionizing radiation induced DNA damage foci and their relation to chromatin organization." Mutation Research/Reviews in Mutation Research **704**(1–3): 78-87.
38. Couedel, C., K. D. Mills, M. Barchi, L. Shen, A. Olshen, R. D. Johnson, A. Nussenzweig, J. Essers, R. Kanaar, G. C. Li, F. W. Alt and M. Jasin (2004). "Collaboration of homologous recombination and nonhomologous end-joining factors for the survival and integrity of mice and cells." Genes Dev **18**(11): 1293-1304.
39. Coussens, L. M. and Z. Werb (2002). "Inflammation and cancer." Nature **420**(6917): 860-867.
40. Critchley, D. R. (2009). "Biochemical and structural properties of the integrin-associated cytoskeletal protein talin." Annual review of biophysics **38**: 235-254.
41. Cuk, K., M. Zucknick, J. Heil, D. Madhavan, S. Schott, A. Turchinovich, D. Arlt, M. Rath, C. Sohn, A. Benner, H. Junkermann, A. Schneeweiss and B. Burwinkel (2013). "Circulating microRNAs in plasma as early detection markers for breast cancer." International Journal of Cancer **132**(7): 1602-1612.
42. Curtin, N. J. (2012). "DNA repair dysregulation from cancer driver to therapeutic target." Nat Rev Cancer **12**(12): 801-817.
43. Czabotar, P. E., G. Lessene, A. Strasser and J. M. Adams (2014). "Control of apoptosis by the BCL-2 protein family: implications for physiology and therapy." Nat Rev Mol Cell Biol **15**(1): 49-63.
44. Deckbar, D., P. A. Jeggo and M. Lobrich (2011). "Understanding the limitations of radiation-induced cell cycle checkpoints." Critical Reviews in Biochemistry and Molecular Biology **46**(4): 271-283.
45. Delaney, G., S. Jacob, C. Featherstone and M. Barton (2005). "The role of radiotherapy in cancer treatment: estimating optimal utilization from a review of evidence-based clinical guidelines." Cancer **104**(6): 1129-1137.

46. Dewan, M. Z., A. E. Galloway, N. Kawashima, J. K. Dewyngaert, J. S. Babb, S. C. Formenti and S. Demaria (2009). "Fractionated but Not Single-Dose Radiotherapy Induces an Immune-Mediated Abscopal Effect when Combined with Anti–CTLA-4 Antibody." Clinical Cancer Research **15**(17): 5379-5388.
47. Diamond, M. S. and M. Farzan (2013). "The broad-spectrum antiviral functions of IFIT and IFITM proteins." Nat Rev Immunol **13**(1): 46-57.
48. Dickey, J. S., C. E. Redon, A. J. Nakamura, B. J. Baird, O. A. Sedelnikova and W. M. Bonner (2009). "H2AX: functional roles and potential applications." Chromosoma **118**(6): 683-692.
49. Dirat, B., L. Bochet, M. Dabek, D. Daviaud, S. Dauvillier, B. Majed, Y. Y. Wang, A. Meulle, B. Salles, S. Le Gonidec, I. Garrido, G. Escourrou, P. Valet and C. Muller (2011). "Cancer-associated adipocytes exhibit an activated phenotype and contribute to breast cancer invasion." Cancer Res **71**(7): 2455-2465.
50. Dyson, N. (1998). "The regulation of E2F by pRB-family proteins." Genes & Development **12**(15): 2245-2262.
51. E, X. and T. F. Kowalik (2014). "The DNA Damage Response Induced by Infection with Human Cytomegalovirus and Other Viruses." Viruses **6**(5): 2155-2185.
52. Eke, I. and N. Cordes (2015). "Focal adhesion signaling and therapy resistance in cancer." Seminars in Cancer Biology **31**: 65-75.
53. Eke, I., E. Dickreuter and N. Cordes (2012). "Enhanced radiosensitivity of head and neck squamous cell carcinoma cells by β1 integrin inhibition." Radiotherapy and Oncology **104**(2): 235-242.
54. Eke, I., K. Storch, I. Kästner, A. Vehlow, C. Faethe, W. Mueller-Klieser, G. Taucher-Scholz, A. Temme, G. Schackert and N. Cordes (2012). "Three-dimensional Invasion of Human Glioblastoma Cells Remains Unchanged by X-ray and Carbon Ion Irradiation In Vitro." International Journal of Radiation Oncology*Biology*Physics **84**(4): e515-e523.
55. el-Deiry, W. S., S. E. Kern, J. A. Pietenpol, K. W. Kinzler and B. Vogelstein (1992). "Definition of a consensus binding site for p53." Nat Genet **1**(1): 45-49.
56. Enserink, J. M. and R. D. Kolodner (2010). "An overview of Cdk1-controlled targets and processes." Cell Division **5**(1): 1-41.
57. Eriksson, D. and T. Stigbrand (2010). "Radiation-induced cell death mechanisms." Tumour Biol **31**(4): 363-372.
58. Eskelinen, E.-L. (2008). New Insights into the Mechanisms of Macroautophagy in Mammalian Cells. International Review of Cell and Molecular Biology, Academic Press. **Volume 266:** 207-247.
59. Fei, P. and W. S. El-Deiry (0000). "P53 and radiation responses." Oncogene **22**(37): 5774-5783.
60. Feofanova, N., J. M. Geraldo and L. M. de Andrade (2014). "Radiation oncology in vitro: trends to improve radiotherapy through molecular targets." Biomed Res Int **2014**: 461687.
61. Fernandez-Fuente, G., P. Mollinedo, L. Grande, A. Vazquez-Barquero and J. L. Fernandez-Luna (2014). "Culture Dimensionality Influences the Resistance of

Glioblastoma Stem-like Cells to Multikinase Inhibitors." Molecular Cancer Therapeutics **13**(6): 1664-1672.
62. Fokas, E., R. Prevo, E. M. Hammond, T. B. Brunner, W. G. McKenna and R. J. Muschel (2014). "Targeting ATR in DNA damage response and cancer therapeutics." Cancer Treat Rev **40**(1): 109-117.
63. Formenti, S. C. and S. Demaria (2013). "Combining Radiotherapy and Cancer Immunotherapy: A Paradigm Shift." Journal of the National Cancer Institute **105**(4): 256-265.
64. Fournier, M. V. and K. J. Martin (2006). "Transcriptome profiling in clinical breast cancer: From 3D culture models to prognostic signatures." Journal of Cellular Physiology **209**(3): 625-630.
65. Frantz, C., K. M. Stewart and V. M. Weaver (2010). "The extracellular matrix at a glance." Journal of Cell Science **123**(24): 4195.
66. Frey, B., Y. Rubner, L. Kulzer, N. Werthmöller, E.-M. Weiss, R. Fietkau and U. S. Gaipl (2014). "Antitumor immune responses induced by ionizing irradiation and further immune stimulation." Cancer Immunology, Immunotherapy **63**(1): 29-36.
67. Friedrich, J., R. Ebner and L. A. Kunz-Schughart (2007). "Experimental anti-tumor therapy in 3-D: Spheroids – old hat or new challenge?" International Journal of Radiation Biology **83**(11-12): 849-871.
68. Friedrich, J., C. Seidel, R. Ebner and L. A. Kunz-Schughart (2009). "Spheroid-based drug screen: considerations and practical approach." Nat. Protocols **4**(3): 309-324.
69. Frith, J. E., B. Thomson and P. G. Genever (2010). "Dynamic three-dimensional culture methods enhance mesenchymal stem cell properties and increase therapeutic potential." Tissue Eng Part C Methods **16**(4): 735-749.
70. Fulda, S., A. M. Gorman, O. Hori and A. Samali (2010). "Cellular Stress Responses: Cell Survival and Cell Death." International Journal of Cell Biology **2010**: 23.
71. Gabarra-Niecko, V., M. D. Schaller and J. M. Dunty (2003). "FAK regulates biological processes important for the pathogenesis of cancer." Cancer Metastasis Rev **22**(4): 359-374.
72. Gamper, A. M. and R. G. Roeder (2008). "Multivalent Binding of p53 to the STAGA Complex Mediates Coactivator Recruitment after UV Damage." Molecular and Cellular Biology **28**(8): 2517-2527.
73. Gattazzo, F., A. Urciuolo and P. Bonaldo (2014). "Extracellular matrix: A dynamic microenvironment for stem cell niche()." Biochimica et Biophysica Acta **1840**(8): 2506-2519.
74. Gewirtz, D. A., S. E. Holt and L. W. Elmore (2008). "Accelerated senescence: an emerging role in tumor cell response to chemotherapy and radiation." Biochem Pharmacol **76**(8): 947-957.
75. Girardi, C., C. De Pittà, S. Casara, G. Sales, G. Lanfranchi, L. Celotti and M. Mognato (2012). "Analysis of miRNA and mRNA Expression Profiles Highlights Alterations in Ionizing Radiation Response of Human Lymphocytes under Modeled Microgravity." PLoS ONE **7**(2): e31293.

76. Gong, P., T. Zhang, D. He and J.-T. Hsieh (2015). "MicroRNA-145 Modulates Tumor Sensitivity to Radiation in Prostate Cancer." Radiation Research **184**(6): 630-638.
77. Gong, X., C. Lin, J. Cheng, J. Su, H. Zhao, T. Liu, X. Wen and P. Zhao (2015). "Generation of Multicellular Tumor Spheroids with Microwell-Based Agarose Scaffolds for Drug Testing." PLoS ONE **10**(6): e0130348.
78. Goodarzi, A. A., A. T. Noon, D. Deckbar, Y. Ziv, Y. Shiloh, M. Löbrich and P. A. Jeggo (2008). "ATM Signaling Facilitates Repair of DNA Double-Strand Breaks Associated with Heterochromatin." Molecular Cell **31**(2): 167-177.
79. Grabarz, A., A. Barascu, J. Guirouilh-Barbat and B. S. Lopez (2012). "Initiation of DNA double strand break repair: signaling and single-stranded resection dictate the choice between homologous recombination, non-homologous end-joining and alternative end-joining." Am J Cancer Res **2**(3): 249-268.
80. Green, D. R. and G. Kroemer (2009). "Cytoplasmic Functions of the Tumor Suppressor p53." Nature **458**(7242): 1127.
81. Gregersen, L. H., A. B. Jacobsen, L. B. Frankel, J. Wen, A. Krogh and A. H. Lund (2010). "MicroRNA-145 Targets <italic>YES</italic> and <italic>STAT1</italic> in Colon Cancer Cells." PLoS ONE **5**(1): e8836.
82. Grivennikov, S. I., F. R. Greten and M. Karin (2010). "Immunity, Inflammation, and Cancer." Cell **140**(6): 883-899.
83. Gu, L. and D. J. Mooney (2016). "Biomaterials and emerging anticancer therapeutics: engineering the microenvironment." Nat Rev Cancer **16**(1): 56-66.
84. Gudkov, A. V. and E. A. Komarova (2003). "The role of p53 in determining sensitivity to radiotherapy." Nat Rev Cancer **3**(2): 117-129.
85. Hainaut, P. and M. Hollstein (2000). "p53 and human cancer: the first ten thousand mutations." Adv Cancer Res **77**: 81-137.
86. Hanahan, D. and L. M. Coussens (2012). "Accessories to the crime: functions of cells recruited to the tumor microenvironment." Cancer Cell **21**(3): 309-322.
87. Hanahan, D. and Robert A. Weinberg "Hallmarks of Cancer: The Next Generation." Cell **144**(5): 646-674.
88. Hanahan, D. and R. A. Weinberg (2011). "Hallmarks of cancer: the next generation." Cell **144**(5): 646-674.
89. Härmä, V., J. Virtanen, R. Mäkelä, A. Happonen, J.-P. Mpindi, M. Knuuttila, P. Kohonen, J. Lötjönen, O. Kallioniemi and M. Nees (2010). "A Comprehensive Panel of Three-Dimensional Models for Studies of Prostate Cancer Growth, Invasion and Drug Responses." PLoS ONE **5**(5): e10431.
90. Harms, K., S. Nozell and X. Chen (2003). "The common and distinct target genes of the p53 family transcription factors." Cellular and Molecular Life Sciences CMLS **61**(7): 822-842.
91. Hehlgans, S., M. Haase and N. Cordes (2007). "Signalling via integrins: implications for cell survival and anticancer strategies." Biochim Biophys Acta **1775**(1): 163-180.
92. Hehlgans, S., K. Storch, I. Lange and N. Cordes (2013). "The novel HDAC inhibitor NDACI054 sensitizes human cancer cells to radiotherapy." Radiotherapy and Oncology **109**(1): 126-132.

93. Helton, E. S. and X. Chen (2007). "p53 modulation of the DNA damage response." Journal of Cellular Biochemistry **100**(4): 883-896.
94. Hennig, J., M. P. McShane, N. Cordes and I. Eke (2014). "APPL proteins modulate DNA repair and radiation survival of pancreatic carcinoma cells by regulating ATM." Cell Death Dis **5**: e1199.
95. Hermeking, H. "p53 Enters the MicroRNA World." Cancer Cell **12**(5): 414-418.
96. Hermeking, H. (2009). "The miR-34 family in cancer and apoptosis." Cell Death Differ **17**(2): 193-199.
97. Hermeking, H. (2012). "MicroRNAs in the p53 network: micromanagement of tumour suppression." Nat Rev Cancer **12**(9): 613-626.
98. Hynes, R. O. (2009). "Extracellular matrix: not just pretty fibrils." Science (New York, N.Y.) **326**(5957): 1216-1219.
99. Huarte, M., M. Guttman, D. Feldser, M. Garber, M. J. Koziol, D. Kenzelmann-Broz, A. M. Khalil, O. Zuk, I. Amit, M. Rabani, L. D. Attardi, A. Regev, E. S. Lander, T. Jacks and J. L. Rinn (2010). "A large intergenic non-coding RNA induced by p53 mediates global gene repression in the p53 response." Cell **142**(3): 409-419.
100. Hwang, H.-W., E. A. Wentzel and J. T. Mendell (2009). "Cell–cell contact globally activates microRNA biogenesis." Proceedings of the National Academy of Sciences of the United States of America **106**(17): 7016-7021.
101. Ichimura, A., Y. Ruike, K. Terasawa, K. Shimizu and G. Tsujimoto (2010). "MicroRNA-34a Inhibits Cell Proliferation by Repressing Mitogen-Activated Protein Kinase Kinase 1 during Megakaryocytic Differentiation of K562 Cells." Molecular Pharmacology **77**(6): 1016-1024.
102. Ikeda, Y., E. Tanji, N. Makino, S. Kawata and T. Furukawa (2012). "MicroRNAs Associated with Mitogen-Activated Protein Kinase in Human Pancreatic Cancer." Molecular Cancer Research **10**(2): 259-269.
103. Irish, J. M., R. Hovland, P. O. Krutzik, O. D. Perez, O. Bruserud, B. T. Gjertsen and G. P. Nolan (2004). "Single cell profiling of potentiated phospho-protein networks in cancer cells." Cell **118**(2): 217-228.
104. Yamada, K. M. and E. Cukierman (2007). "Modeling tissue morphogenesis and cancer in 3D." Cell **130**(4): 601-610.
105. Ye, G., G. Fu, S. Cui, S. Zhao, S. Bernaudo, Y. Bai, Y. Ding, Y. Zhang, B. B. Yang and C. Peng (2011). "MicroRNA 376c enhances ovarian cancer cell survival by targeting activin receptor-like kinase 7: implications for chemoresistance." Journal of Cell Science **124**(3): 359-368.
106. Jackson, S. P. and J. Bartek (2009). "The DNA-damage response in human biology and disease." Nature **461**(7267): 1071-1078.
107. Järveläinen, H., A. Sainio, M. Koulu, T. N. Wight and R. Penttinen (2009). "Extracellular Matrix Molecules: Potential Targets in Pharmacotherapy." Pharmacological Reviews **61**(2): 198-223.
108. Jasin, M. and R. Rothstein (2013). "Repair of Strand Breaks by Homologous Recombination." Cold Spring Harbor Perspectives in Biology **5**(11).

109. Joerger, A. C. and A. R. Fersht (2007). "Structure-function-rescue: the diverse nature of common p53 cancer mutants." Oncogene **26**(15): 2226-2242.
110. John-Aryankalayil, M., S. T. Palayoor, D. Cerna, C. B. Simone, 2nd, M. T. Falduto, S. R. Magnuson and C. N. Coleman (2010). "Fractionated radiation therapy can induce a molecular profile for therapeutic targeting." Radiat Res **174**(4): 446-458.
111. John-Aryankalayil, M., S. T. Palayoor, A. Y. Makinde, D. Cerna, C. B. Simone, 2nd, M. T. Falduto, S. R. Magnuson and C. N. Coleman (2012). "Fractionated radiation alters oncomir and tumor suppressor miRNAs in human prostate cancer cells." Radiat Res **178**(3): 105-117.
112. Josson, S., S.-Y. Sung, K. Lao, L. W. K. Chung and P. A. S. Johnstone (2008). "Radiation modulation of microRNA in prostate cancer cell lines." The Prostate **68**(15): 1599-1606.
113. Kahn, J., P. J. Tofilon and K. Camphausen (2012). "Preclinical models in radiation oncology." Radiation Oncology **7**(1): 1-5.
114. Kalbasi, A., C. H. June, N. Haas and N. Vapiwala "Radiation and immunotherapy: a synergistic combination." The Journal of Clinical Investigation **123**(7): 2756-2763.
115. Karin, M. (2009). "NF-κB as a Critical Link Between Inflammation and Cancer." Cold Spring Harbor Perspectives in Biology **1**(5).
116. Katt, M. E., A. L. Placone, A. D. Wong, Z. S. Xu and P. C. Searson (2016). "In Vitro Tumor Models: Advantages, Disadvantages, Variables, and Selecting the Right Platform." Frontiers in Bioengineering and Biotechnology **4**: 12.
117. Kauppila, S., F. Stenback, J. Risteli, A. Jukkola and L. Risteli (1998). "Aberrant type I and type III collagen gene expression in human breast cancer in vivo." J Pathol **186**(3): 262-268.
118. Kenny, P. A., G. Y. Lee, C. A. Myers, R. M. Neve, J. R. Semeiks, P. T. Spellman, K. Lorenz, E. H. Lee, M. H. Barcellos-Hoff, O. W. Petersen, J. W. Gray and M. J. Bissell (2007). "The morphologies of breast cancer cell lines in three-dimensional assays correlate with their profiles of gene expression." Molecular Oncology **1**(1): 84-96.
119. Khodarev, N. N., M. Beckett, E. Labay, T. Darga, B. Roizman and R. R. Weichselbaum (2004). "STAT1 is overexpressed in tumors selected for radioresistance and confers protection from radiation in transduced sensitive cells." Proceedings of the National Academy of Sciences of the United States of America **101**(6): 1714-1719.
120. Kim, Y.-C., G. Gerlitz, T. Furusawa, F. Catez, A. Nussenzweig, K.-S. Oh, K. H. Kraemer, Y. Shiloh and M. Bustin (2009). "Activation of ATM depends on chromatin interactions occurring before induction of DNA damage." Nat Cell Biol **11**(1): 92-96.
121. Kinner, A., W. Wu, C. Staudt and G. Iliakis (2008). "Gamma-H2AX in recognition and signaling of DNA double-strand breaks in the context of chromatin." Nucleic Acids Res **36**(17): 5678-5694.
122. Kita, K., S. Sugaya, L. Zhai, Y. P. Wu, C. Wano, S. Chigira, J. Nomura, S. Takahashi, M. Ichinose and N. Suzuki (2003). "Involvement of LEU13 in

Interferon-Induced Refractoriness of Human RSa Cells to Cell Killing by X Rays." Radiation Research **160**(3): 302-308.
123. Krempler, A., D. Deckbar, P. A. Jeggo and M. Lobrich (2007). "An imperfect G2M checkpoint contributes to chromosome instability following irradiation of S and G2 phase cells." Cell Cycle **6**(14): 1682-1686.
124. Kruse, J.-P. and W. Gu (2009). "Modes of p53 Regulation." Cell **137**(4): 609-622.
125. Kulzer, L., Y. Rubner, L. Deloch, A. Allgäuer, B. Frey, R. Fietkau, J. Dörrie, N. Schaft and U. S. Gaipl (2014). "Norm- and hypo-fractionated radiotherapy is capable of activating human dendritic cells." Journal of Immunotoxicology **11**(4): 328-336.
126. Kuribayashi, K., N. Finnberg, J. R. Jeffers, G. P. Zambetti and W. S. El-Deiry (2011). "The relative contribution of pro-apoptotic p53-target genes in the triggering of apoptosis following DNA damage in vitro and in vivo." Cell Cycle **10**(14): 2380-2389.
127. Lara-Gonzalez, P., F. G. Westhorpe and S. S. Taylor (2012). "The spindle assembly checkpoint." Curr Biol **22**(22): R966-980.
128. Lau, T.-L., C. Kim, M. H. Ginsberg and T. S. Ulmer (2009). "The structure of the integrin αIIbβ3 transmembrane complex explains integrin transmembrane signalling." The EMBO Journal **28**(9): 1351-1361.
129. Leung, C. M., T. W. Chen, S. C. Li, M. R. Ho, L. Y. Hu, W. S. Liu, T. T. Wu, P. C. Hsu, H. T. Chang and K. W. Tsai (2014). "MicroRNA expression profiles in human breast cancer cells after multifraction and single-dose radiation treatment." Oncol Rep **31**(5): 2147-2156.
130. Levental, K. R., H. Yu, L. Kass, J. N. Lakins, M. Egeblad, J. T. Erler, S. F. Fong, K. Csiszar, A. Giaccia, W. Weninger, M. Yamauchi, D. L. Gasser and V. M. Weaver (2009). "Matrix crosslinking forces tumor progression by enhancing integrin signaling." Cell **139**(5): 891-906.
131. Li, B. and J. H. C. Wang (2011). "Fibroblasts and Myofibroblasts in Wound Healing: Force Generation and Measurement." Journal of tissue viability **20**(4): 108-120.
132. Li, C., H. T. Nguyen, Y. Zhuang, Z. Lin, E. K. Flemington, Y. Zhuo, S. P. Kantrow, G. F. Morris, D. E. Sullivan and B. Shan (2012). "Comparative profiling of miRNA expression of lung adenocarcinoma cells in two-dimensional and three-dimensional cultures." Gene **511**(2): 143-150.
133. Li, F., H. Chen, Y. Huang, Q. Zhang, J. Xue, Z. Liu and F. Zheng (2015). "miR-34c plays a role of tumor suppressor in HEC1-B cells by targeting E2F3 protein." Oncol Rep **33**(6): 3069-3074.
134. Li, F. and G. Sethi (2010). "Targeting transcription factor NF-κB to overcome chemoresistance and radioresistance in cancer therapy." Biochimica et Biophysica Acta (BBA) - Reviews on Cancer **1805**(2): 167-180.
135. Li, J., B. A. Ballif, A. M. Powelka, J. Dai, S. P. Gygi and V. W. Hsu (2005). "Phosphorylation of ACAP1 by Akt regulates the stimulation-dependent recycling of integrin β1 to control cell migration." Developmental cell **9**(5): 663-673.

136. Li, X. H., C. T. Ha, D. Fu and M. Xiao (2012). "Micro-RNA30c Negatively Regulates REDD1 Expression in Human Hematopoietic and Osteoblast Cells after Gamma-Irradiation." PLoS ONE **7**(11): e48700.
137. Lieber, M. R. (2010). "The mechanism of double-strand DNA break repair by the nonhomologous DNA end-joining pathway." Annu Rev Biochem **79**: 181-211.
138. Lin, R.-Z. and H.-Y. Chang (2008). "Recent advances in three-dimensional multicellular spheroid culture for biomedical research." Biotechnology Journal **3**(9-10): 1172-1184.
139. Lisby, M. and R. Rothstein (2009). "Choreography of recombination proteins during the DNA damage response." DNA Repair (Amst) **8**(9): 1068-1076.
140. Liu, B., Y. Chen and D. K. St. Clair (2008). "ROS and p53: versatile partnership." Free radical biology & medicine **44**(8): 1529-1535.
141. Livak, K. J. and T. D. Schmittgen (2001). "Analysis of Relative Gene Expression Data Using Real-Time Quantitative PCR and the $2^{-\Delta\Delta CT}$ Method." Methods **25**(4): 402-408.
142. Lord, C. J. and A. Ashworth (2012). "The DNA damage response and cancer therapy." Nature **481**(7381): 287-294.
143. Lorusso, G. and C. Ruegg (2008). "The tumor microenvironment and its contribution to tumor evolution toward metastasis." Histochem Cell Biol **130**(6): 1091-1103.
144. Lu, P., K. Takai, V. M. Weaver and Z. Werb (2011). "Extracellular Matrix Degradation and Remodeling in Development and Disease." Cold Spring Harbor perspectives in biology **3**(12): 10.1101/cshperspect.a005058 a005058.
145. Lu, P., V. M. Weaver and Z. Werb (2012). "The extracellular matrix: A dynamic niche in cancer progression." The Journal of Cell Biology **196**(4): 395-406.
146. Luca, A. C., S. Mersch, R. Deenen, S. Schmidt, I. Messner, K. L. Schafer, S. E. Baldus, W. Huckenbeck, R. P. Piekorz, W. T. Knoefel, A. Krieg and N. H. Stoecklein (2013). "Impact of the 3D microenvironment on phenotype, gene expression, and EGFR inhibition of colorectal cancer cell lines." PLoS One **8**(3): e59689.
147. Lucero, H. A. and H. M. Kagan (2006). "Lysyl oxidase: an oxidative enzyme and effector of cell function." Cellular and Molecular Life Sciences CMLS **63**(19-20): 2304-2316.
148. Luo, J., J. Chen and L. He (2015). "mir-129-5p Attenuates Irradiation-Induced Autophagy and Decreases Radioresistance of Breast Cancer Cells by Targeting HMGB1." Medical Science Monitor : International Medical Journal of Experimental and Clinical Research **21**: 4122-4129.
149. Martin, K. J., D. R. Patrick, M. J. Bissell and M. V. Fournier (2008). "Prognostic Breast Cancer Signature Identified from 3D Culture Model Accurately Predicts Clinical Outcome across Independent Datasets." PLoS ONE **3**(8): e2994.

150. Mbeunkui, F. and D. J. Johann, Jr. (2009). "Cancer and the tumor microenvironment: a review of an essential relationship." Cancer Chemother Pharmacol **63**(4): 571-582.
151. Mehta, G., A. Y. Hsiao, M. Ingram, G. D. Luker and S. Takayama (2012). "Opportunities and Challenges for use of Tumor Spheroids as Models to Test Drug Delivery and Efficacy." Journal of controlled release : official journal of the Controlled Release Society **164**(2): 192-204.
152. Melchjorsen, J., H. Kristiansen, R. Christiansen, J. Rintahaka, S. Matikainen, S. R. Paludan and R. Hartmann (2009). "Differential regulation of the OASL and OAS1 genes in response to viral infections." J Interferon Cytokine Res **29**(4): 199-207.
153. Metheetrairut, C. and F. J. Slack (2013). "MicroRNAs in the Ionizing Radiation Response and in Radiotherapy." Current opinion in genetics & development **23**(1): 12-19.
154. Mihara, M., S. Erster, A. Zaika, O. Petrenko, T. Chittenden, P. Pancoska and U. M. Moll (2003). "p53 Has a Direct Apoptogenic Role at the Mitochondria." Molecular Cell **11**(3): 577-590.
155. Minafra, L. and V. Bravatà (2014). "Cell and molecular response to IORT treatment." Translational Cancer Research **3**(1): 32-47.
156. Minami, T., S. Jiang, K. Schadler, J.-i. Suehiro, T. Osawa, Y. Oike, M. Miura, M. Naito, T. Kodama and S. Ryeom (2013). "The Calcineurin-NFAT-Angiopoietin 2 signaling axis in lung endothelium is critical for the establishment of lung metastases." Cell reports **4**(4): 709-723.
157. Miranti, C. K. and J. S. Brugge (2002). "Sensing the environment: a historical perspective on integrin signal transduction." Nat Cell Biol **4**(4): E83-E90.
158. Mirzayans, R., B. Andrais, A. Scott and D. Murray (2012). "New Insights into p53 Signaling and Cancer Cell Response to DNA Damage: Implications for Cancer Therapy." Journal of Biomedicine and Biotechnology **2012**: 16.
159. Mithieux, S. M. and A. S. Weiss (2005). Elastin. Advances in Protein Chemistry, Academic Press. **Volume 70:** 437-461.
160. Mitra, S. K. and D. D. Schlaepfer (2006). "Integrin-regulated FAK–Src signaling in normal and cancer cells." Current Opinion in Cell Biology **18**(5): 516-523.
161. Mo, Z.-H., X.-D. Wu, S. Li, B.-Y. Fei and B. Zhang (2014). "Expression and clinical significance of microRNA-376a in colorectal cancer." Asian Pacific journal of cancer prevention : APJCP **15**(21): 9523-9527.
162. Morgan, W. F. and M. B. Sowa (2005). "Effects of ionizing radiation in nonirradiated cells." Proc Natl Acad Sci U S A **102**(40): 14127-14128.
163. Moser, M., K. R. Legate, R. Zent and R. Fässler (2009). "The Tail of Integrins, Talin, and Kindlins." Science **324**(5929): 895-899.
164. Mott, J. D. and Z. Werb (2004). "Regulation of matrix biology by matrix metalloproteinases." Current Opinion in Cell Biology **16**(5): 558-564.
165. Nagata, S., R. Hanayama and K. Kawane (2010). "Autoimmunity and the Clearance of Dead Cells." Cell **140**(5): 619-630.

166. Najafi, M., R. Fardid, G. Hadadi and M. Fardid (2014). "The Mechanisms of Radiation-Induced Bystander Effect." Journal of Biomedical Physics & Engineering **4**(4): 163-172.
167. Nguyen, H. T., C. U. I. Li, Z. Lin, Y. A. N. Zhuang, E. K. Flemington, M. E. Burow, Y. I. Lin and B. I. N. Shan (2012). "The microRNA expression associated with morphogenesis of breast cancer cells in three-dimensional organotypic culture." Oncology reports **28**(1): 117-126.
168. Nikjoo, H., D. Emfietzoglou, T. Liamsuwan, R. Taleei, D. Liljequist and S. Uehara (2016). "Radiation track, DNA damage and response-a review." Rep Prog Phys **79**(11): 116601.
169. Nyga, A., U. Cheema and M. Loizidou (2011). "3D tumour models: novel in vitro approaches to cancer studies." Journal of Cell Communication and Signaling **5**(3): 239-248.
170. Nyga, A., U. Cheema and M. Loizidou (2011). "3D tumour models: novel in vitro approaches to cancer studies." J Cell Commun Signal **5**(3): 239-248.
171. O'Shea, J. J., D. M. Schwartz, A. V. Villarino, M. Gadina, I. B. McInnes and A. Laurence (2015). "The JAK-STAT Pathway: Impact on Human Disease and Therapeutic Intervention." Annual Review of Medicine **66**(1): 311-328.
172. OKAICHI, K., M. IDE-KANEMATSU, N. IZUMI, N. MORITA, Y. OKUMURA and M. IHARA (2008). "Variations in Sensitivity to Ionizing Radiation in Relation to p53 Mutation Point." Anticancer Research **28**(5A): 2687-2690.
173. Oren, M. and V. Rotter (2010). "Mutant p53 Gain-of-Function in Cancer." Cold Spring Harbor Perspectives in Biology **2**(2).
174. Ozbek, S., P. G. Balasubramanian, R. Chiquet-Ehrismann, R. P. Tucker and J. C. Adams (2010). "The evolution of extracellular matrix." Mol Biol Cell **21**(24): 4300-4305.
175. Palayoor, S. T., M. John-Aryankalayil, A. Y. Makinde, M. T. Falduto, S. R. Magnuson and C. N. Coleman (2014). "Differential expression of stress and immune response pathway transcripts and miRNAs in normal human endothelial cells subjected to fractionated or single-dose radiation." Mol Cancer Res **12**(7): 1002-1015.
176. Paraskevopoulou, M. D., G. Georgakilas, N. Kostoulas, I. S. Vlachos, T. Vergoulis, M. Reczko, C. Filippidis, T. Dalamagas and A. G. Hatzigeorgiou (2013). "DIANA-microT web server v5.0: service integration into miRNA functional analysis workflows." Nucleic Acids Research **41**(Web Server issue): W169-W173.
177. Paszek, M. J., N. Zahir, K. R. Johnson, J. N. Lakins, G. I. Rozenberg, A. Gefen, C. A. Reinhart-King, S. S. Margulies, M. Dembo, D. Boettiger, D. A. Hammer and V. M. Weaver (2005). "Tensional homeostasis and the malignant phenotype." Cancer Cell **8**(3): 241-254.
178. Pattabiraman, D. R. and R. A. Weinberg (2014). "Tackling the cancer stem cells – what challenges do they pose?" Nature reviews. Drug discovery **13**(7): 497-512.

179. Pawlik, A., P. Delmar, S. Bosse, L. Sainz, C. Petat, G. Pietu, D. Thierry and D. Tronik-Le Roux (2009). "Changes in transcriptome after in vivo exposure to ionising radiation reveal a highly specialised liver response." Int J Radiat Biol **85**(8): 656-671.
180. Pollard, J. W. (2004). "Tumour-educated macrophages promote tumour progression and metastasis." Nat Rev Cancer **4**(1): 71-78.
181. Pouwels, J., J. Nevo, T. Pellinen, J. Ylänne and J. Ivaska (2012). "Negative regulators of integrin activity." Journal of Cell Science **125**(14): 3271-3280.
182. Price, K. J., A. Tsykin, K. M. Giles, R. T. Sladic, M. R. Epis, R. Ganss, G. J. Goodall and P. J. Leedman (2012). "Matrigel Basement Membrane Matrix influences expression of microRNAs in cancer cell lines." Biochemical and Biophysical Research Communications **427**(2): 343-348.
183. Purdy, J. A. (2008). "Dose to normal tissues outside the radiation therapy patient's treated volume: a review of different radiation therapy techniques." Health Phys **95**(5): 666-676.
184. Quail, D. F. and J. A. Joyce (2013). "Microenvironmental regulation of tumor progression and metastasis." Nat Med **19**(11): 1423-1437.
185. Quante, M., S. P. Tu, H. Tomita, T. Gonda, S. S. W. Wang, S. Takashi, G. H. Baik, W. Shibata, B. DiPrete, K. S. Betz, R. Friedman, A. Varro, B. Tycko and T. C. Wang (2011). "Bone marrow-derived myofibroblasts contribute to the mesenchymal stem cell niche and promote tumor growth." Cancer cell **19**(2): 257-272.
186. Rashi-Elkeles, S., R. Elkon, S. Shavit, Y. Lerenthal, C. Linhart, A. Kupershtein, N. Amariglio, G. Rechavi, R. Shamir and Y. Shiloh (2011). "Transcriptional modulation induced by ionizing radiation: p53 remains a central player." Mol Oncol **5**(4): 336-348.
187. Rygaard, J. and C. O. Povlsen (1969). "Heterotransplantation of a human malignant tumour to "Nude" mice." Acta Pathol Microbiol Scand **77**(4): 758-760.
188. Robinson, S. C. and L. M. Coussens (2005). "Soluble mediators of inflammation during tumor development." Adv Cancer Res **93**: 159-187.
189. Rodier, F. and J. Campisi (2011). "Four faces of cellular senescence." J Cell Biol **192**(4): 547-556.
190. Ross, D. T., U. Scherf, M. B. Eisen, C. M. Perou, C. Rees, P. Spellman, V. Iyer, S. S. Jeffrey, M. Van de Rijn, M. Waltham, A. Pergamenschikov, J. C. E. Lee, D. Lashkari, D. Shalon, T. G. Myers, J. N. Weinstein, D. Botstein and P. O. Brown (2000). "Systematic variation in gene expression patterns in human cancer cell lines." Nature Genetics **24**(3): 227-235.
191. Rozario, T. and D. W. DeSimone (2010). "The extracellular matrix in development and morphogenesis: A dynamic view." Developmental Biology **341**(1): 126-140.
192. Rutnam, Z. J., T. N. Wight and B. B. Yang (2013). "miRNAs regulate expression and function of extracellular matrix molecules()." Matrix biology : journal of the International Society for Matrix Biology **32**(2): 74-85.
193. Santivasi, W. L. and F. Xia (2014). "Ionizing radiation-induced DNA damage, response, and repair." Antioxid Redox Signal **21**(2): 251-259.

194. Sarcar, B., S. Kahali, A. H. Prabhu, S. D. Shumway, Y. Xu, T. Demuth and P. Chinnaiyan (2011). "Targeting radiation-induced G(2) checkpoint activation with the Wee-1 inhibitor MK-1775 in glioblastoma cell lines." Mol Cancer Ther **10**(12): 2405-2414.
195. Sausville, E. A. and A. M. Burger (2006). "Contributions of human tumor xenografts to anticancer drug development." Cancer Res **66**(7): 3351-3354, discussion 3354.
196. Schaue, D., J. A. Ratikan, K. S. Iwamoto and W. H. McBride (2012). "Maximizing Tumor Immunity With Fractionated Radiation." International Journal of Radiation Oncology*Biology*Physics **83**(4): 1306-1310.
197. Sharp, H. J., E. K. Wansley, C. T. Garnett, M. Chakraborty, K. Camphausen, J. Schlom and J. W. Hodge (2007). "Synergistic antitumor activity of immune strategies combined with radiation." Front Biosci **12**: 4900-4910.
198. Shattil, S. J., C. Kim and M. H. Ginsberg (2010). "The final steps of integrin activation: the end game." Nature reviews. Molecular cell biology **11**(4): 288-300.
199. Shepperd, Lindsey A., John C. Meadows, Alicja M. Sochaj, Theresa C. Lancaster, J. Zou, Graham J. Buttrick, J. Rappsilber, Kevin G. Hardwick and Jonathan B. A. Millar (2012). "Phosphodependent Recruitment of Bub1 and Bub3 to Spc7/KNL1 by Mph1 Kinase Maintains the Spindle Checkpoint." Current Biology **22**(10): 891-899.
200. Short, S. C., F. M. Buffa, S. Bourne, M. Koritzinsky, B. G. Wouters and S. M. Bentzen (2007). "Dose- and time-dependent changes in gene expression in human glioma cells after low radiation doses." Radiat Res **168**(2): 199-208.
201. Simone, C. B., 2nd, M. John-Aryankalayil, S. T. Palayoor, A. Y. Makinde, D. Cerna, M. T. Falduto, S. R. Magnuson and C. N. Coleman (2013). "mRNA Expression Profiles for Prostate Cancer following Fractionated Irradiation Are Influenced by p53 Status." Transl Oncol **6**(5): 573-585.
202. Singleton, B. K., C. S. Griffin and J. Thacker (2002). "Clustered DNA damage leads to complex genetic changes in irradiated human cells." Cancer Res **62**(21): 6263-6269.
203. Smith, M. L., D. Gourdon, W. C. Little, K. E. Kubow, R. A. Eguiluz, S. Luna-Morris and V. Vogel (2007). "Force-induced unfolding of fibronectin in the extracellular matrix of living cells." PLoS Biol **5**(10): e268.
204. Soon, P. and H. Kiaris (2013). "MicroRNAs in the tumour microenvironment: big role for small players." Endocrine-Related Cancer **20**(5): R257-R267.
205. Spaeth, E. L., J. L. Dembinski, A. K. Sasser, K. Watson, A. Klopp, B. Hall, M. Andreeff and F. Marini (2009). "Mesenchymal Stem Cell Transition to Tumor-Associated Fibroblasts Contributes to Fibrovascular Network Expansion and Tumor Progression." PLoS ONE **4**(4): e4992.
206. Spoerri, L., Z. Oo, J. Larsen, N. Haass, B. Gabrielli and S. Pavey (2015). Cell Cycle Checkpoint and DNA Damage Response Defects as Anticancer Targets: From Molecular Mechanisms to Therapeutic Opportunities. Stress Response Pathways in Cancer. G. T. Wondrak, Springer Netherlands**:** 29-49.

207. Stauder, R., W. Eisterer, J. Thaler and U. Gunthert (1995). "CD44 variant isoforms in non-Hodgkin's lymphoma: a new independent prognostic factor." Blood **85**(10): 2885-2899.
208. Stegeman, H., J. H. A. M. Kaanders, M. M. G. Verheijen, W. J. M. Peeters, D. L. Wheeler, M. Iida, R. Grénman, A. J. van der Kogel, P. N. Span and J. Bussink (2013). "Combining radiotherapy with MEK1/2, STAT5 or STAT6 inhibition reduces survival of head and neck cancer lines." Molecular Cancer **12**: 133-133.
209. Storch, K. and N. Cordes (2016). "The impact of CDK9 on radiosensitivity, DNA damage repair and cell cycling of HNSCC cancer cells." Int J Oncol **48**(1): 191-198.
210. Storch, K., I. Eke, K. Borgmann, M. Krause, C. Richter, K. Becker, E. Schrock and N. Cordes (2010). "Three-Dimensional Cell Growth Confers Radioresistance by Chromatin Density Modification." Cancer Research **70**(10): 3925-3934.
211. Storch, K., I. Eke, K. Borgmann, M. Krause, C. Richter, K. Becker, E. Schröck and N. Cordes (2010). "Three-Dimensional Cell Growth Confers Radioresistance by Chromatin Density Modification." Cancer Research **70**(10): 3925-3934.
212. Surget, S., M. P. Khoury and J. C. Bourdon (2013). "Uncovering the role of p53 splice variants in human malignancy: a clinical perspective." Onco Targets Ther **7**: 57-68.
213. Tian, H., Z. Gao, H. Li, B. Zhang, G. Wang, Q. Zhang, D. Pei and J. Zheng (2015). "DNA damage response--a double-edged sword in cancer prevention and cancer therapy." Cancer Lett **358**(1): 8-16.
214. Tibbitt, M. W. and K. S. Anseth (2009). "Hydrogels as extracellular matrix mimics for 3D cell culture." Biotechnol Bioeng **103**(4): 655-663.
215. Tibbitt, M. W. and K. S. Anseth (2012). "Dynamic microenvironments: the fourth dimension." Sci Transl Med **4**(160): 160ps124.
216. Toledo, F. and G. M. Wahl (2007). "MDM2 and MDM4: p53 regulators as targets in anticancer therapy." The international journal of biochemistry & cell biology **39**(7-8): 1476-1482.
217. Tredan, O., C. M. Galmarini, K. Patel and I. F. Tannock (2007). "Drug resistance and the solid tumor microenvironment." J Natl Cancer Inst **99**(19): 1441-1454.
218. Trinchieri, G. (2010). "Type I interferon: friend or foe?" J Exp Med **207**(10): 2053-2063.
219. Tripathi, P., Y. Wang, M. Coussens, K. R. Manda, A. M. Casey, C. Lin, E. Poyo, J. D. Pfeifer, N. Basappa, C. M. Bates, L. Ma, H. Zhang, M. Pan, L. Ding and F. Chen (2014). "Activation of NFAT signaling establishes a tumorigenic microenvironment through cell autonomous and non-cell autonomous mechanisms." Oncogene **33**(14): 1840-1849.
220. Tsai, M. H., J. A. Cook, G. V. Chandramouli, W. DeGraff, H. Yan, S. Zhao, C. N. Coleman, J. B. Mitchell and E. Y. Chuang (2007). "Gene expression

profiling of breast, prostate, and glioma cells following single versus fractionated doses of radiation." Cancer Res **67**(8): 3845-3852.
221. Tsunoda, T., Y. Takashima, T. Fujimoto, M. Koyanagi, Y. Yoshida, K. Doi, Y. Tanaka, M. Kuroki, T. Sasazuki and S. Shirasawa (2010). "Three-dimensionally Specific Inhibition of DNA Repair-Related Genes by Activated KRAS in Colon Crypt Model." Neoplasia (New York, N.Y.) **12**(5): 397-404.
222. Uze, G. and D. Monneron (2007). "IL-28 and IL-29: newcomers to the interferon family." Biochimie **89**(6-7): 729-734.
223. Vaupel, P. (2004). "Tumor microenvironmental physiology and its implications for radiation oncology." Seminars in Radiation Oncology **14**(3): 198-206.
224. Vlachos, I. S., N. Kostoulas, T. Vergoulis, G. Georgakilas, M. Reczko, M. Maragkakis, M. D. Paraskevopoulou, K. Prionidis, T. Dalamagas and A. G. Hatzigeorgiou (2012). "DIANA miRPath v.2.0: investigating the combinatorial effect of microRNAs in pathways." Nucleic Acids Research **40**(Web Server issue): W498-W504.
225. Vousden, K. H. and K. M. Ryan (2009). "p53 and metabolism." Nat Rev Cancer **9**(10): 691-700.
226. Wang, J., D. Duncan, Z. Shi and B. Zhang (2013). "WEB-based GEne SeT AnaLysis Toolkit (WebGestalt): update 2013." Nucleic Acids Research **41**(W1): W77-W83.
227. Weaver, V. M., O. W. Petersen, F. Wang, C. A. Larabell, P. Briand, C. Damsky and M. J. Bissell (1997). "Reversion of the Malignant Phenotype of Human Breast Cells in Three-Dimensional Culture and In Vivo by Integrin Blocking Antibodies." The Journal of Cell Biology **137**(1): 231-245.
228. Weidhaas, J. B., I. Babar, S. M. Nallur, P. Trang, S. Roush, M. Boehm, E. Gillespie and F. J. Slack (2007). "MicroRNAs as Potential Agents to Alter Resistance to Cytotoxic Anticancer Therapy." Cancer Research **67**(23): 11111.
229. Weiswald, L. B., D. Bellet and V. Dangles-Marie (2015). "Spherical Cancer Models in Tumor Biology()." Neoplasia **17**(1): 1-15.
230. West, C. M. and G. C. Barnett (2011). "Genetics and genomics of radiotherapy toxicity: towards prediction." Genome Medicine **3**(8): 52-52.
231. Weterings, E. and D. J. Chen (2008). "The endless tale of non-homologous end-joining." Cell Res **18**(1): 114-124.
232. Whiteside, T. L. (2008). "The tumor microenvironment and its role in promoting tumor growth." Oncogene **27**(45): 5904-5912.
233. Wilderman, M. J., J. Sun, A. S. Jassar, V. Kapoor, M. Khan, A. Vachani, E. Suzuki, P. A. Kinniry, D. H. Sterman, L. R. Kaiser and S. M. Albelda (2005). "Intrapulmonary IFN-β Gene Therapy Using an Adenoviral Vector Is Highly Effective in a Murine Orthotopic Model of Bronchogenic Adenocarcinoma of the Lung." Cancer Research **65**(18): 8379-8387.
234. Willis, N. and N. Rhind (2009). "Regulation of DNA replication by the S-phase DNA damage checkpoint." Cell Division **4**(1): 1-10.

235. Wirth, M., J. Joachim and S. A. Tooze (2013). "Autophagosome formation—The role of ULK1 and Beclin1–PI3KC3 complexes in setting the stage." Seminars in Cancer Biology **23**(5): 301-309.
236. Wise, S. G. and A. S. Weiss (2009). "Tropoelastin." The International Journal of Biochemistry & Cell Biology **41**(3): 494-497.
237. Wozniak, M. A., R. Desai, P. A. Solski, C. J. Der and P. J. Keely (2003). "ROCK-generated contractility regulates breast epithelial cell differentiation in response to the physical properties of a three-dimensional collagen matrix." J Cell Biol **163**(3): 583-595.
238. Xiaofei, E. and T. F. Kowalik (2014). "The DNA damage response induced by infection with human cytomegalovirus and other viruses." Viruses **6**(5): 2155-2185.
239. Zaidel-Bar, R., S. Itzkovitz, A. Ma'ayan, R. Iyengar and B. Geiger (2007). "Functional atlas of the integrin adhesome." Nature cell biology **9**(8): 858-867.
240. Zamarron, B. F. and W. Chen (2011). "Dual roles of immune cells and their factors in cancer development and progression." Int J Biol Sci **7**(5): 651-658.
241. Zhan, J.-f., L.-h. Chen, Y.-w. Yuan, G.-z. Xie, A.-m. Sun, Y. Liu and Z.-x. Chen (2011). "STAT1 promotes radioresistance of CD44+/CD24−/low cells in breast cancer." Experimental Biology and Medicine **236**(4): 418-422.
242. Zhao, Y., I. C. Lou and R. B. Conolly (2012). "Computational modeling of signaling pathways mediating cell cycle checkpoint control and apoptotic responses to ionizing radiation-induced DNA damage." Dose Response **10**(2): 251-273.
243. Zhao, L., X. Lu and Y. Cao (2013). "MicroRNA and signal transduction pathways in tumor radiation response." Cellular Signalling **25**(7): 1625-1634.
244. Zheng, G. X. Y., A. Ravi, G. M. Gould, C. B. Burge and P. A. Sharp (2011). "Genome-wide impact of a recently expanded microRNA cluster in mouse." Proceedings of the National Academy of Sciences **108**(38): 15804-15809.
245. Zhou, Y.-L., Y.-J. Xu and C.-W. Qiao (2015). "MiR-34c-3p suppresses the proliferation and invasion of non-small cell lung cancer (NSCLC) by inhibiting PAC1/MAPK pathway." International Journal of Clinical and Experimental Pathology **8**(6): 6312-6322.
246. Zhu, J., G. Xiong, C. Trinkle and R. Xu (2014). "Integrated extracellular matrix signaling in mammary gland development and breast cancer progression." Histology and histopathology **29**(9): 1083-1092.
247. Zlotorynski, E. (2015). "DNA damage response: The spliceosome cashes in at the ATM." Nat Rev Mol Cell Biol **16**(8): 454-454.
248. Zois, C. E. and M. I. Koukourakis (2009). "Radiation-induced autophagy in normal and cancer cells: Towards novel cytoprotection and radio-sensitization policies?" Autophagy **5**(4): 442-450.
249. Zschenker, O., T. Streichert, S. Hehlgans and N. Cordes (2012). "Genome-wide gene expression analysis in cancer cells reveals 3D growth to affect ECM and processes associated with cell adhesion but not DNA repair." PLoS One **7**(4): e34279.